



# ISJET

## INTERNATIONAL SCIENTIFIC JOURNAL OF ENGINEERING AND TECHNOLOGY

Volume 6 No. 2 July-December 2022



ISSN 2586-8527 (Online)

Panyapiwat Institute of Management

Indexed in the Thai-Journal Citation Index (TCI 2)

**INTERNATIONAL SCIENTIFIC  
JOURNAL OF ENGINEERING AND TECHNOLOGY  
(ISJET)**

---

**Volume 6 No. 2 July-December 2022**

**ISSN 2586-8527 (Online)  
PANYAPIWAT INSTITUTE OF MANAGEMENT**

**INTERNATIONAL SCIENTIFIC JOURNAL OF ENGINEERING AND THCHNOLOGY (ISJET)**

**Volume 6 No. 2 July-December 2022**

**ISSN 2586-8527 (Online)**

**Copyright**

Panyapiwat Institute of Management

85/1 Moo 2, Chaengwattana Rd.,

Bang Talat, Pakkred,

Nonthaburi, 11120, Thailand

Tel. +66 2855 1560

Fax +66 2855 0392

E-mail: [isjet@pim.ac.th](mailto:isjet@pim.ac.th)

Website: <https://ph02.tci-thaijo.org/index.php/isjet/index>

**Copyright©2017, Panyapiwat Institute of Management**



## INTERNATIONAL SCIENTIFIC JOURNAL OF ENGINEERING AND THCHNOLOGY (ISJET)

Volume 6 No. 2 July-December 2022 ISSN 2586-8527 (Online)

### **Objective:**

International Scientific Journal of Engineering and Technology will be dedicated to serving as a forum to share knowledge on research advances in all fields of sciences: Engineering, Technology, Innovation, Information Technology, Management Information System, Logistics and Transportation, Agricultural Science and Technology, Animal Science and Aquaculture, Food Science, and other areas in Sciences and Technology. Submissions are welcomed from both PIM as well as other Thai and foreign institutions.

### **Scope:**

Engineering, Technology, Innovation Technology, Management Information System, Logistics and Transportation, Agricultural Science and Technology, Animal Science and Aquaculture, Food Science, and other areas in Sciences and Technology

### **Type of Article:**

- Research article
- Academic article
- Book review
- Review article

### **Languages of academic works:**

Article written in either English languages are accepted for publication.

### **Reviewing Policy:**

1. Any manuscript to be accepted for publication must have been reviewed and approved by at least three peer reviewers in that particular field or related fields.
2. The submitted manuscript must have never been published in any other periodical, and must not be in the approving process for publication by any other periodical. Also, the author must not plagiarize the work of other people.
3. The article, expression, illustrations, and tables that are published in the Journal are the sole responsibility of the author, and definitely not that of Panyapiwat Institute of Management.
4. The Editorial Board of International Scientific Journal of Engineering and Technology reserves right for decision making on publishing any article in the Journal.

### **Frequency of Publication:**

Twice a year

- The first issue: January-June
- The second issue: July-December

### **Publication and Access Charges:**

There are no charges to submit and publish all types of articles. Full articles in pdf format can be downloaded freely from the journal website at <https://ph02.tci-thaijo.org/index.php/isjet/index>

ISJET Journal Editorial Board  
The office of Research and Development  
Panyapiwat Institute of Management  
85/1 Moo 2, Chaengwattana Rd.,  
Bang Talat, Pakkred, Nonthaburi, 11120, Thailand  
Tel. +66 2855 1560  
Fax +66 2855 0392  
E-mail: [isjet@pim.ac.th](mailto:isjet@pim.ac.th)  
Website: <https://ph02.tci-thaijo.org/index.php/isjet/index>

# INTERNATIONAL SCIENTIFIC JOURNAL OF ENGINEERING AND TECHNOLOGY (ISJET)

Volume 6 No. 2 July-December 2022

ISSN 2586-8527 (Online)

## Advisors Board

Assoc. Prof. Dr. Somrote Komolavanij	Panyapiwat Institute of Management, Thailand
Assoc. Prof. Dr. Pisit Charnkeitkong	Panyapiwat Institute of Management, Thailand
Assoc. Prof. Dr. Paritud Bhandhubanyong	Panyapiwat Institute of Management, Thailand
Assoc. Prof. Dr. Chom Kimpan	Panyapiwat Institute of Management, Thailand
Prof. Dr. Rattikorn Yimnirun	Vidyasirimedhi Institute of Science and Technology, Thailand

## Editor-in-chief

Assoc. Prof. Dr. Parinya Sanguansat	Panyapiwat Institute of Management, Thailand
-------------------------------------	--

## Associate Editor of Engineering and Technology

Asst. Prof. Dr. Phannachet Na Lamphun	Panyapiwat Institute of Management, Thailand
---------------------------------------	--

## Associate Editor of Information Technology

Asst. Prof. Dr. Nivet Chirawichitchai	Panyapiwat Institute of Management, Thailand
---------------------------------------	--

## Associate Editor of Science

Dr. Wirin Sonsrettee	Panyapiwat Institute of Management, Thailand
----------------------	--

## Associate Editor of Logistics and Transportation

Dr. Tantikorn Pichpibul	Panyapiwat Institute of Management, Thailand
-------------------------	--

## Associate Editor of Agriculture Science and Food Technology

Asst. Prof. Dr. Korawit Chaisu	Panyapiwat Institute of Management, Thailand
--------------------------------	--

## Editorial Board

Prof. Dr. Chidchanok Lursinsap	Chulalongkorn University, Thailand
Prof. Dr. Parames Chutima	Chulalongkorn University, Thailand
Prof. Dr. Phadungsak Rattanadecho	Thammasat University, Thailand
Prof. Dr. Prasanta Kumar Dey	Aston Business School, Aston University, UK
Prof. Dr. Rosemary R. Seva.	De La Salle University, Philippines
Prof. Dr. Sandhya Babel	Sirindhorn International Institute of Technology, Thailand
Prof. Dr. Takashi Yukawa	Nagaoka University of Technology, Japan
Prof. Dr. Thanaruk Theeramunkong	Sirindhorn International Institute of Technology, Thailand
Prof. Duane P. Bartholomew	University of Hawaii at Manoa Honolulu, USA
Assoc. Prof. Dr. Chawalit Jeenanunta	Sirindhorn International Institute of Technology, Thailand
Assoc. Prof. Dr. Nattapon Chantarapanich	Kasetsart University, Sriracha Campus, Thailand
Assoc. Prof. Dr. Panich Intra	Rajamangala University of Technology Lanna, Thailand
Assoc. Prof. Dr. Ruengsak Kawtummachai	Panyapiwat Institute of Management, Thailand
Assoc. Prof. Dr. Wilaiporn Lee	King Mongkut's University of Technology North Bangkok, Thailand
Asst. Prof. Dr. Adisak Joomwong	Maejo University, Thailand
Asst. Prof. Dr. Anan Boonpan	Panyapiwat Institute of Management, Thailand
Asst. Prof. Dr. Rangsimma Chanphana	Chulalongkorn University, Thailand
Asst. Prof. Dr. Thongchai Kaewkiriya	Panyapiwat Institute of Management, Thailand
Dr. Anand Mary	Faculty of Dentistry, University of Puthisastra, Cambodia
Dr. Jochen Hermann Josef Amrehn	Nanjing Tech University Pujiang Institute, China
Dr. Nattakarn Phaphoom	TD Tawandang Company Limited, Thailand
Dr. Nattaporn Chotyakul	Panyapiwat Institute of Management, Thailand

## Journal Secretary

Ms. Suchinda Chaluai	Panyapiwat Institute of Management, Thailand
----------------------	--

**INTERNATIONAL SCIENTIFIC JOURNAL OF ENGINEERING AND TECHNOLOGY (ISJET)**

Volume 6 No. 2 July-December 2022

ISSN 2586-8527 (Online)

**Peer Reviewers**

Prof. Dr. Parames Chutima

Assoc. Prof. Dr. Paitoon Siri Oran

Assoc. Prof. Dr. Papot Jaroenapibal

Assoc. Prof. Dr. Parinya Sanguansat

Assoc. Prof. Dr. Sangsuree Vasuponggayya

Assoc. Prof. Dr. Wilaiporn Lee

Asst. Prof. Dr. Chutima Beokhaimook

Asst. Prof. Dr. Duenpen Kochakornjarupong

Asst. Prof. Dr. Kanyarat Lueangprasert

Asst. Prof. Dr. Nipat Jongsawat

Asst. Prof. Dr. Nivet Chirawichitchai

Asst. Prof. Dr. Panomkhawn Riyamongkol

Asst. Prof. Dr. Sukumal Kitisin

Dr. Kwankamon Dittakan

Chulalongkorn University, Thailand

Panyapiwat Institute of Management, Thailand

Khon Kaen University, Thailand

Panyapiwat Institute of Management, Thailand

Prince of Songkla University, Hatyai Campus, Thailand

King Mongkut's University of Technology North Bangkok,  
Thailand

Rangsit University, Thailand

Thaksin University Phatthalung, Thailand

Burapha University Sa Kaeo, Thailand

Rajamangala University of Technology Thanyaburi,  
Thailand

Panyapiwat Institute of Management, Thailand

Naresuan University, Thailand

Kasetsart University, Thailand

Prince of Songkla University, Thailand

**INTERNATIONAL SCIENTIFIC JOURNAL OF ENGINEERING AND TECHNOLOGY (ISJET)**

Volume 6 No. 2 July-December 2022

ISSN 2586-8527 (Online)

PANYAPIWAT INSTITUTE OF MANAGEMENT

85/1 Moo 2, Chaengwattana Rd.,

Bang Talat, Pakkred, Nanthaburi, 11120 Thailand

Dear Colleagues,

Information and artificial intelligence undeniably play an important role in our modern society. The ability to use the information at the right time can give companies an edge over the competition. However, developing information from data is not always easy and can be time-consuming. This is where artificial intelligence comes into play. Artificial intelligence, such as neural networks can adapt to changing inputs and are able to produce the best result that provides the information needed. This can lead to more effectiveness and efficiency in the work process, as shown in research articles: Deep Constitutional Neural Networks based on VGG-16 Transfer Learning for Abnormalities Peeled Shrimp Classification, Fluke Eggs Detection and Classification Using Deep Convolution Neural Network, Identifying ATM Fraud Transactions in Thailand using Outlier Detection with Location-Based Grouping and Behavior Feature. The other multidisciplinary contents of the research articles are Comparison of Keyword Etraction Methods for Crowdfunding Projects Based on the Web Data, Developing of Grip Comfort of Perfume Bottles by Applying the Concepts of Product Design and Development and Hybrid Optimization Technique, Reverse Logistics Networks for Infected Medical Waste Management in Epidemic Outbreaks under Uncertainty: A Case Study of COVID-19 in Pathum Thani, Thailand

All authors and readers from around the world are invited to visit the website <https://ph02.tci-thaijo.org/index.php/isjet/index>. This link will grant you to submit your research to publish in our journal or will access to electronic versions of all issues of our journal. On behalf of the Editorial Board, I would like to take this opportunity to thank everyone who has complimented our goal by contributing to the ISJET.

With kind regards,

Asst. Prof. Dr. Phannachet Na Lamphun  
Associat Editor Engineering and Technology  
[isjet@pim.ac.th](mailto:isjet@pim.ac.th)

**INTERANTIONAL SCIETIFIC JOURNAL OF ENGINEERIN AND TECHNOLOGY (ISJET)**

## CONTENTS

- **Comparison of Keyword Etraction Methods for Crowdfunding Projects Based on Web-Data** 1  
*Wenting Hou and Jian Qu*
- **Deep Constitutional Neural Networks based on VGG-16 Transfer Learning for Abnormalities Peeled Shrimp Classification** 13  
*Tamnawat Valeeprakhon, Korawit Orkphol, and Penpun Chaihuadjaroen*
- **Development of Grip Comfort of Perfume Bottle by Applying the Concepts of Product Design and Development and Hybrid Optimization Technique** 24  
*Suchada Rianmora and Pervez Alam Khan*
- **Fluke Eggs Detection and Classification Using Deep Convolution Neural Network** 40  
*Natthaphon Hongcharoen, Parinya Sanguansat, and Sanparith Marukatat*
- **Identifying ATM Fraud Transactions in Thailand using Outlier Detection with Location-Based Grouping and Behavior Feature** 54  
*Natsuda Kaothanthong and Roongtawan Laimek*
- **Reverse Logistics Network Design for Infected Medical Waste Management in Epidemic Outbreaks under Uncertainty: A Case Study of COVID-19 in Pathum Thani, Thailand** 66  
*Pornpawee Supsermpol, Sun Olapiriyakul, and Navee Chiadamrong*



# Comparison of Keyword Etraction Methods for Crowdfunding Projects Based on Web-Data

Wenting Hou<sup>1</sup> and Jian Qu<sup>2</sup>

<sup>1,2</sup>Faculty of Engineering and Technology, Panyapiwat Institute of Management, Nonthaburi, Thailand  
E-mail: 6372100134@stu.pim.ac.th, jianqu@pim.ac.th

Received: October 15, 2021 / Revised: December 17, 2021 / Accepted: December 17, 2021

**Abstract**—With the development of technology, there are more and more crowdfunding projects. However, it is hard for a human to understand such projects easily. Therefore, this study aims to provide a better solution for extracting keywords from each crowdfunding project so that everyone can quickly understand the core of these projects. In this study, we compared the performance of four keyword extraction methods on crowdfunding projects. The experimental results show that Bert performs better in precision, recall, and f-measure than NLTK, LIAAD, and Harvest algorithms. Moreover, we compared four pre-training models based on Bert and found that the distills-based-multilingual-cased-v1 model worked better than others with 74.0% in precision and 85.0% in F-measure.

In addition, we also created a corpus of 106,869 pairs of text and its keyword for keyword extraction based on crowdfunding projects.

**Index Terms**—Crowdfunding Projects, Web-data, Searching API, Keyword Extraction, Bert Model

## I. INTRODUCTION

Why extract keywords?

In the era of the information explosion, information can be easily accessed on the internet, but humans cannot easily understand most of them. We need to

extract some information that we are interested in. We can employ keyword extraction for such tasks. The extraction of keywords can also be called text label extraction. For example, “today’s roast pork is really good”, the word in the text “roast pork” can be considered a keyword or a label of this sentence. This keyword can express the meaning of the sentence to a certain extent. For example, if the word “roast pork” is used in a text classification task, it can imply information with the category of “food”. There are normally two groups of methods for such keyword extraction: supervised and unsupervised methods. The supervised approach can achieve high accuracy, but the disadvantage is that it requires many labeled data and high labor costs. Compared with the supervised methods, the unsupervised methods have lower data requirements. Therefore, the application of such a method in the field of keyword extraction is more popular. In this study, we compare some of the common unsupervised keyword extraction algorithms, namely NLTK, Harvest, LIAAD, and a supervised method, namely Bert.

Why extract keywords from crowdfunding projects?

We found the failure rate of crowdfunding projects in 2015<sup>1</sup>, 2017<sup>2</sup>, 2019<sup>3</sup>, 2020<sup>4</sup>, and 2021<sup>5</sup>, and we compared the failure rate of 2015, 2017, 2019, and 2021, as shown in Fig.1. From Fig.1 we can see that the failure rate of crowdfunding projects is high and has been rising except 2021.

<sup>1</sup><https://www.weiyangx.com/122711.html>

<sup>2</sup><https://zhuanlan.zhihu.com/p/32325090>

<sup>3</sup><https://medium.com/@daniel.kupka>

<sup>4</sup><https://www.amz123.com/thread-348221.htm>

<sup>5</sup><https://www.kickstarter.com/help/stats>

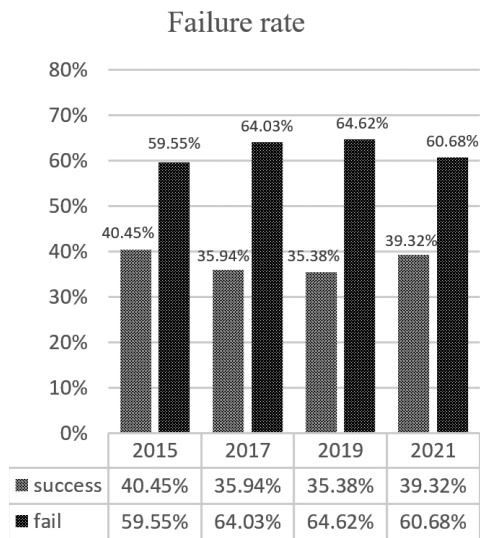


Fig. 1. Failure rate of crowdfunding projects

There are two reasons for the decline in the failure rate in 2021. Firstly, there were fewer crowdfunding projects this year, as shown in Table I. Although Kickstarter only displays all the data since its establishment in 2009, we can calculate that there were only 73,068 projects published in 2021 and there were 92,518 projects published in 2020. There was a 21% reduction in the number of projects published. Secondly, the failure rate in 2021 was updated on December 2, 2021, missing a month. These two reasons lead to the decline in the failure rate in 2021.

TABLE I  
COMPARISON OF NUMBER OF PROJECTS PUBLISHED IN 2020  
AND 2021

List	2009-2019	2009-2020	2009-2021	2020	2021
Number of projects published	378000	470518	543586	92518	73068
Number of successful projects	133724	175169	212713	41445	37544

Since the high failure rate of crowdfunding projects, so we wanted to use keyword extraction to understand the main content of the project, which can be used to determine the feasibility of the project further. For example, the Fontus project claimed that it is a self-filling water bottle, especially designed to fit your bicycle. This water bottle will refill itself as you ride on your bike. It can create 0.5 liters of water per hour out of solar power and air. This device was designed to capture the moisture content in the air, condense it and store it as safe drinking water. The air stream you generate while riding is used here in place of a fan to pass large amounts of air into the chambers without needing extra energy sources. If you look at how the Fontus bottle advertises its ability to absorb water

from the air, it seems logical to the layman. The Fontus bottle claims to be a small dehumidifier: it sucks air into the bottle and condenses to trap moisture when the air cools, using small solar panels to power the process. We all know how dehumidifiers work, so it seems simple enough. However, to produce 0.5 liters of water in 1 hour as Fontus claims, a 250-watt solar panel with a surface area of 1.5 square meters is required to operate at 100% efficiency! This is a huge, rooftop-sized solar panel--definitely not the small panel that Fontus is equipped with. It is less than 1/6 of the required panel size. Secondly, condensing moisture from humidity into water requires 9000 BTU/gal, if the air is already at the dewpoint, 100% humidity. 0.5 liters of water requires 1195 BTU to condense. If this water bottle was the efficient of a central air conditioner, this would use 92 watt-hrs of electricity. But Peltier solid-state cooling is like 10th the efficiency of air conditioning systems, so Fontus bottle needs about one kilowatt-hr. to make 0.5 liters of water in 100% humidity conditions. Although Fontus is equipped with a 250-watt solar panel, it would need four hours of work. This is a pretty huge contrast to the 0.5 liters per hour. In summary, this water bottle sounds logical but technically impossible.

Now, the product seems to have died, pitting many investors. It is because we do not know enough to see that Fontus does not have technical support to deliver the product. If we get the "self-filling water bottle" keyword extracted from the web data, we can quickly know the project. If we get the "produce 0.5 liters of water in 1 hour" keyword extracted from the web data, we can use it to search for feasibility on the Internet. Therefore, keyword extraction on crowdfunding projects is very important, due to such keywords might provide a better understanding of the project.

This is a relatively frontier research, we focus on keyword extraction and contradiction detection on crowdfunding projects. Most research on fake information is focused on fake news from social media, and research on fake crowdfunding projects is limited. So we decided to explore this direction, we thought that this innovative research will be more popular on crowdfunding platforms. This study is only the first step, the first step is the comparison of keyword extraction on crowdfunding projects, and the next step is the knowledge extraction to identify possible fake projects.

## II. RELATED STUDIES

There are many methods for extracting keywords, roughly divided into the following three categories: statistical-based methods, graph-based methods, and semantic model-based methods. The statistical methods which we will explain include Term-Frequency (TF), Term Frequency-Inverse Document Frequency (TFIDF), Natural Language Toolkit (NLTK) [1] and

Yet Another Keyword Extractor (YAKE). Term-Frequency (TF) is the simplest method, which calculates the score by the frequency of words in the document. The main problem with word frequency is that it does not consider structural and semantic information and cannot distinguish synonyms. TFIDF is a simple but effective method proposed by Salton [2] in 1988, and it calculates each term in a text by considering two factors: one is the term's word frequency in the document, i.e., TF, and another is the Inverse Document Frequency (IDF), which measures how many texts contain the term. IDF is mainly used to penalize those terms that appear in many texts, and these terms are usually some irrelevant deactivation words, etc. The whole core idea of TFIDF [3] is that the importance of a term in a document depends on the frequency of the term in the document and the number of occurrences in other documents. However, the TFIDF algorithm also has obvious drawbacks. It is not comprehensive enough to measure the importance of a word by its frequency simply, and sometimes the important words may not appear many times [4]. NLTK is a well-known natural language processing library for Python [5], which comes with classification, word separation and other functions. In this study, we combined RAKE and NLTK to form RAKE-NLTK, it achieved 62.4% of F-measure based on the GMB corpora [1]. If applied to crowdfunding project, the results might be different. Harvest Text [6] is a library that focuses on unsupervised (weak) methods and can integrate domain knowledge (e.g., types, aliases) for simple and efficient processing and analysis of a domain-specific text. It has many features such as text cleaning, new word discovery, sentiment analysis, entity recognition linking, keyword extraction, knowledge extraction, syntactic analysis, etc. David Gotz et al. [7] presented an intelligent visual analytic system called Harvest, which was designed to empower everyday business users to derive insight from large amounts of data. They found that there was a 75% reduction in error rate on average. When a task was performed using Many Eyes, it achieved 22% of error rate; when a task was performed using HARVEST, it achieved 5.6% of error rate. They attributed the sharp drop in error rate to Harvest's ability that can let users easily explore data from different angles. Yet Another Keyword Extractor (YAKE) is an unsupervised keyword extraction algorithm[8]. It relies on statistical features of text extracted from a single document to select the most important keywords in the text. Ricardo Campos et al. [9] proposed YAKE to extract keywords from single documents, and compared it with RAKE, TextRank, SingleRank and TFIDF. Based on the Schutz2008 database, YAKE achieved 9.1% of F-measure, TextRank achieved 8.2% of F-measure, TFIDF achieved 4.3% of F-measure, SingleRank achieved 3.7% of F-measure, RAKE achieved 0.6% of

F-measure. So, YAKE performed better. The core idea of the statistical-based approach is to calculate the score of each word or phrase in the text, and it is possible that all words can be sorted with the scores, then the top n words with the highest scores are obtained as the keywords of the text [10]. The statistical features include co-occurrence frequency, symmetric conditional probability, modified association measure, chi-square, mean distance, length similarity, and word frequency. In medical or biological fields, many information extraction systems and studies rely on a certain corpus. Qu et al. [11] proposed a new approach to address English medical OOV terms. Unlike most existing methods for translating English OOV terms into Chinese, their candidates are selected by a machine learning system with the support of different features, and the best candidate selection results in the highest correct rate of 86.79% using features such as lift, frequency, and distance together. This suggests we may employ more features to find a better keyword.

Secondly, the Graph-Based Approaches include PageRank [12], TextRank, SingleRank, TopicRank, and PositionRank. PageRank was first used to calculate the importance of web pages, and TextRank is a graph-based ranking algorithm for text [13]. The basic idea is derived from Google's Page Rank algorithm, which automatically extracts many meaningful words or phrases from a given text. The original text is split into sentences. In each sentence, deactivated words are filtered out, and only words of the specified lexical nature are retained. It results in a collection of sentences and a collection of words [14]. TopicRank treats topics as clusters of similar key phrases [15], which are ranked according to their importance in the document, then top n most relevant topics are selected, and each topic selects one most important key phrase to represent the core keywords of the document.

Thirdly, Semantic Models include Linear Discriminant Analysis (LDA) [16], Hidden Markov Model (HMM) [17], Recurrent Neural Networks (RNN), and Bidirectional Encoder Representations from Transformers (Bert), etc. The keyword or phrase extraction based on semantic models is generally supervised learning. It treats keyword extraction as an annotation task to determine whether the word is a keyword or not; or after classifying the text, it automatically learns the weight score of each word in the text based on the attention layer, and extracts keywords according to the score. These methods are all supervised learning and require labeled data for training the model. Zhang et al. [18] proposed a 2-layer RNN model that treats keyword and key phrase extraction as an annotation classification task to determine whether each word is a keyword or a key phrase. The first layer of the model is used for the keyword recognition task, and the second layer is

used for the key phrase recognition task. Fusion weights the loss functions of two tasks as the final loss function. The proposed RNN model achieved 80.97% of F-measure on automatically extracting keyphrases from single tweets. BERT is a pre-trained language model, and the full name is Bidirectional Encoder Representations from Transformer. It means that it is a bidirectional encoder representation based on Transformer [19]. As the name suggests, Bert uses the Transformer. It can take the word that precedes and follows it into account while processing a word to get its meaning in the context. We know that Transformer’s attention mechanism has a good effect on feature extraction of words in context. Overall, the Bert model uses the popular feature extractor Transformer and implements a bi-directional language model, giving it good performance. Yili Qian et al. [20] proposed a

text keyword extraction method based on Bert, and compared it with TFIDF, TextRank, and LDA. Based on 300 scientific papers downloaded from Wanfang database, TFIDF achieved 36.4% of F-measure, TextRank achieved 40.7% of F-measure, LDA achieved 42.0% of F-measure, a keyword extraction algorithm based on Bert and multi class feature fusion achieved 43.6% of F-measure. The results show that the combination algorithm based on Bert is better than the single extraction algorithm. However, there is still room for improvement. For example, Bert uses the original Transformer. Although it is powerful, now there are some more powerful and improved versions; another place left to be improved is the Mask mechanism of Bert, which can be used to train the Bidirectional language model, but this will lead to inconsistency between pre-training and fine-tuning on downstream tasks.



Fig. 2. The overall flow chart of the study

input	url	title	summary
"Star Citizen"	robertsspaceindustries.com/	... Space Industries   Follow the development of Star C...	查看此网页的中文翻译, 请点击 翻译此页 Roberts Space Industries is the official go-to website for all news about Star Citizen and Squadron 42. It also hosts the online store for game items...
	starcitizen.mmos.com/	Home Page : Star Citizen	查看此网页的中文翻译, 请点击 翻译此页 Star Citizen is a space trading and combat sim. It will run on windows and linux. It was 100% crowd funded on
	starcitizen.howar31.com/	首頁   Star Citizen - 星際公民中文社群網	這裡是 Star Citizen 星際公民 中文社群網, 在這裡將會提供星際入門指南、民生與軍用品介紹、船艦交通工具展示、UEE地球聯合帝國最新消
	fanyi.baidu.com	star citizen - 百度翻译	star citizen 英[stɑ:(r) 'sɪtɪzn] 美[stɑ:r 'sɪtɪzn] 网络 星际公民; [例句]But as of early November, the focus had shifted to issues such as the move by Gong Li, the film star, to become a Singaporean citizen. 但到11月初, 焦点转移到了影星成为新加坡公民之类的问题上。
	豆瓣	星际公民 Star Citizen (豆瓣)	2019年2月16日 Star Citizen 星际公民的视频, 攻略, 评测, 图片, 评分, 讨论, 帮助你判断是否好玩, 发现更多相似好玩游戏及爱玩这些游戏的
	starcitizen.jeuxonline.info/	Star Citizen	Star Citizen : mise à jour Alpha 3.10 et accès gratuit Jusqu'au 23 septembre Star Citizen 12 septembre 42 Après
	www.vxbao.com/game/558...html	星际公民Star Citizen中文版下载_星际公民Star	2017年5月20日 《StarCitizen中文版》(星际公民)是一款模拟经营游戏, 它除了一款PC平台的星际游戏之外, 它更是一个深化, 一个众筹神话。
	starcitizen.wikia.com/	Star Citizen Wiki   Fandom	Agents of Mayhem • Battalion 1944 • Battleborn • Battlefield • Borderlands • Brothers in Arms • Bulletstorm
	知乎	如何评价太空游戏新作《星际公民》(Star	2018年4月20日 而这就是《Star Citizen》最大的问题: 大把的精力花在飞船设计上。做几个土豪版飞船看得见摸得着, 群众喜闻乐见, 还能
	www.kickstarter.com/projects/c...	Star Citizen by Cloud Imperium Games	Cloud Imperium Games Corporation 正在 Kickstarter 上为 Star Citizen 筹款! Reclaim the stars in the exciting new Space

Fig. 3. Example of snippet retrieval

### III. OUR APPROACH

In this section, we describe our approach, and it has two major steps: information retrieval and keyword extraction, as shown in Fig. 2. Next, we introduce the information retrieval and the keyword extraction.

#### A. Information Retrieval

We found a list of the highest-funded crowdfunding projects on Wikipedia<sup>1</sup>. With the data from Wikipedia, we used the Internet to retrieve information. The first step is snippet retrieval of the project. We separated the retrieved snippet into three different fields in the database: URL, title, and summary. Moreover, input is the project's name, as shown in Fig. 3.

The name of the crowdfunding projects may be ambiguous, thus the retrieved information may not be related to the project. For example, we search for the "EOS" project, and there may be a person or a song called "EOS". Therefore, we need to find an efficient way for making our query text less ambiguous. There are four ways of constructing the query text: searching the name of the project, searching the name of the project and its category, searching the name of the project and its crowdfunding platform, and searching the name of the project plus category plus crowdfunding platform, as shown in Table II. We compare A to the name of the project, B to the category of the project, C to the crowdfunding platform of the project.

TABLE II  
FOUR DIFFERENT SEARCH METHODS

Search Method	Instance	Shortening
"name+category"	"Star Citizen+电子游戏"	"A+B"
"name"	"Star Citizen"	"A"
"name+category+platform"	"Star Citizen+电子游戏+Kickstarter"	"A+B+C"
"name+platform"	"Star Citizen+Kickstarter"	"A+C"

**Note:** A = name of the project itself, B=category of the project, C = crowdfunding platform of the project

We conducted a test to find out which search method is better. We searched the first 20 projects of the list of highest-funded crowdfunding projects on Wikipedia. Each project intercepted ten snippets, 20 projects intercepted 200 snippets. The feedback snippets of each search method are different, So we got 800 different snippets in total. We used 800 snippets to compare the effective ratios in these four search methods. We judged the correctness of each snippet. When the input is "A", the number of correct snippets is 143, the effective ratio is 71.5%; And when the

input is "A+B", the number of correct snippets is 180, the effective ratio is 90%; When the input is "A+C", the number of correct snippets is 115, the effective ratio is 57.5%; And when the input is "A+B+C", the number of correct snippets is 129, the effective ratio is 64.5%. By calculating 800 snippets, we found that searching the name of the project and its category to retrieve snippets is the most efficient and least intrusive way of constructing the query text. The effective ratio is arranged from high to low, as shown in Table III.

TABLE III  
EFFECTIVE RATIOS OF DIFFERENT INPUT  
OF SNIPPET RETRIEVAL

Input	Number of Valid Snippets	Effective Ratio
"A+B"	180	90%
"A"	143	71.5%
"A+B+C"	129	64.5%
"A+C"	115	57.5%

In summary, this study selected the input "A+B" for Internet snippet retrieval. We set up a programmable search engine by calling the API. We changed the region, language, and website in the basic setting of the programmable search engine. The region is set to all regions, which returns more contents; the language is set to simplified Chinese, because this study is more concerned with extracting Chinese characters. The websites to be searched are shown in Table IV. These ten websites often appeared when we searched project information manually.

TABLE IV  
LIST OF WEBSITES

Number	Website
1	http://www.doc88.com
2	sogou.com
3	weibo.com
4	www.zhihu
5	www.bing.com
6	www.csdn.net
7	www.sohu.com
8	https://zol.com.cn
9	www.baidu.com
10	www.google.com

Then we used MySQL to create a database and created a table containing ID, Keyword, URL, Title, Summary. Next, we employed Google Search API to retrieve information automatically, and such information was saved into the database.

<sup>1</sup>[https://en.wikipedia.org/wiki/List\\_of\\_highest-funded\\_crowdfunding\\_projects](https://en.wikipedia.org/wiki/List_of_highest-funded_crowdfunding_projects) (last accessed on 1 October 2021)

B. Keyword Extraction

We reviewed papers to find seven best keyword extraction methods. Of these seven methods, only four perform well in Chinese. These four methods are NLTK, LIAAD, Harvest, and Bert. Among these four methods, there is only one supervised method called Bert. So we make up for this shortcoming by comparing four models based on Bert.

Firstly, we compared NLTK, LIAAD, Harvest, and Bert using three different types of documents. Although we limited the language to simplified Chinese, there were still English results. “testen” is a pure English document; “testch” is a pure Chinese document; the “test” document is half Chinese and half English. The results show that the Bert model is better, and the selected candidates are closer to the document’s meaning, as shown in Table V.

TABLE V  
DIFFERENT METHODS FOR EXTRACTING KEYWORDS

	Testen	Testch	Test
Original text	The iBackPack has the capability to hold all of your electronics. There is an optional built-in WiFi connection and batteries galore. It includes a 20,000 mAh primary, 8,000 mAh secondary, and a half a dozen other batteries that ensure your electronics are constantly charged.	兵马俑，即秦始皇兵马俑，亦简称秦兵马俑或秦俑，第一批全国重点文物保护单位，第一批中国世界遗产，位于今陕西省西安市临潼区。兵马俑是古代墓葬雕塑的一个类别。古代实行人殉，奴隶是奴隶主生前的附属品，奴隶主死后奴隶要作为殉葬品为奴隶主陪葬。兵马俑即制成兵马（战车、战马、士兵）形状的殉葬品。	基于广受赞誉的 Stellaris PC 游戏，Stellaris Infinite Legacy 提供了您喜欢的 4x 棋盘游戏，其中包括个性化的定制内容和突如其来的故事，使 Stellaris PC 游戏与众不同。Stellaris Infinite Legacy 是一款可供 2 至 4 名玩家使用的 2 小时 4x 棋盘游戏，其简单规则会根据您在游戏中的选择而增长
NLTK	‘000 mah secondary’, ‘000 mah primary’, ‘wifi connection’, ‘optional built’, ‘constantly charged’	‘士兵（形状的殉葬品）’, ‘兵马俑即制成兵马’战车’, ‘第一批全国重点文物保护单位’, ‘第一批中国世界遗产’, ‘战马’	‘stellaris infinite legacy 是一款可供 2 至 4 名玩家使用的 2 小时 4x 棋盘游戏’, ‘stellaris infinite legacy 提供了您喜欢的 4x 棋盘游戏’, ‘基于广受赞誉的 stellaris pc 游戏’, ‘使 stellaris pc 游戏与众不同’, ‘其简单规则会根据您在游戏中的选择而增长’
Harvest	/	‘兵马俑’, ‘奴隶主’, ‘殉葬品’, ‘奴隶’, ‘临潼区’	‘游戏’, ‘棋盘’, ‘赞誉’, ‘玩家’, ‘个性化’ ‘基于广受赞誉的 stellaris’,
Bert	‘dozen’, ‘electronics’, ‘batteries’, ‘20’, ‘wifi’	‘第一批中国世界遗产’, ‘第一批全国重点文物保护单位’, ‘奴隶主死后奴隶要作为殉葬品为奴隶主陪葬’, ‘兵马俑是古代墓葬雕塑的一个类别’, ‘奴隶是奴隶主生前的附属品’	‘其简单规则会根据您在游戏中的选择而增长’, ‘其中包括个性化的定制内容和突如其来的故事’, ‘legacy 提供了您喜欢的 4x 棋盘游戏’, ‘legacy 是一款可供 2 至 4 名玩家使用的 2 小时 4x 棋盘游戏’
LIAAD	‘the’, ‘your’, ‘electronics’, ‘ibackpack’, ‘has’	‘兵马俑，即秦始皇兵马俑，亦简称秦兵马俑或秦俑，第一批全国重点文物保护单位，第一批中国世界遗产，位于今陕西省西安市临潼区。兵马俑是古代墓葬雕塑的一个类别。古代实行人殉，奴隶是奴隶主生前的附属品，奴隶主死后奴隶要作为殉葬品为奴隶主陪葬。兵马俑即制成兵马（战车、战马、士兵）形状的殉葬品’	‘stellaris’, ‘infinite’, ‘legacy’, ‘名玩家使用的’, ‘棋盘游戏，其简单规则会根据您在游戏中的选择而增长’,

However, individual cases do not represent the whole, and we will use more data to determine whether the Bert model is the most suitable method for this study. Next, we will explain to you the four methods we compared.

1) NLTK

NLTK is a natural language processing library for Python. A virtual example is shown in Table VI.

TABLE VI  
A VIRTUAL EXAMPLE OF NLTK

Original text	兵马俑，即秦始皇兵马俑，亦简称秦兵马俑或秦俑，是第一批全国重点文物保护单位
Input	C1C2C3P1C4C5C6C7C8C9C10P2C11C12C13C14C15C16C17C18C19C20P3C21C22C23C24C25C26C27C28C29C30C31C32C33C34
Output	C21C22C23C24C25C26C27C28C29C30C31C32C33C34, C4C5C6C7C8C9C10
Answer	是第一批全国重点文物保护单位 即秦始皇兵马俑

### 2) LIAAD

Yake is a lightweight unsupervised automatic keyword extraction method mentioned. A virtual example is shown in Table VII.

TABLE VII  
A VIRTUAL EXAMPLE OF LIAAD

Original Text	兵马俑，即秦始皇兵马俑，亦简称秦兵马俑或秦俑，是第一批全国重点文物保护单位
Input	C1C2C3P1C4C5C6C7C8C9C10P2C11C12C13C14C15C16C17C18C19C20P3C21C22C23C24C25C26C27C28C29C30C31C32C33C34
Output	C1C2C3P1C4C5C6C7C8C9C10P2C11C12C13C14C15C16C17C18C19C20P3C21C22C23C24C25C26C27C28C29C30C31C32C33C34
Answer	兵马俑，即秦始皇兵马俑，亦简称秦兵马俑或秦俑，是第一批全国重点文物保护单位

### 3) Harvest

HarvestText has many features such as keyword extraction, knowledge extraction, etc. In this study, we used it to obtain keywords in the text based on algorithms such as Textrank, tfidf, etc., using JIEBA for word separation and TFIDF for extraction. A virtual example is shown in Table VIII.

TABLE VIII  
A VIRTUAL EXAMPLE OF HARVEST

Original Text	兵马俑，即秦始皇兵马俑，亦简称秦兵马俑或秦俑，是第一批全国重点文物保护单位
Input	C1C2C3P1C4C5C6C7C8C9C10P2C11C12C13C14C15C16C17C18C19C20P3C21C22C23C24C25C26C27C28C29C30C31C32C33C34
Output	C1C2C3, C14C15C16C17
Answer	兵马俑 秦兵马俑

### 4) Bert

BERT is a pre-trained language model mentioned. In this study, we used it for keyword extraction. A virtual example is shown in Table IX.

TABLE IX  
A VIRTUAL EXAMPLE OF BERT

Original Text	兵马俑，即秦始皇兵马俑，亦简称秦兵马俑或秦俑，是第一批全国重点文物保护单位
Input	C1C2C3P1C4C5C6C7C8C9C10P2C11C12C13C14C15C16C17C18C19C20P3C21C22C23C24C25C26C27C28C29C30C31C32C33C34
Output	C21C22C23C24C25C26C27C28C29C30C31C32C33C34, C1C2C3
Answer	是第一批全国重点文物保护单位 兵马俑

Secondly, we compared four pre-trained models based on Bert for keyword extraction. Assuming that the most similar candidate to the document is a good keyword/keyphrase representing the document, converting the document and the candidate into a vector, we used the cosine similarity between the vectors to calculate the similarity between the candidate and the document. The top five most similar candidates of the document are used as the resultant keywords, as shown in the Table X. M1=quora-distilbert-multilingual, M2=distilbert-base-nli-mean-tokens, M3=distiluse-base-multilingual-cased-v1, M4=distiluse-base-multilingual-cased-v2. After comparison, we found that the M2 worked better, showing excellent performance in the similarity task. We applied the comparison to the large-scale data in an attempt to draw a conclusion that was not individual cases. We searched all 120 projects to generate 5340 snippets. For these 5340 snippets, we used four models based on Bert to generate 64,044 keywords, such information was saved into the database, as shown in Fig. 4. These 64,044 keywords are the large-scale data for further research.

TABLE X  
KEYWORD EXTRACTION UNDER DIFFERENT MODELS BASED ON BERT

Model	Top 5	Characteristic
Human results	‘兵马俑’， ‘亦简称秦兵马俑或秦俑’， ‘第一批中国世界遗产’， ‘第一批全国重点文物保护单位’， ‘兵马俑是古代墓葬雕塑的一个类别’	
M1	‘兵马俑即制成兵马’， ‘兵马俑是古代墓葬雕塑的一个类别’， ‘形状的殉葬品’， ‘古代实行人殉’， ‘奴隶主死后奴隶要作为殉葬品为奴隶主陪葬’	Use parallel data in more than 50 languages and fine-tune
M2	‘第一批中国世界遗产’， ‘第一批全国重点文物保护单位’， ‘奴隶主死后奴隶要作为殉葬品为奴隶主陪葬’， ‘兵马俑是古代墓葬雕塑的一个类别’， ‘奴隶是奴隶主生前的附属品’	STSB performance: 85.16

TABLE X  
KEYWORD EXTRACTION UNDER DIFFERENT MODELS BASED ON BERT (CON.)

Model	Top 5	Characteristic
M3	‘亦简称秦兵马俑或秦俑’， ‘兵马俑’， ‘兵马俑即制成兵马俑’， ‘即秦始皇兵马俑’， ‘兵马俑是古代墓葬雕塑的一个类别’	Support 15 languages
M4	‘第一批中国世界遗产’， ‘奴隶是奴隶主生前的附属品’， ‘亦简称秦兵马俑或秦俑’， ‘奴隶主死后奴隶要作为殉葬品为奴隶主陪葬’， ‘兵马俑是古代墓葬雕塑的一个类别’	Support more than 50 languages

input	summaryID	summary	kw1	kw2	kw3	kw4
Star Citizen + 电子游戏	1	(You can download and play Star Citizen Alpha 3....	电子游戏	download	alpha	alpha
Star Citizen + 电子游戏	1	(You can download and play Star Citizen Alpha 3....	会公示有助于你了解公共主页用途的信息	会公示有助于你了解公共主页用途的信息	公共主页信息公示查看更多	公共主页信息公示查看更多
Star Citizen + 电子游戏	1	(You can download and play Star Citizen Alpha 3....	download	facebook	会公示有助于你了解公共主页用途的信息	会公示有助于你了解公共主页用途的信息
Star Citizen + 电子游戏	2	(RSI's Spectrum is our integrated community and p...	rsi	integration	community	community
Star Citizen + 电子游戏	2	(RSI's Spectrum is our integrated community and p...	game	interaction	integrated	integrated
Star Citizen + 电子游戏	2	(RSI's Spectrum is our integrated community and p...	spectrum	forums	integration	integration
Star Citizen + 电子游戏	3	(电子游戏. Satisfactory. 电子游戏. 这个公共主页赞了. IGN. 公共主页发布的...	这个公共主页赞了	这个公共主页赞了	这个公共主页赞了	电子游戏
Star Citizen + 电子游戏	3	(电子游戏. Satisfactory. 电子游戏. 这个公共主页赞了. IGN. 公共主页发布的...	4月30日20	公共主页发布的近期帖子	公共主页发布的近期帖子	war
Star Citizen + 电子游戏	3	(电子游戏. Satisfactory. 电子游戏. 这个公共主页赞了. IGN. 公共主页发布的...	公共主页发布的近期帖子	4月30日20	电子游戏	公共主页发布的近期帖子
Star Citizen + 电子游戏	4	(《星际公民》(英文: Star Citizen) 是已经在 Microsoft Windows和Lin...	星际公民	也有正在开发中的单人	星际公民	星际公民
Star Citizen + 电子游戏	4	(《星际公民》(英文: Star Citizen) 是已经在 Microsoft Windows和Lin...	windows和linux公开的太空模拟电子游戏	星际公民是一个mmorpg游戏	windows和linux公开的太空模拟电子游戏	星际公民是一个mmorpg游戏
Star Citizen + 电子游戏	4	(《星际公民》(英文: Star Citizen) 是已经在 Microsoft Windows和Lin...	星际公民是一个mmorpg游戏	windows和linux公开的太空模拟电子游戏	星际公民是一个mmorpg游戏	windows和linux公开的太空模拟电子游戏

Fig. 4. Example of different keywords extracted by four models based on Bert in database

#### IV. RESULTS AND DISCUSSION

In this section, as shown in Fig.5, we describe the results of information retrieval and keyword extraction.

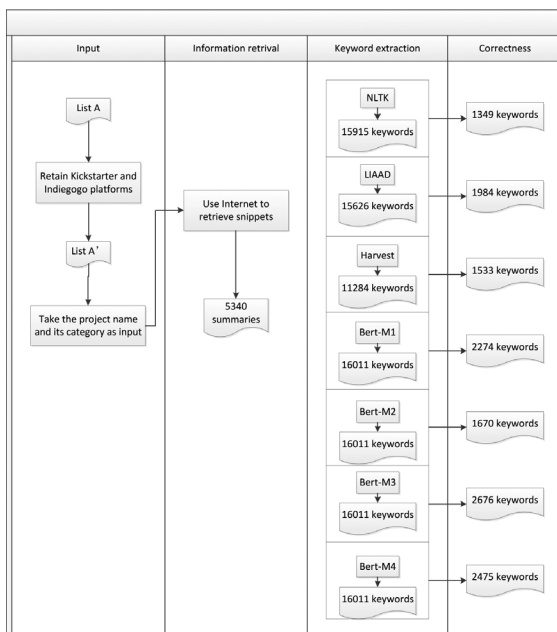


Fig. 5. The overall flow chart of the project with results

#### A. Data Source

This study used two datasets: List A, List A'. List A is the original dataset on Wikipedia, which is a list of the highest-funded crowdfunding projects (including those that failed to receive funding), and List A' is a list of projects from A with only Kickstarter and IndieGoGo platforms retained. In this study, we focus on the keyword extraction of the 5340 summaries retrieved from 120 projects in List A' to select a better method and model.

For these 5340 snippets, we used NLTK, LIAAD, and Harvest to generate 42,825 keywords, and used four models based on Bert to generate another set of 64,044 keywords. We hired five master students to help us mark the correctness of these keywords. Finally, we created a corpus to storage those tagged 106,869 pairs of text and its keyword for keyword extraction based on crowdfunding projects.

#### B. Method Comparison

After the keyword extraction, the next step is evaluation. The project-related keywords will be selected from all the keywords extracted. Different methods resulted in 58836 keywords. We artificially marked correctness to derive the precision, recall, and F-measure of each method in the field of crowdfunding projects.



TABLE XI  
TOTAL NUMBER OF KEYWORDS IN DIFFERENT METHODS

Method	Total Number of Keywords	Correctness
NLTK	15915	1349
LIAAD	15626	1984
Harvest	11284	1533
Bert	16011	2676

There are 120 projects. Each project retrieves 100 summaries, sometimes less than 100, and ends up with 5340. We took 5340 summaries as input, and set the number of keywords extracted to 3 for each method. Thus, NLTK got 15915 keywords, LIAAD got 15626 keywords, Harvest got 11284 keywords, and Bert got 16011 keywords. As shown in Table XI, Harvest extracts the least keywords because it is based on the jieba-tfidf algorithm for keyword extraction, while JIEBA is only applicable to only Chinese word separation<sup>1</sup>, so the difference between the Harvest and other methods is as high as four thousand, but the content of this study focuses on Chinese content, so we only consider the precision rate, recall rate, and F-measure.

As shown in Table XII, the results show that the Bert model works better because the selected candidates are closer to the document's meaning.

TABLE XII  
COMPARISON OF DIFFERENT METHODS

Method	Total Number of Keywords	Effective number	Precision	Recall	F-measure
NLTK	15915	1349	8.5%	1	15.6%
LIAAD	15626	1984	12.7%	1	22.5%
Harvest	11284	1533	13.6%	1	23.9%
Bert(V1)	16011	2676	16.7%	1	28.6%

From Fig. 6 we can see that NLTK has the lowest F-measure, only 15.6%. Bert has the highest F-measure, with 28.6%. It is better than the other three methods, the most important reason is that only Bert can obtain the bidirectional feature representation of the context among these four keyword extraction methods. So, Bert is the most suitable method for extracting keywords on crowdfunding projects.

Comparison of Different Methods

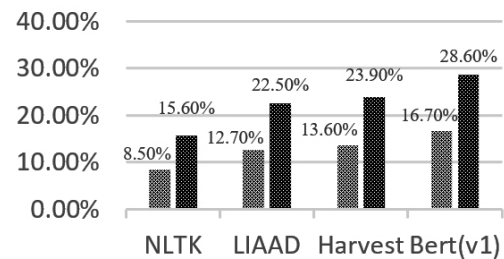


Fig. 6. Comparison of different methods

### C. Model Comparison

Next, the comparison of different models based on Bert is shown in Table XIII. Different models resulted in 64044 keywords, we marked the correctness of keywords and calculated the F-measure of each model, as shown in Table XIII. M1=quora-distilbert-multilingual, M2=distilbert-base-nli-mean-tokens, M3=distiluse-base-multilingual-cased-v1, M4=distiluse-base-multilingual-cased-v2. And "0" means incorrect, "1" means correct. From Table XIII, we can see that M3 works better.

TABLE XIII  
COMPARISON OF DIFFERENT MODELS WITH 64044 KEYWORDS

	Total Number of Keywords	1	0	Precision	Recall	F-Measure
M1	16011	2274	13737	14.2%	1	24.9%
M2	16011	1670	14341	10.4%	1	18.8%
M3	16011	2676	13335	16.7%	1	28.6%
M4	16011	2475	13536	15.5%	1	26.8%

From Fig.7 we can see that M3 has the highest F-measure of 28.6%. While M2 only has 18.8% of F-measure. Although an example shows that M2 performs better, but large-scale data shows that M3 performs well.

<sup>1</sup><https://github.com/fxsjy/jieba> (last accessed on 1 October 2021)

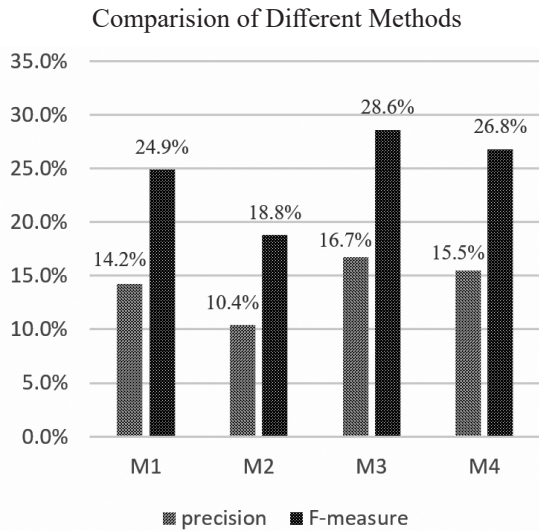


Fig. 7. Comparison of different models

In order to find out the effect of data size, we divided the number of snippets feedback into four sub-sets: TOP25, TOP50, TOP75 and TOP100. We compared the performance of Bert-M1, Bert-M2, Bert-M3 and Bert-M4 under these four sub-sets. When only the first 25 snippets were taken for each project, M3 achieved the highest F-measure of 30.0%; When the first 50 snippets were taken for each project, M3 achieved the highest F-measure of 30.1%; When the first 75 snippets were taken for each project, M3 achieved the highest F-measure of 29.1%; When the first 100 snippets were taken for each project, M3 achieved the highest F-measure of 28.6%. We found that the performance of M3 is always the best model regardless of the size of the data, as shown in Table XIV.

TABLE XIV  
COMPARISON OF DIFFERENT METHODS ON  
DIFFERENT SIZES OF DATA

Method	TOP N	TOP25	TOP50	TOP75	TOP100
NLTK	True	881	1293	1340	1349
	Total	8449	13625	15348	15915
	Precision	10.4%	9.5%	8.7%	8.5%
LIAAD	Recall	65.3%	95.8%	99.3%	100%
	F-score	<b>18.0%</b>	<b>17.3%</b>	<b>16.1%</b>	<b>15.6%</b>
	True	1283	1877	1974	1984
Harvest	Total	8382	13395	15062	15626
	Precision	15.3%	14.0%	13.1%	12.7%
	Recall	64.7%	94.6%	99.5%	100%
Bert-M1	F-score	<b>24.8%</b>	<b>24.4%</b>	<b>23.2%</b>	<b>22.5%</b>

Method	TOP N	TOP25	TOP50	TOP75	TOP100
Bert-M2	True	967	1443	1523	1533
	Total	6401	10125	11070	11284
	Precision	15.1%	14.3%	13.8%	13.6%
Bert-M3	Recall	63.1%	94.1%	99.3%	100%
	F-score	<b>24.4%</b>	<b>24.8%</b>	<b>24.2%</b>	<b>23.9%</b>
	True	1461	2121	2251	2274
Bert-M4	Total	8500	13717	15444	16011
	Precision	17.2%	15.5%	14.6%	14.2%
	Recall	64.2%	93.3%	99.0%	100%
Harvest	F-score	<b>27.1%</b>	<b>26.6%</b>	<b>25.4%</b>	<b>24.9%</b>
	True	1076	1551	1649	1670
	Total	8500	13717	15444	16011
NLTK	Precision	12.7%	11.3%	10.7%	10.4%
	Recall	64.4%	92.9%	98.7%	100%
	F-score	<b>21.2%</b>	<b>20.1%</b>	<b>19.3%</b>	<b>18.8%</b>
LIAAD	True	1674	2465	2634	2676
	Total	8500	13717	15444	16011
	Precision	19.7%	18.0%	17.1%	16.7%
Bert-M1	Recall	62.6%	92.1%	98.4%	100%
	F-score	<b>30.0%</b>	<b>30.1%</b>	<b>29.1%</b>	<b>28.6%</b>
	True	1550	2277	2439	2475
Bert-M2	Total	8500	13717	15444	16011
	Precision	18.2%	16.6%	15.8%	15.5%
	Recall	62.6%	92.0%	98.5%	100%
Bert-M3	F-score	<b>28.2%</b>	<b>28.1%</b>	<b>27.2%</b>	<b>26.8%</b>

We also compared the performance of NLTK, LIAAD and Harvest under these four sub-sets, as shown in Table XIV. From the data point of view, the smaller the TOPN, the smaller the recall rate. However, as TOPN becomes larger, the accuracy rate will also decrease under normal circumstances. So the performance can be judged by the F-measure in combination. We found TOP25 always had the highest F-measure, because the noise was minimal at this time. We can think that the higher the ranking of the snippets retrieved on the Internet, the more relevant the snippet and the project, and the higher the correct keyword extraction rate. But there are two exceptions: when the method is Bert-M3, TOP50 has the highest F-measure of 30.1%; and when the method is Harvest, TOP50 has the highest F-measure of 24.8%. These two methods have better anti-noise performance, because they change little with the change of TOPN.

In summary, the experimental results show that the M3 model performs best When the first 50 snippets are taken for each project.

In addition, in order to show that when the first 50 snippets are taken for each project, Bert's M3 model is the most suitable method for this study, we compared the keywords extracted by Bert with the keywords extracted by human. We computed the ratio of the edit distance to the length of max (string1, string 2). 0 means that the sequences are identical, while 1.0 means that they have nothing in common. When the ratio of the edit distance is between 0-0.6, we think that the keywords extracted by Bert are true. We used the keywords extracted manually as the ground truth, and found that F-measure was as high as 74.0%, F-measure was as high as 85.0%. The details are shown in Table XV.

TABLE XV  
COMPARISON OF KEYWORDS EXTRACTED BY  
MACHINE AND HUMAN

Human Results	M3	M3-Edit Distance	Precision	Recall	F-Measure
3192	2465	1823	74.0%	100%	85.0%

## V. CONCLUSION AND FUTURE WORK

In this research, we proposed Bert to extract keywords from crowdfunding projects, and compared it with NLTK, LIAAD and Harvest, Bert performed best. Compared with the four models based on Bert, M3 performed best. Based on 106,869 pairs of keywords, Bert's M3 model is the best keyword extraction method for crowdfunding projects. And when retrieving TOP50 snippets, M3 performed better, it achieved 85.0% of F-measure. Keyword extraction is widely used in the field of NLP. If we can accurately describe the document with a few simple keywords, we can understand whether an article is what we need by just looking at a few keywords, which will greatly improve our information acquisition efficiency.

In the future, we plan to study the effect of mixing these Bert models on the keyword extraction of crowdfunding projects. Because the five candidates selected by M3 are not all optimal in TABLE IX: it does not propose the word “第一批中国世界遗产”, while M2 does. So, we may consider a mixture of several models. For example, we may use the M3 to select the first two candidates and use the M2 to select the first three candidates, so that the combined five candidates will be more similar to the text than the candidates selected by a single model. We think selecting candidates by a mixture of different models will be more similar to the keywords that were selected by human.

## ACKNOWLEDGEMENTS

The first author conducted the experiment and drafted the manuscript. The last author guided and advised the experiment and co-drafted the manuscript. The first and second authors contribute 50% equally to this work.

## REFERENCES

- [1] X. Schmitt, S. Kubler, J. Robert et al., "A replicable comparison study of NER software: StanfordNLP, NLTK, OpenNLP, SpaCy, Gate," in *Proc. 2019 Sixth International Conference on Social Networks Analysis, Management and Security*, 2019, pp. 338-343.
- [2] G. B. Salton and C. Buckley, "Term-Weighting Approaches In Automatic Text Retrieval," *Information Processing and Management*, vol. 24, no. 5, pp. 513-523, Jan. 1988.
- [3] T. Joachims, "A Probabilistic Analysis of the Rocchio Algorithm with TFIDF for Text Categorization," in *Proc. The 14th International Conference on Machine Learning*, 1997, pp. 143-151.
- [4] L. Huang, Y. Wu, and Q. J. C. S. Zhu, "Research and Improvement of Keyword Automatic Extraction Method," *Journal of Computer Science*, vol. 41, no. 6, pp. 204-207, Jun. 2014.
- [5] E. Loper and S. Bird, "NLTK: The Natural Language Toolkit," in *Proc. The COLING/ACL 2006 Interactive Presentation Sessions*, 2006, pp. 69-72.
- [6] C. M. Bowman, P. B. Danzig, D. R. Hardy et al., "The harvest Information Discovery and Access System," *Computer Networks and ISDN Systems*, vol. 28, no. 1-2, pp. 119-125, Dec. 1995.
- [7] D. Gotz, Z. When, J. Lu et al., "Harvest: an Intelligent Visual Analytic Tool for the Masses," in *Proc. The First International Workshop on Intelligent Visual Interfaces for Text Analysis*, 2010, pp. 1-4.
- [8] R. Campos, V. Mangaravite, A. Pasquali et al., "YAKE! Keyword Extraction from Single Documents Using Multiple Local Features," *Information Sciences*, vol. 509, pp. 257-289, Jan. 2020.
- [9] R. Campos, V. Mangaravite, A. Pasquali et al., "A Text Feature Based Automatic Keyword Extraction Method for Single Documents," in *Proc. European Conference on Information Retrieval*, 2018, pp. 684-691.
- [10] R. Campos, V. Mangaravite, A. Pasquali et al., "Yake! Collection-Independent Automatic Keyword Extractor," in *Proc. European Conference on Information Retrieval*, 2018, pp. 806-810.
- [11] J. Qu, T. Theeramunkong, C. Nattee et al., "Web Translation of English Medical OOV Terms to Chinese with Data Mining Approach," *Science and Technology Asia*, vol. 16, no. 2, pp. 26-40, Jun. 2011.
- [12] L. Page, S. Brin, R. Motwani et al., (1998, Jan. 28). *The PageRank Citation Ranking: Bringing Order to the Web*. [Online]. Available: <http://ilpubs.stanford.edu:090/422/>
- [13] R. Mihalcea and P. Tarau, "TextRank: Bringing Order into Text," in *Proc. The 2004 Conference on Empirical Methods in Natural Language Processing*, 2004, pp. 404-411.
- [14] W. Li and J. Zhao, "TextRank Algorithm by Exploiting Wikipedia for Short Text Keywords Extraction," in *Proc. 2016 3rd International Conference on Information Science and Control Engineering*, 2016, pp. 683-686.
- [15] A. Bougouin, F. Boudin, and B. Daille, "Topicrank: Graph-Based Topic Ranking for Keyphrase Extraction," in *Proc. The 6th International Joint Conference on Natural Language Processing*, 2013, pp. 543-551.
- [16] A. M. Martinez and A. C. Kak, "PCA Versus LDA," *IEEE Transactions on Pattern Analysis and Machine Intelligence*, vol. 23, no. 2, pp. 228-233, Feb. 2001.
- [17] S. Vogel, H. Ney, and C. Tillmann, "HMM-Based Word Alignment in Statistical Translation," in *Proc. The 16th International Conference on Computational Linguistics*, 1996, pp. 836-841.
- [18] Q. Zhang, Y. Wang, Y. Gong et al., "Keyphrase Extraction Using Deep Recurrent Neural Networks on Twitter," in *Proc. The 2016 Conference on Empirical Methods in Natural Language Processing*, 2016, pp. 836-845.

- [19] J. Devlin, M.W. Chang, K. Lee et al., "Bert: Pre-Training of Deep Bidirectional Transformers for Language Understanding," in *Proc. The 2019 Conference of the North American Chapter of the Association for Computational Linguistics: Human Language Technologies*, 2019, pp. 4171-4186.
- [20] Y. Qian, C. Jia, and Y. Liu, "Bert-Based Text Keyword Extraction," *Journal of Physics: Conference Series*, vol. 1992, no. 4, p. 042077, Aug. 2021.



**Wenting Hou** is currently studying for the Master of Engineering (Engineering and Technology), Panyapiwat Institute of Management, Thailand. Her research interests are natural language processing, information retrieval.



**Jian Qu** is a full-time lecturer at the Faculty of Engineering and Technology, Panyapiwat Institute of Management. He received Ph.D. with Outstanding Performance award from Japan Advanced Institute of Science and Technology, Japan, in 2013. He received B.B.A with Summa Cum Laude honors from Institute of International Studies of Ramkhamhaeng University, Thailand, in 2006, and M.S.I.T from Sirindhorn International Institute of Technology, Thammasat University, Thailand, in 2010. His research interests are natural language processing, intelligent algorithms, machine learning, machine translation, information retrieval, and image processing.

# Deep Constitutional Neural Networks based on VGG-16 Transfer Learning for Abnormalities Peeled Shrimp Classification

Tamnuwat Valeeprakhon<sup>1</sup>, Korawit Orkphol<sup>2</sup>, and Penpun Chaihuadjaroen<sup>3</sup>

<sup>1,2,3</sup>Department of Computer Engineering, Faculty of Engineering at Sriracha, Kasetsart University Sriracha Campus.

E-mail: tamnuwat@eng.src.ku.ac.th, korawit@eng.src.ku.ac.th, penpun@eng.src.ku.ac.th

Received: September 27, 2021 / Revised: October 29, 2021 / Accepted: November 10, 2021

**Abstract**—Peeled white leg shrimp is an important exports economic product of many countries within the coastal areas. In the shrimp processing, shrimps are beheaded and peeled with an automatic machine; after that, the peeled shrimps will be inspected to classify the well-peeled shrimps from the abnormal peeled shrimps. However, the inspection process is conducted in manual work, and this may result in misinterpretation and reduce the manufacturing efficiency due to exhausted humans. Nowadays, machine learning plays an important role in food industries for monitoring manufacturing quality activities. This powerful technology has made significant breakthroughs in this field and their performances greatly surpass human work. In this paper, a deep convolutional neural network based on VGG-16 transfer learning for abnormalities in peeled shrimp classification is proposed. This method makes up two of the main steps preprocessing and model network definition. The dataset preprocessing aims to prepare the provided dataset to suit our classification model by aligning images into the C shape pattern, cropping, and resizing images to meet the need of VGG-16 input layer requirement. The network model definition aims to build the classification model by considering the VGG-16 transfer learning model. This model was customized by replacing the old classification layer with our designed fully connected layers and was trained by using the best parameters conducted in the experimental process. The results obtained from our VGG-16 model achieve 98.36% of accuracy with 0.0213 seconds for classification time, and it produces better results than other comparative models.

**Index Terms**—Abnormalities Peeled Shrimp, VGG-16, Transfer learning, Image classification

## I. INTRODUCTION

White leg shrimp or *Litopenaeus Vannamei* is a type of marine shrimp that is native to South America and commonly found in the coastal regions of the Eastern Pacific Ocean from northern Mexico to northern Peru [1]. Nowadays, white leg shrimp farming is widely popular worldwide because these shrimps have a fast growth rate, good adaptability the various environmental conditions, and high consumer demands. According to a survey of global shrimp exports, shrimp frozen is the world's 137th most traded product, with a moreover total trade of \$19 billion [2].

White leg shrimp is an important export economic product of many countries such as India, Ecuador, Vietnam, Thailand, etc. [3]. The exported shrimp must be processed to preserve freshness and high quality. However, preserving the shrimp quality is very difficult because the dead shrimps will be decomposed rapidly through the Self-Autolysis process; the internal organs in the shrimp head release enzymes such as Tyrosine, Tryptophane, and Cystine. These enzymes spread to the other organs, and the external microorganisms enter the shrimps, causing the flesh color of the shrimps to turn opaque white to yellow, indicating the shrimps were degraded quality [4].

Freezing is one of the most popular shrimp processing to preserve the shrimp quality by reducing the temperature of the shrimp to below  $-18^{\circ}$  degrees, the water in the shrimp turns into ice. This process will preserve the freshness and quality better than other food processing techniques [4]. Frozen shrimp is a product that has been processed by freezing processing. It is popular in many countries because it is cheap, easy to cook, and has a variety of health benefits. The exported frozen shrimp consists of frozen whole shrimp, frozen peeled shrimp, frozen

peeled and tail-on shrimp, frozen be-headed shrimp, and frozen boiled shrimp [5].

The frozen peeled shrimp is the most popular frozen exported shrimp the processing of this frozen shrimp consists of several steps: The first step, the shrimps are washed in clear water at a temperature below 0° degrees to reduce the microorganism, the next step, these shrimp are sorted according to their size, then, these shrimps are beheaded to reduce the self-Autolysis of the chemicals in internal organs in the head of shrimp, the next step, the behead shrimps are peeled to reduce microbial contamination, then, the peeled shrimps are inspected for classifying the abnormalities of peeled shrimps and fixing them, and the last step, the peeled shrimp are frozen at a temperature below -18° degrees to preserve the quality of their shrimps [6].

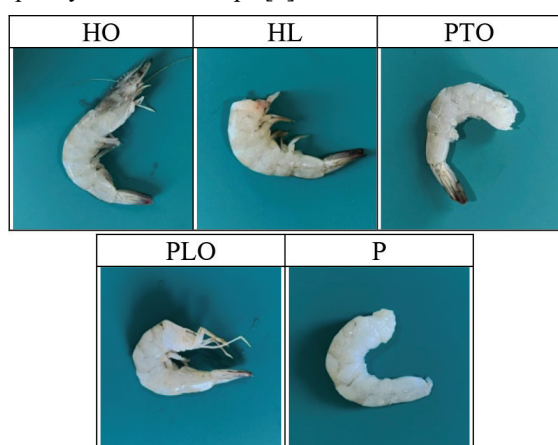


Fig. 1. The Abnormalities of peeled shrimps. Normal peeled shrimp (P) and abnormal peeled shrimp consists of: Whole or Head-on (HO), Headless (HL), Peeled tail-on (PTO), and Peeled leg-on (PLO)

The inspection process detects the abnormalities of peeled shrimps since the shrimps are peeled by a high-speed automatic machine. Sometimes, the employees will detect the abnormalities of peeled shrimps with incomplete problems consisting of four types as follows: whole or head-on (HO) is un-peeled shrimp and their head has not been cut, headless (HL) is un-peeling, but their head has been cut, peeled tail-on (PTO) is peeled shrimp but their tail has remained, and peeled leg-on (PLO) is peeled shrimp, but their leg has not been removed. An example normally (P) and the abnormalities peeled shrimp images are shown in Fig. 1. However, classification and inspection of peeled shrimps are difficult and still depend on manual work, as a consequence of misjudgments and reduce the manufacturing efficiency because exhausted humans.

Nowadays, computer vision technology plays an important role in the food industry, mainly including food safety and quality evaluation [7], food process monitoring and packaging [8], and foreign object detection [9]. This technology has more advantages

than human manual work, and this may result in increasing manufacturing efficiency and reliability and releasing humans from labor. Moreover, computer vision is becoming popular in the food industry, especially the shrimp industry. In the past few years, computer vision techniques have been applied to the field of the shrimp industry as follows: Trung Thanh N Thai proposed the a method for estimating shrimp population density and calculating the size of the shrimp based on computer vision techniques [10], R. P. Surya Sanker presented the infected shrimp with the white spot disease classification based KNN machine learning [11], Dah Jye Lee provided the method for evaluating the quality of shrimp based on image processing techniques [12], Dong Zhang proposed the method for grading shape of shrimps by using Evolution-constructed based machine learning [13], and Zihao Liu presented the method for segmenting the touching pairs of cooked shrimp in order to evaluate the quality of their shrimp [14].

The majority of the research focused on shrimp segregation, size monitoring quality control, and disease detection using image processing and machine learning techniques. However, there are no researchers on the peeled shrimp quality inspection. The automated peeled shrimp inspection is very challenging since nobody has done this before and the developed applications should outperform human efficiency. Transfer learning is a class of machine learning techniques and it is very popular in image classification tasks by using the existing knowledge to solve different problems. This powerful technology is used in many real industrial applications and it can classify the quality of a product via appearance images [15]. In order to classify the abnormalities of peeled shrimps, a transfer learning technique will become to solve this problem.

This paper proposed a deep learning method based on VGG-16 [16] transfer learning network architecture to classify the abnormalities of the peeled shrimp which consists of four types: HO, HL, PTO, and PLO. Our proposed method includes two main steps: dataset preprocessing, and definition of a training network composed of a pre-trained model, feature extraction, and the abnormalities peeled shrimp classification.

The remainder of this paper is organized as follows: The first part is aimed to introduce a statement of the problem. The second part describes the experimental setup for the white leg shrimp classification with transfer learning. In the third part, the experimental results are presented. The fourth in the art, the experimental analysis is discussed by comparing with other transfer learning and traditional supervised learning methods. Finally, the last part summarizes the paper and, future work is carried out.

## II. METHODOLOGY

Our proposed approach aims to classify the abnormalities of peeled shrimp images, and it makes up of two main steps: Data preprocessing, and VGG-16 architecture definition. Since the provided dataset was photographed with disordering and the size of image does not meet the need of the VGG-16 input layer requirement. Data preprocessing aims to prepare the provided dataset by aligning all the peeled shrimps in images into the same pattern and resizing these images to match the requirement of the VGG-16. The use of VGG-16 as transfer learning requires a classification layer customization. The VGG-16 architecture definition aims to customize the classification layer by replacing the old one with our fully connected layer architecture. Our proposed approach is presented as the following.

### A. Data Preprocessing

The dataset is obtained from the peeled shrimp images that are simulated to cover all forms of the peeled shrimp abnormalities and these images will be grouped according to their class. Each image is taken with the same focal length in the same environment and a resolution of 1,280x960 pixels.

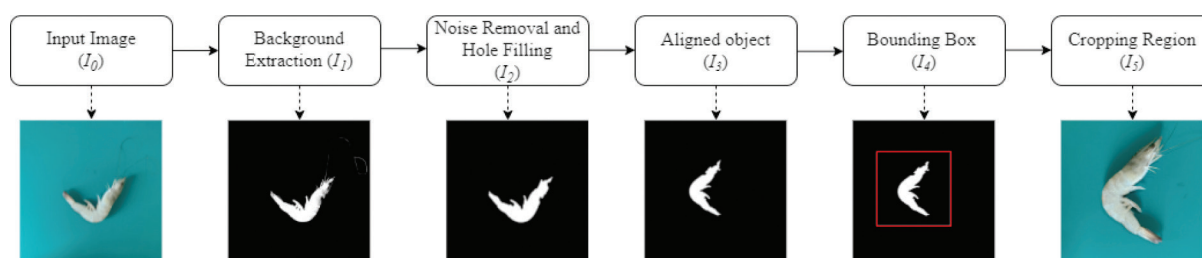


Fig. 2. Overview of the dataset preprocessing method

#### 1) Background Extraction

The segmentation-based color [17] is the powerful method for extracting the interested object from a color image by considering values of the color spaces. It is very important to select the right color space for the right jobs as they will provide a good result on extracting objects. The color spaces selection is determined by the distribution of each value of each color channel, and their value should be clearly differentiated from each others. Fig. 3 shows the distributed values of each color space of a shrimp image, and the result shows that CIELab [18] color space provides a different distribution of each channel value than other candidate color spaces i.e., HSV [19], RGB [20], YCbCr [21].

The CIELab color space is a device-independent color model. This color model is not relative to any

The VGG-16 requires a complex dataset with a specific symmetrical size of image for building a powerful classification model. However, the provided dataset is generated from disordered images, and there are no symmetrical sizes that can directly affect our classification model efficiency. To overcome these problems, aligning and resizing the image will be applied. Image alignment is a process to compute the transformation that aligns the dataset into the same pattern, and image resizing is the process to reduce the dimension of images. However, resizing the large image to a smaller size may result in a loss of quality and missing features of interesting objects in case of these objects are very smaller than the image size. Therefore, the object should be cropped with an asymmetrical size before resizing to maintain the high quality and good features of the objects.

Fig. 2 gives an overview of the data preprocessing procedure consisting of four main steps: (1) The background extraction based on color segmentation, (2) noise and hole removal using morphological operation opening follow by closing, (3) the image alignment based on skeletonization, and (4) object region identification based symmetrical bounding box calculation and cropping region.

particular devices and covers the entire range of human color perception.

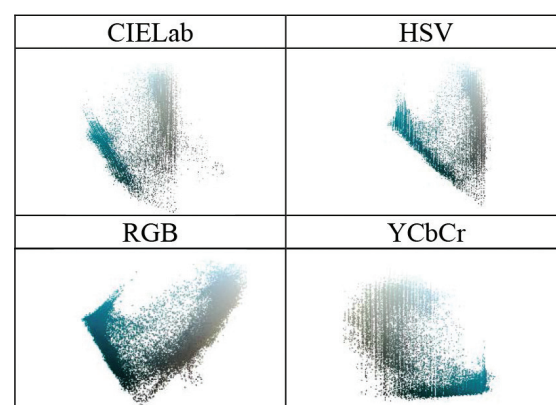


Fig. 3. The distribution values of CIELab, HSV, RGB, and YCbCr color space

Therefore, the CIELab is a useful color model in image processing to segment object jobs where L, A, and B represent Lightness, the position of color between red and green, and the position of color between yellow and blue, respectively. In this research, the CIELab color segmentation can extract the background from a shrimp object by converting input image  $I_0$  from RGB color space into the CIELab color space, then limiting the range of L to 50-100, and B to 0-127. The result of this step is a binary image, as shown in Fig. 2 with  $I_1$ .

2) Noise Removal and Hole Filling

Once the background was extracted off from the object, noises and holes are always appear over the segmented binary image. Noise is a small group of white pixels surrounded by a lake of black pixels, while a hole is a group of back pixels surrounded by white pixels of an interested object. The removal of holes and noises can be performed by using image processing techniques with morphological opening followed by closing [22]. The morphological opening operation is powerful for handling small noise by eroding an image and then dilating the eroded images, while the morphological closing operation is great for filling small holes by dilating an image and then eroding the dilated image. The result after using the opening and closing operation is shown in Fig. 4 with  $I_2$ .

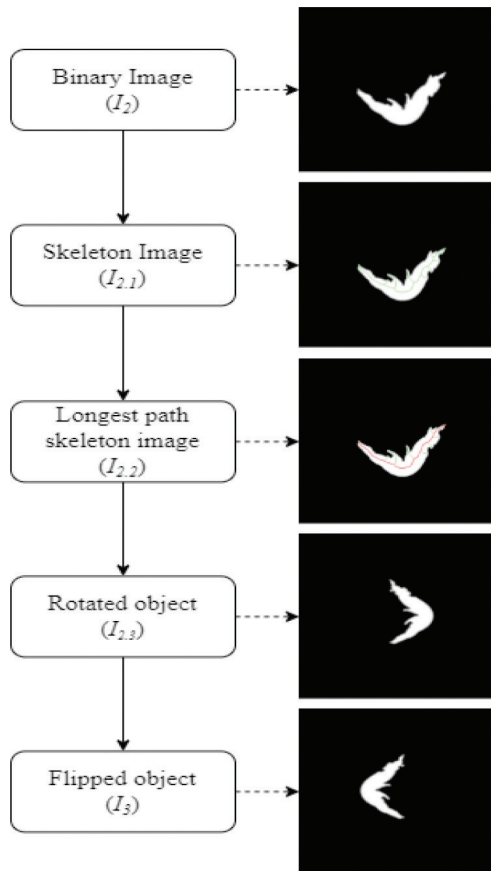


Fig. 4. Overview of object alignment method

3) Object Alignment

The binary image  $I_2$  was presented after noises and holes removing, then the object alignment will be calculated. Fig. 4 shows an overview of an object alignment procedure by considering the characteristic of a skeleton of shrimp that has a shape like the C and these shrimps will be aligned into this pattern.

The skeleton is extracted from  $I_2$  by reducing a white region in a binary image to a skeletal remnant that largely preserves the extent and connectivity of the original region. The skeleton can be expressed in terms of morphological erosions and openings [23] by using formula 1-2 and the skeletonized image is shown in Fig. 4.

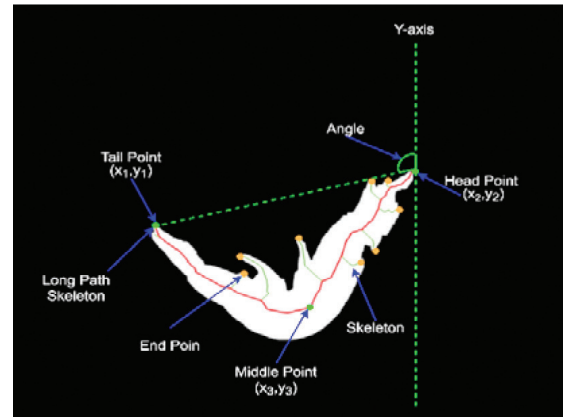


Fig. 5. Skeleton of an object represents in green color, the long path of the skeleton represents the red color and the angle of rotation represents the green angle.

The skeleton is made up of many branches connected to many paths. The C pattern will be identified by observing the longest path of the skeleton as shown in Fig. 5. The longest path is identified by finding every endpoint (The orange and green points) of the skeleton and pairing these points in order to find the length between the paired points. The longest path of the skeleton is a path between the endpoint at the head of the shrimp and the endpoint at the tail of the shrimp (The green points) where a path formed by these points provide a maximum length.

$$S(A) = \bigcup_{k=0}^K S_k(A) \tag{1}$$

$$S_k(A) = \bigcup_{k=0}^K \{(A! kB) - [(A! kB) \circ B]\} \tag{2}$$

Where B is a structure element,  $(A! kB)$  indicates k successive erosions of A, and K is the last iterative step before A erodes to an empty set.

$$\theta = \cos^{-1} \left( \frac{Y_1 - Y_2}{\sqrt{(x_1 - x_2)^2 + (Y_1 - Y_2)^2}} \right) \tag{3}$$

Where  $Y_1 = \max(y_1, y_2)$  and  $Y_2 = \min(y_1, y_2)$



The shrimp will be aligned into the C pattern by rotating this shrimp to the vertical with the Angle of Rotation (AoR). Fig. 5 shows the AoR which is the angle between the Y-axis and the line between the head point and the tail point of the shrimp, this angle is performed with formula 3, and the rotated image is shown in Fig. 4 ( $I_{2,3}$ ). However, the shrimp can be flipped on the left or right hand. If the shrimp was flipped to the right hand, it would be flipped back to the left by observing the middle point of the longest path of the skeleton. The x coordinate of this point would be less than the x coordinate of the head and tail points. The flipped image is shown in Fig. 4 ( $I_3$ ).

#### 4) Symmetrical Bounding Box Calculation and Cropping Region

The most of the images are used to train the machine learning models are symmetrical size, so the cropped images must also be symmetrical. The Bounding Box (BB) is a popular method for identifying the cropping region that fits the interested object [24] as shows in Fig. 6 with the red rectangle. However, this method is not suitable for this research because the cropped object is asymmetrical. The Symmetrical Bounding Box (SBB) is our modified of Bounding Box (BB) method to calculate the cropping region in order to crop an interested object with a symmetrical size. This method uses a list of boundary points for calculating their cropping region.

The Border Following (BF) is one of the fundamental techniques in the image processing of digitized binary images, it is used to address the boundary of object region by driving a sequence of coordinates or the chain codes from the boundary between white region and background [25]. Once the BF was applying, the result of this method represents a list of the pixel coordinates of region boundary as formula 4, then SBB will be calculated by using the formula 5-6.

$$list_x = [x_1, x_2, x_3, \dots, x_n] \quad (4)$$

$$list_y = [y_1, y_2, y_3, \dots, y_n]$$

$$cropping = (start_x, start_y) \text{ to } (end_x, end_y) \quad (5)$$

$$start_i = \frac{\min(list_i)}{2} + \frac{\max(list_i)}{2} - \frac{\partial}{2} - \beta \quad (6)$$

$$end_i = \frac{\min(list_i)}{2} + \frac{\max(list_i)}{2} + \frac{\partial}{2} + \beta$$

$$\partial = \max(\max(list_x) - \min(list_x), \max(list_y) - \min(list_y))$$

Where,  $i \in \{x, y\}$  and  $\beta$  is margin size

Fig. 6 shows a result obtained from SBB with a margin of 100 with the green rectangle. This method provides a starting point and ending point in order to crop a region with a symmetrical rectangle surrounding the interesting object while the BB provides a rectangle that fits the object as the red rectangle. All input images will be cropped with the

symmetrical rectangle obtained from SSB, and the cropped images have a space between the object and the border in order to prevent miss featured in the feature extraction process all of the cropped images are resized into 224x244 pixels to serve the requirement of the VGG-16 input layer. Table I shows the example cropped images categorized by class of the abnormalities of peeled shrimp.

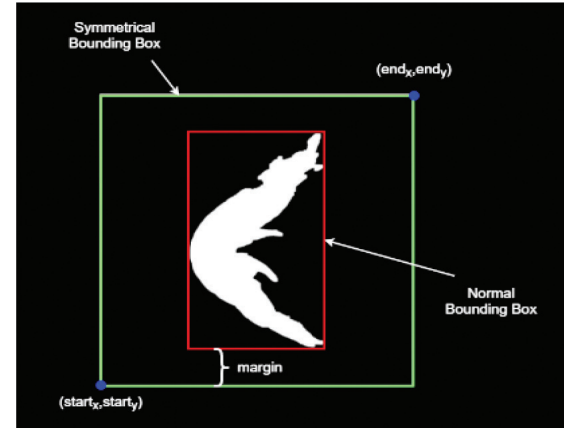


Fig. 6. The green rectangle is a result obtained by SBB and the red rectangle is a result obtained by BB the symmetrical.





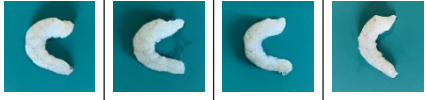
#### B. Dataset and VGG-16 Architecture Definition

Transfer learning is a machine learning method based on a convolutional neural network. This method uses existing knowledge to solve different tasks but related filed of problems. Generally, the machine learning method requires a sufficient dataset and perfect network architecture to build a model for classifying multi-class of problems through the learning process. However, the transfer learning method uses less dataset and learning time than other machine learning methods because it uses a pre-trained weight as the starting point for learning cause the speed up for training and the performance of the classification model has been improved.

##### 1) Dataset

The peeled shrimp dataset consists of a total 5,074 of color images out of which 880 are normal peeled shrimps (P), 1004 are abnormal unpeeled shrimps, and their head still on (HO), 1,272 are abnormal unpeeled shrimps but their heads are beheaded (HL), 950 are abnormal peeled shrimps but their tail still on (PTO), and 968 are abnormal peeled shrimps but their leg still on (PLO). Table I shows the example labeled dataset by classes. All images are pre-processed and normalized resulting in an image size of 224x224 with all pixel values in a range of 0-1 that meet the need of the VGG-16 input layer requirement. This dataset is split randomly into three parts for training, validating, and testing our classification model. The first spitted dataset is used to fit the model and consists of 60% of all datasets and the remaining is equally split for validating and testing (20% for validation and 20% for testing).

TABLE I  
THE ABNORMALITIES PEED SHRIMP DATASET

Label	Type	Class	Status	Example	Sample
0	Whole or Head-on	HO	Abnormal		1,004
1	Headless	HL	Abnormal		1,272
2	Peeled Tail-on	PTO	Abnormal		950
3	Peeled Leg-on	PLO	Abnormal		968
4	Peeled	P	Normal		880

## 2) VGG-16 Architecture

VGG-16 is sixteen layers based on convolutional neural network architecture used by the Visual Geometry Group from Oxford University to obtain outstanding results in the ILSVRC2014 (Large Scale Visual Recognition Challenge 2014) competition [16]. It was still considered to be an excellent model in the classification task. This model uses a set of weights pre-trained on ImageNet and it achieves 92.5% which currently in top five test accuracy in ImageNet [26].

Fig. 7 shows the architecture of the VGG-16 network consists of thirteen convolutional layers and three fully connected layers. However, the use of the VGG-16 as a transfer learning will require to freeze all the weight layers from trainable to non-trainable and create a new fully connected layers that fits the new dataset instead of the three old layers on top of the output layers from the base model. The characteristics of VGG-16 used in our work are as follows:

- The input layer uses 224x224x3 pixels of image size.
- The whole convolution layer uses a kernel size of 3x3 with a stride size of 1 and sets the padding as the same. The used pooling layers are max pooling with 2x2 layers with a stride size of 2. VGG 16 uses the Rectified Linear Unit as the activation function with the formula (7).

$$\text{Relu}(x) = \max(0, x) \quad (7)$$

- In the classification task, cross-entropy is used as a loss function to assess the true and predicted value with formula (8)  $y(x_i)$  where represents the true label and  $\hat{y}(x_i)$  represents the prediction label. The loss of each batch is shown in formula (9) where n represents the category number and m is the sample number in the batch.

$$H = -\sum_{i=1}^n y(x_i) \log(\hat{y}(x_i)) \quad (8)$$

$$\text{loss} = -\frac{1}{m} \sum_{j=1}^m \sum_{i=1}^n y = y_{ji} \log(\hat{y}_{ji}) \quad (9)$$

- The output layer uses Softmax as a probability distribution which is the highest probability with the formula (10). In order to classify tasks, there are five categories m in multi-classification prediction. The label Y has m values where  $y^{(i)} \in \{0, 1, \dots, m\}$  is a category in sample space.  $p = (y = j | x)$  represents the probability that x belongs to an exact category  $j=1, 2, \dots, m$ . The classifier parameters represent as  $\theta = [\theta_1^i, \theta_2^i, \dots, \theta_m^i]$ . Thus, the probability will belong to a certain class.

$$h_{\theta}(x^{(i)}) = \begin{bmatrix} p(y^{(i)} = 0 | x^{(i)}; \theta) \\ p(y^{(i)} = 1 | x^{(i)}; \theta) \\ \vdots \\ p(y^{(i)} = m | x^{(i)}; \theta) \end{bmatrix} = \frac{1}{\sum_{j=1}^m e^{\theta_j^i x^{(i)}}} \begin{bmatrix} e^{\theta_0^i x^{(i)}} \\ e^{\theta_1^i x^{(i)}} \\ \vdots \\ e^{\theta_m^i x^{(i)}} \end{bmatrix} \quad (10)$$

The old classification layer with three fully connected was replaced with our designed classification layer that is suited for our task as shown in Fig. 6. Our proposed model-based transfer learning is trained by using the best parameters conducted in the experiment process consisting of the optimization

algorithm with Adam, training iterate with 1000 epoch, 128 of batch size and learning rate with 0.001. The overfitting problem will be eliminated by setting the early stopping with 3 of patience which refers to the number of epochs with no improvement after training and it will be stopped.

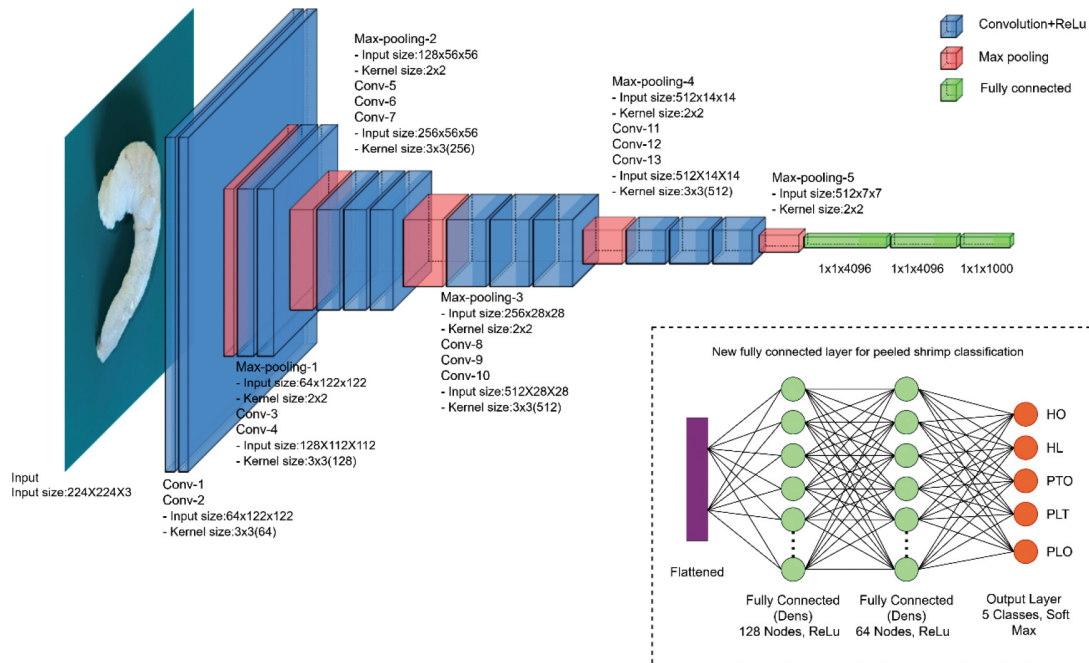


Fig. 7. VGG 16 network architecture by freezing the last three old Fc layers and replaces it with our designed Fc layers.

### III. RESULTS AND DISCUSSION

The experimental results of our proposed the VGG-16 transfer learning based on the abnormalities peeled shrimp classification are statistically described as accurate compared with the difference models including five transfer learning models and three supervised learning models by considering the various confusion matrix-based performance matrices. These metrics consist of four main indicators: (1) Accuracy is characterized as the percentage of relevant results measuring all the correctly classification class. (2) Precision is used to evaluate exactness of a classification model. (3) Recall is the measure of completeness of a classification model. (4) F-measure is defined as the weighted harmonic mean of precision and recall [28].

All experimental methods in this paper were programmed in Python version 3 and there ware

implemented on the NVIDIA DGX1 AI cloud server, CPU Dual 20-core Intel Xeon E5-2698 v4 2.2 GHz, GPUs 8X NVIDIA Tesla V100, and 512 GB 2,133 MHz DDR4 of system memory.

In order to evaluate our proposed models, it is necessary to run the training model with several times to determine the average accuracy because the classification model requires random data for training, validation and testing, which may result in an accuracy instability.

Table II represents the results obtained from VGG-16 models running in 35 times, our testing results achieve 98.36% in average of accuracy with 0.0213 seconds on a classification time and the model size is 64.54 MB. All indicators produce good and consistent results, and the standard deviation of all indicators is very small since our proposed method provides the result clustered around the mean.

TABLE II  
THE COMPARISON MEAN OF ACCURACY, PRECISION, RECALL, F-MEASURE, PREDICTION TIME AND MODELS SIZE

Method	Model	Accuracy (%)	Precision (%)	Recall (%)	F-measure (%)	Time (Sec)	Size (MB)
Transfer Learning	VGG16	98.36	98.46	98.45	98.42	0.0213	64.54
	MobileNet	97.45	97.54	97.59	97.55	0.0159	19.49
	Xception	94.95	95.24	95.15	95.09	0.0240	91.70
	Resnet-50	97.44	97.54	97.56	97.50	0.0249	102.56
	Densnet	98.06	98.18	98.18	98.13	0.0514	82.25
	Inception	96.18	96.25	96.44	96.28	0.0076	93.37
Supervised Learning	SVM	74.81	75.64	77.33	75.03	0.0091	0.400
	CNN	91.01	91.32	91.46	91.19	0.0093	2.170
	RNN	77.95	78.02	79.65	77.00	0.0004	0.280

Fig. 8(a) represents the training and validating accuracy curves of the VGG-16 model which was trained with a pre-processed dataset. These curves are increasing and flattening closely to 100% of accuracy. Fig. 8(b) represents the training and validation loss curves that the validation loss is slightly greater than the training loss. These curves are decreasing and flat to the point of stability after 100 epochs until the end. This kind of curve represents the best fit learning

curve [29]. Fig. 8(c) represents the confusion matrix of the impact of false class rates. This matrix provides the rich of true positives and true negatives accuracy for each class while false positives and false negatives are very small. Therefore, it can be concluded that the VGG-16 model training has a good effect, keeping a few losses, owing to validating the accuracy and avoiding being affected by the over-fitting problem.

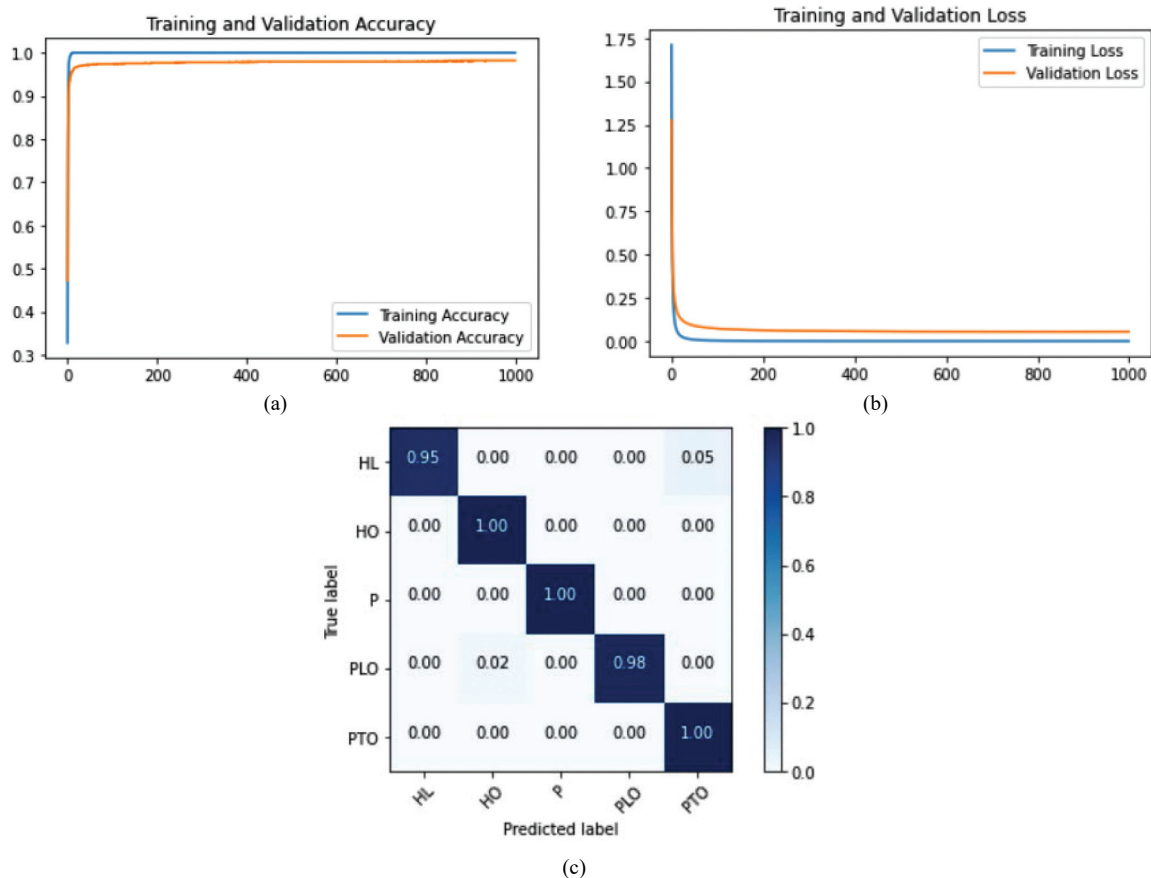


Fig. 8. Training and Validating analysis over 1,000 epochs: (a) Training and validating accuracy analysis, (b) Training and validating loss analysis, (c) Confusion Matrix analyses of VGG-16 trained with preprocessed dataset.

Fig. 9 represents the comparison accuracy between the VGG-16 models that were trained with and without a preprocessed dataset. These models were trained with the same parameter setting and were ran in 35 times with 1000 epochs. Each time,

the accuracy of the VGG-16 model was trained with a preprocessed dataset is higher than the VGG-16 model trained with a normal dataset. Thus, the preprocessed dataset optimizes the classification model's accuracy.

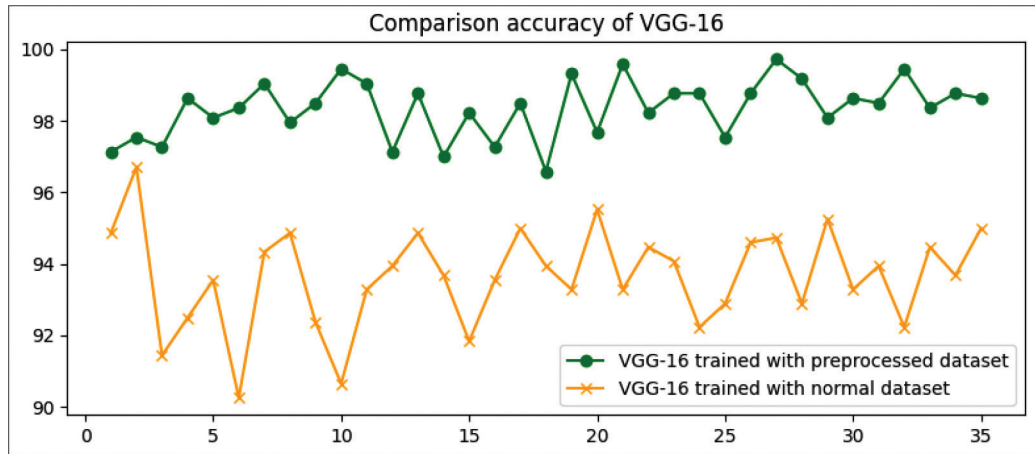


Fig. 9. The comparison accuracy between VGG-16 was trained with preprocessed dataset and VGG-16 was trained with normal dataset with 1000 epochs running in 35 times.

All of these models are compared to ones of our proposed model in order to verify that it is superior. The comparison of results between our proposed model and other comparative models by considering performance indicators are presented. Table II represents all indicators results obtained from different models based on the abnormalities peeled shrimp classification running in 35 times. These models were trained with the preprocessed dataset by using the same parameter setting. The VGG-16 model provides higher accuracy than other competitive models with 98.36% and all indicators is accurate in the same high accuracy. It is clear that the VGG-16 is more accurate than other transfer learning models and supervised learning models.

The VGG-16 has a greater accuracy than a simple CNN because the fundamental architecture of the VGG-16 is based on CNN, but it is more complexity and has been trained with a larger dataset, so it will require less learning time and deliver a higher accuracy when trained with a new dataset.

Furthermore, The VGG-16 has a significantly greater accuracy as compared to SVM and RNN since it has a better feature extraction process by adding the convolutional layer and pooling layer connected in a complex architecture. This process will generate good attributes that are easy to classify in the classification layer. However, an RNN uses this process with only simple architecture and an SVM don't have these process.

Moreover, The VGG-16 is more accurate than other transfer learning methods. Every transfer learning approach is based on CNN with various degrees of complexity of architecture. The proper

method should be well structured and have sufficient complexity in order to suit the new dataset. The outcome is the sole criterion for selecting a method. Therefore, the VGG-16 is suitable for this study.

The classification time and model size are important indicators for measuring the performance of the classification models. Since the classification model size directly affects the classification speed. The results show that the models that were built with complex architecture tend to be a larger size and often take a lot of time to classify than models that were built with minimal architecture. The VGG-16 was built 16 layers deep which is faster than the Resnet-50 which was built 50 layers deep. On the other hand, RNN is a less complicated architecture than the VGG-16, therefore it takes less classification time than the VGG-16. However, the complicatedness and size of classification models don't have an effect on classification accuracy.

In summary, even though all of the models are based on the abnormalities peeled shrimps' classification. The VGG-16 with our designed classification layer was able to produce better results than the other competitive models and all indicators demonstrated the effectiveness of the VGG-16. Aligning and resizing images through data preprocessing is very important to increase the accuracy of our classification model. The size of models directly affects the classification times. The model with complex architecture tends to be large and it takes a long time to make a classification. The VGG-16 took less time to classify than the larger models. However, the model's size and classification speed do not affect the accuracy of classification models.

In order to evaluate the quality level of the results obtained from our proposed model. It is important to compare our proposed model with other competitive models since many models can investigate the abnormalities of peeled shrimp. CNN [29], RNN [30], and SVM [31] are commonly used classification approach, and there are frequently used as the preferred primary since many of the advanced models today are inspired by these models. MobileNet [32], Xception [33], Resnet-50 [34], Densnet [35], and Inception [36] are the transfer learning models that achieve the top class accuracy in ImageNet tests and are frequently used in classification tasks as the same things as the prior models.

#### IV. CONCLUSION

In this paper, a deep convolutional neural network with the VGG-16 based transfer learning for the abnormalities peeled shrimp classification is proposed. The major contribution of this work is the successful development of an effective methodology for classifying the abnormalities of peeled shrimp. The provided dataset was preprocessed by aligning images based on skeleton calculation, cropping images with the symmetrical bounding boxes, and resizing images to meet the need of the VGG-16 input layer requirement. The VGG-16 model was customized with our designed classification layers and was trained with our designed parameters. All indicator results obtained from our classification model show that the VGG-16 with our designed classification layer offers better accuracy than others. The preprocessed dataset with our method directly effects to increase the accuracy of classification models.

In future work, our provided method will be applied to the real production line. However, the peeled shrimps in the real production line are always stick together. The segmentation of stick peeled shrimp is our primary work.

#### ACKNOWLEDGMENT

We would like to thank the Digital Academy Thailand and the Faculty of Engineering at Sriracha, Kasetsart University, Sriracha Campus, for supporting the facilities for this study.

#### REFERENCES

- [1] M. Z. Herzberg, A. I. C. Córdova, and R. O. Cavallic, "Biological Viability of Producing White Shrimp *Litopenaeus Vannamei* in Seawater Floating Cages," *Aquaculture*, vol. 259, no. 1-4, pp. 283-289, Sep. 2006.
- [2] A. Farhana, "The Export Trend of Shrimp Industries in Bangladesh: An Analysis," *Scientific Research Journal*, vol. 5, no. 4, pp. 80-95, Sep. 2017.
- [3] R. Warangkhan, "Model for Forecasting the Export Volume of Frozen Shrimp," *RMUTSB Academic Journal*, vol. 8, no. 1, pp. 70-82, Jun. 2020.
- [4] L. M. Díaz-Tenorio, F. García-Carreño, and Ramon Pacheco-Aguilar "Comparison of Freezing and Thawing Treatments On Muscle Properties of White Leg Shrimp (*Litopenaeus Vannamei*)," *Journal of Food Biochemistry*, vol. 31, no. 5, pp. 563-576, Oct. 2007.
- [5] C. Jotikasthira, "The Development of Thailand's Potentials and Exports of Shrimp Processed for Southeast Asia," *Journal of Bangkokthonburi University*, vol. 8, no. 1, pp. 59-72, Jan. 2019.
- [6] D. Sylvain, "Shrimp Quality and Safety Management Along the Supply Chain in Benin," Ph.D. thesis, Dept. Nutrition and Health Sciences, Wageningen Univ. Wageningen, NLD, 2015.
- [7] G. A. Leiva-Valenzuela and J. M. Aguilera, "Automatic Detection of Orientation and Diseases in Blueberries Using Image Analysis to Improve Their Postharvest Storage Quality," *Journal of Food Control*, vol. 33, pp. 166-173, Sep. 2013.
- [8] H. Zareiforouh, S. Minaei, M. R. Alizadeh et al., "Design, Development And Performance Evaluation of an Automatic Control System for Rice Whitening Machine Based on Computer Vision and Fuzzy Logic," *Computers and Electronics in Agriculture*, vol. 124, pp. 14-22, Jun. 2016.
- [9] P. A. Coelho, S. N. Torres, W. E. Ramirez et al., "A machine Vision System For Automatic Detection of Parasites *Edotea Magellanica* Shell-off Cooked *Clammulina Edulis*," *Journal of Food Engineering*, vol. 181, pp. 84-91, Jul. 2016.
- [10] T. T. N. Thai, N. S. Thanh, and P. C. Viet, "Computer Vision Based Estimation of Shrimp Population Density and Size," in *Proc. International Symposium on Electrical and Electronocs (ISEE)*, 2021. pp.145-148.
- [11] R. P. S. Sankar, V. Jenitta, and B. Kannapiran, "Diagnosis of Shrimp Condition Using Intelligent Technique," in *Proc. International Conference on Electrical, Instrumentation and Communication Engineering (ICEICE)*, 2017, pp.1-5.
- [12] L. J. Dah, X. Guangming, R. M. Lane et al., "An Efficient Shape Analysis Method for Shrimp Quality Evaluation," in *Proc. International Conference on Control, Automation, Robotics and Vision (ICARCV)*, 2012, pp. 865-870.
- [13] D. Zhang, K. D. Lillywhite, D. J. Lee et al., "Automatic Shrimp Shape Grading Using Evolution Constructed Features," *Computers and Electronics in Agriculture*, vol. 100, pp. 116-122, Jan. 2014.
- [14] Z. Liu, C. Fang, and Z. Wei, "Recognition-Based Image Segmentation of Touching Pairs of Cooked Shrimp (*Penaeus Orientalis*) Using Improved Pruning Algorithm for Quality Measurement," *Journal of Food Engineering*, vol. 195, pp. 166-181, Feb. 2017.
- [15] K. Weiss, T. M. Khoshgoftaar, and D. Wang, "A Survey of Transfer Learning," *Journal of Big Data*, pp. 1-40, May. 2016.
- [16] K. Simonyan and A. Zisserman, "Very Deep Convolutional Networks for Large-Scale Image Recognition," *Computer Vision and Pattern Recognition*, vol. 6, pp. 1-14, Sep. 2015.
- [17] G. Q. Jiang, C.-J. Zhao, and J.-Y. Qi, "The Research of Image Segmentation Based on Color Characteristic," in *Proc. International Conference on Machine Learning and Cybernetics*, 2011, pp. 1-12,
- [18] S. Bansal and D. Aggarwal, "Color Image Segmentation Using Cielab Color Space Using ant Colony Optimization," *International Journal of Computer Applications*, vol. 29, no. 9, pp. 28-34, Sep. 2011.
- [19] P. Ganesan, V. Rajini, B. S. Sathish et al., "HSV Color Space Based Segmentation of Region of Interest in Satellite Images," in *Proc. International Conference on Control, Instrumentation, Communication and Computational Technologies*, 2014, pp. 1-10.
- [20] C. Zhang, W. Yang, Z. Liu et al., "Color image segmentation in rgb color space based on color saliency," in *Proc. International Conference on Computer and Computing Technologies in Agriculture*, 2013, pp. 101-105.
- [21] K. B. Shaik, P. Ganesan, and V. Kalist, "Comparative Study of Skin Color Detection And Segmentation in HSV and YCbCr

- Color Space,” *Procedia Computer Science*, vol. 57, pp. 41-48, Dec. 2015.
- [22] N. Jamil, T. M. T. Sembok, and Z. A. Bakar, “Noise Removal and Enhancement of Binary Images Using Morphological Operations,” in *Proc. International Symposium on Information Technology*, 2008, pp. 1-6.
- [23] P. Maragos and R. W. Schafer, “Morphological Skeleton Representation and Coding of Binary Images,” *IEEE Transactions on Acoustics, Speech, and Signal Processing*, vol. 34, no. 5, pp. 1228-1244, Oct. 1986.
- [24] G. Toussaint, “Solving Geometric Problems with the Rotating Calipers,” in *Proc. IEEE MELECON 83*, 2000, pp. 1-12.
- [25] S. Suzuki and K. Abe, “Topological structural analysis of digitized binary images by border following,” *Computer Vision, Graphics, and Image Processing*, vol. 30, no. 1, pp. 32-46, Apr. 1985.
- [26] J. Gu, P. Yu, X. Lu et al., “Leaf Species Recognition Based on VGG16 Networks and Transfer Learning,” in *Proc. IEEE 5th Advanced Information Technology, Electronic and Automation Control Conference*, 2021, pp. 2189-2193.
- [27] M. Sokolova, N. Japkowicz, and S. Szpakowicz, “Beyond Accuracy, F-Score and Roc: A Family of Discriminant Measures For Performance Evaluation,” *Advances in Artificial Intelligence*, vol. 4304, pp. 1015-1021, Jan. 2006.
- [28] T. Viering and M. Loog, “The Shape of Learning Curves: A Review,” *ArXiv*, vol. 1, pp. 1-46, Mar. 2021.
- [29] A. Saad, A. M. Tareq, and A.-Z. Saad, “Understanding of a Convolutional Neural Network,” in *Proc. International Conference on Engineering and Technology*, 2017, pp. 1-6.
- [30] B. Siddhartha, S. Václav, and K. Ashish. *Recurrent Neural Network*. Elsevier Academic Press, Massachusetts: USA, 2020, pp. 52-64.
- [31] Z. Yongli, “Support Vector Machine Classification Algorithm and its Application,” in *Proc. International Conference on Information Computing and Applications*, 2012, pp.179-186.
- [32] A. G. Howard, M. Zhu, B. Chen et al., “Mobilenets: Efficient Convolutional Neural Networks for Mobile Vision Applications,” *Computer Vision and Pattern Recognition*, vol. 1, pp. 1-9, Apr. 2017.
- [33] F. Chollet, “Xception: Deep Learning with Depthwise Separable Convolutions,” in *Proc. IEEE Conference on Computer Vision and Pattern Recognition*, 2017, pp. 1-8.
- [34] K. He, X. Zhang, S. Ren et al., “Deep residual Learning for Image Recognition,” in *Proc. IEEE Conference on Computer Vision and Pattern Recognition*, 2016 pp. 770-778.
- [35] G. Huang, Z. Liu, L. V. D. Maaten et al., “Densely Connected Convolutional Networks,” in *Proc. IEEE Conference on Computer Vision and Pattern Recognition*, 2018, pp. 1-9.
- [36] C. Szegedy, V. Vanhoucke, S. Ioffe et al., “Rethinking the Inception Architecture for Computer Vision,” in *Proc. IEEE Conference Computer Vision and Pattern Recognition*, 2015, pp. 4700-4708.



**Tamnuwat Valeprakhon** is a lecturer at the Department of Computer Engineering, Faculty of Engineering at Sriracha, Kasetsart University, Sriracha campus, Thailand. He graduated M.Eng in Computer Engineering from Khon Kaen University, Thailand. He was granted a scholarship from the National Science and Technology Development Agency (NSTDA) for studying at the Kochi University of Technology, Japan. His research interests including of Computer Vision, Image Processing, and Artificial Intelligence.



**Korawit Orkphol** is a lecturer at the Department of Computer Engineering, Faculty of Engineering at Sriracha, Kasetsart University, Sriracha campus, Thailand. He graduated Ph.D. in Computer Science and Technology from Harbin Engineering University, P.R. Harbin, China. His research field including of Artificial Intelligence, Machine Learning, and Natural Language Processing.



**Penpun Chaihuadjaroen** is an Assistant Professor at the Department of Computer Engineering, Faculty of Engineering at Sriracha, Kasetsart University, Sriracha campus, Thailand. She graduated M.S in Computer Science from King Mongkut’s Institute of Technology Ladkrabang, Thailand. Her research field including of Computer Vision and Image Processing.

# Development of Grip Comfort of Perfume Bottle by Applying the Concepts of Product Design and Development and Hybrid Optimization Technique

Suchada Rianmora<sup>1</sup> and Pervez Alam Khan<sup>2</sup>

<sup>1,2</sup>School of Manufacturing Systems and Mechanical Engineering, Sirindhorn International Institute of Technology, Thammasat University, Pathumthani, Thailand  
E-mail: suchada@siit.tu.ac.th, m6222040716@g.siiit.tu.ac.th

Received: September 27, 2021 / Revised: October 28, 2021 / Accepted: November 1, 2021

**Abstract**—This study mostly relied on online customer reviews to reveal a problem with gripping comfort in perfume bottles, which was limiting customer willingness to purchase. The absence of ergonomic design owing to inappropriate dimensions in large-volume perfume bottles was the primary reason for problems with comfortable gripping. As voted by local users in the preference survey, a rectangular-shaped bottle was used as the foundation of this study. Taguchi's experiment design was created according to the extraction of dimensions from a rectangular bottle. Based on the experimental design, bottle samples were fabricated by using the rapid prototyping (RP) process – a 3D Printer. Kansei words were applied to elicit customer feelings on bottle samples for grip comfort. For evaluating the responses and determining the proper dimension factors that resulted in the most comfortable grip and ergonomically designed perfume bottle, Grey relational analysis was used in this study.

**Index Terms**— Content Analysis, Ergonomics Design, Grey Relational Analysis, Grip comfort perfume Bottle, Product Design and Development, Taguchi Method.

## I. INTRODUCTION

Perfume has now become an essential component of our daily lives. They are pleasant-smelling fluid-based items that many individuals utilize in their regular lifestyle. They are being worn all over the world by people of different genders, ages, and cultures. For years, they act as a symbol of personal style [1]. Perfume is becoming one of the most popular products among all fashionable labels. Because each brand has some distinct products, the emergence of brands has generated a scenario of confusion among consumers' purchase intentions. They may be in the

form of the aesthetic appearance of perfume bottles or distinction in fragrance [2]. The global perfume market is growing at a compound annual growth rate of 3.9% from 2019 to 2025 [3]. In the context of Thailand, revenues generated from the perfume industry amount to US\$266.9 million in 2021, and the market is expected to grow at a compound annual growth rate of 3.80% [4]. This demonstrates the need of studying many facets of perfume attributes. Many investigations have emphasized various elements, such as examining purchase intent based on factors related to the perfume bottle package design [5]-[9], any other researchers also studied odor perception [10], [11] and perfume bottle form [12]-[15]. Most of these studies are based on survey methods where the pre-determined product attributes are fixed. This study used content analysis of internet reviews, which allows for a more in-depth look at customers' genuine perceptions by considering the whole spectrum of criteria addressed [16]. Customer reviews have evolved into a space where customers may express their feelings about the products they have used, primarily through their level of satisfaction. These reviews also provide a unique set of information comprising positive and negative comments, as well as ratings, allowing market researchers to run various analyses and identify the features that are highly appealing, as well as those that are criticized and need to be improved [17]-[19]. Online retail platforms as well as some general discussion platforms, where customers share their feeling about various aspects of a particular product in the form of reviews have become a major source of the voice of the customer aiding to examine customers' needs and preferences as well as design requirements.

An in-depth investigation of these needs, preferences, and design criteria may lead to the identification of the product's features or the crucial element, which could lead to product innovation in the form of inventing a new product or revamping an



existing one [19]. This study looked at user reviews on *Fragrantica.com*'s general discussion forum. *Fragrantica* is an online encyclopedia of perfume that also has a community of perfume lovers who offer their opinions on a variety of topics, including the scent, brand name, shape, size, material, and color of the perfume bottle, and nearly anything else about perfume [20]. As stated above, this study used *Fragrantica.com*'s general discussion forum to examine reviews linked to various features of perfume bottles and identify difficulties people have with perfume bottles that have not yet been addressed by researchers or that need to be improved. After analyzing many opinions on the discussion form, it was discovered that buyers had difficulty gripping the perfume bottle comfortably due to the bottle's insufficient proportions. Difficulty in gripping may also cause problems like carpal tunnel syndrome and trigger finger [21]. Following an examination of various articles (described in the research background section of this study), it was determined that several researchers appear to have employed multi-criteria decision-making techniques to improve the aesthetic of perfume bottles. No one, however, has investigated what proportion of perfume bottles is most pleasant in the customer's hands. In this study, we attempted to find online reviews where customers mentioned the issue of comfort grip, match it with local users via an online survey, optimize the bottle dimension via a multi-criteria decision-making method, and obtain customer feeling on grip comfort on the optimized bottle size via Kansei engineering. In order to access the depth of human emotions and understand customer needs, Kansei engineering translates human emotion to a quantifiable value where Grey relation analysis aids decision-making in uncertain contexts and circumstances involving several attributes by comparing each alternative to an ideal outcome.

## II. RESEARCH BACKGROUND

This section will be mentioned about the related works and backgrounds of perfume design and characteristics where the existing designs and physical characteristics of perfume bottles were studied via the perceptions and experiences of the customers who commented on some ideas and reviews through the online-block platform. The results were also presented in this section as the preliminary study before going to the design stage in the next section.

### A. Studies on "Perfume Attributes"

Consumers value packaging and bottle design because they are the first quality that a product shares with them. It is the catalyst for a possible purchase [9]. The Influence of perfume packaging on Jordanian female customer purchasing behavior

was investigated by Al Saed et al. [7], who found that all aspects of perfume packaging, except package material, have a substantial impact on consumer purchasing behavior. Chen et al. [22] researched customer's psychological impressions of perfume bottle form and concluded that aesthetically pleasing forms attract more customer preference. Sivagnanasundaram et al. [6] looked at the shape, material, and color of packaging in relation to gender. He found that there was a unisexual preference for the rectangular bottle, regardless of color or material. Similarly, men and women appear to like red-squared and blue-squared bottles equally, but males prefer black-squared bottles more. Lesot et al. used machine learning methodologies to investigate the forms of perfume bottles and the emotions associated with each shape, concluding that shapes influence consumers' emotions when they are introduced to packaging [15]. Wei et al. employed Kansei engineering and Type I quantification theory to perform a study on perfume bottle designs, demonstrating that the integrated model works well for recommending new product design and development using various parts of the bottle and visuals of the respective product. Tien-You et al. [1] investigated customer preferences for perfume bottle forms and found that circle shapes are the most appealing to buyers [22].

The *fuzzy analytic hierarchy process* was utilized by Chen et al. [12] to show that it can be used to generate alternative designs during the conceptual stage of design, providing perfume bottle designers an advantage. Lin et al. [13] created new perfume bottle designs based on client preferences using grey relational analysis, grey prediction, and the technique for "order of preference" by similarity to the ideal solution. Elango et al. [5] looked into the aspects that influence consumer purchasing decisions for local brand perfume packaging in Bangkok in 2020, and discovered that visual package design has an effect on consumer purchasing intents. According to the results of his consumer behavior survey, 71 % of respondents bought perfume in the 50-100 ml range per bottle. He also revealed that 72 % of those respondents wear perfume every day. As a result, another size to satisfy consumer behavior is 100 ml, which is a nice amount for customers who use perfume on a daily basis. They believe it is good to invest in and do not need to buy a new bottle of perfume on a regular basis. The customer's ease when holding the bottle to spray perfume is also influenced by the shape. They may decide not to buy the product if it does not fit their palm nicely.

Based on the studies mentioned above, there was clear that shape and size of perfume bottle that provide better grip comfort are one of the most influential factors for customer purchase intention apart from fragrance. Therefore, we looked for grip

comfort reviews on the internet. And the output is described in the next section.

*B. Online Customer Reviews and Analysis*

Reviews are no longer a choice for online users, but rather an expectation [24]-[26]. When a customer wants to find out more about a product or compare other product options, they have access to thousands of reviews that include both positive and negative feedback from other customers which serve as a guide for purchasing a new product [25]. The close evaluation of positive feedback will indicate the product’s most popular feature, whilst the evaluation of negative feedback will reflect the feature that needs to be improved [18], [19]. Previous research has revealed that online reviews are often used for product innovation. Kim et al. [27] used online reviews as a resource to improve various aspects of a washing machines. Rianmora et al. [28], [29] customized gimbal stabilizer and salad spinner respectively based on data from online user assessments. Online reviews were used by Kim et al. [30] for the product innovation of MP3 players and mobile headsets. Similarly, fragrantica.com [20] was used in this study to investigate the ergonomics of the perfume bottle design. The reviews were gathered using the general discussion form [31]-[36], and the analysis was performed. The reviews are shown in Tables I and II.

Based on the reviewed results, the following data were obtained:

- a. Mainly 100 ml. or more long volume bottles are harder to grip.
- b. The majority of rectangular and square bottles are hard to grip.
- c. People with carpal tunnel syndrome had high difficulty in holding long rectangular and squared bottles.
- d. In addition, a variety of other and irregularly shaped enormous-sized bottles were difficult to hold.
- e. The spray position also makes it hard to grip bottles.

According to the comments and findings from the target users, these can be made clear that the bottles lack a good ergonomic characteristics, and this would be better to design the bottle for fitting the user’s palm during spraying or holding quickly.

TABLE I  
PREFERRED SIZE REVIEW [31]-[36]

No.	Review
1	“30 ml and 50 ml work best for me, because I tend to rotate the scents and also I don’t want to keep the bottles for too long in hot weather conditions. As for what bottles look prettiest. In my view this depends on the design of the bottles: some look best in 50 ml (the dainty stuff), some look best in 100 ml (the bold designs).”
2	“I prefer the nice BIG bottles, that way I do not fret about running out!”
3	“I usually prefer buying 30 ml and 50 ml bottles... unless it’s a scent from my top 5, of which I would definitely buy 100 ml.”

TABLE II  
ONLINE PRODUCT REVIEW [31]-[36]

Product	Review
	“I recently got Da Man (Amber) and I love it, especially. The dry down. Just one annoyance, though. The bottle is really clumsy for spraying. My hands have to be completely dry and my index finger stretches too far to spray. Ergonomics must not be Da’s strong point.”
	“For the rectangular and square bottles, I have carpal tunnel in my hands and by far the worst for me would be the big square or rectangle-shaped bottles. I have a 100 ml bottle, it is very big to hold and spray.”
	“100 ml bottle is like a heavy brick, impossible to hold and spray by one hand.”

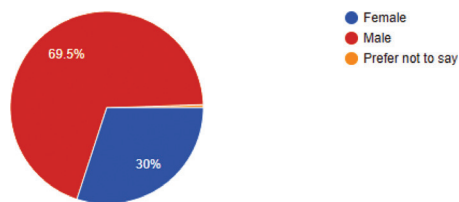
C. Role of Ergonomics in Package Design

Companies rapidly coming up with innovative products have significantly generated a scenario of fierce competition among each other. This rivalry among the companies has shortened the product's life cycle. Identifying a product's attribute which creates value for consumers is the key to innovation [37]. In this case, ergonomics appears to be the most important attribute that needs to be improved, which can also act as an innovation. Ergonomically designed items place a higher priority on comfort than aesthetics, making them simple and enjoyable to use [38]. Since corporations compete on the ease of use of their products, ergonomic features are recognized as critical [39], [40]. Researchers agree that, if the user experiences, such as safe usage and comfort, are not met, the affective and cognitive parts of the design are rendered ineffective [39], [41], [42]. Improper size in relation to shape may also make gripping more difficult, resulting in a decrease in consumer willingness to buy.

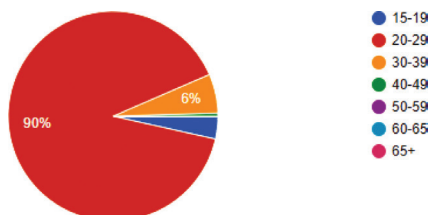
III. CUSTOMER PERCEPTION

Analyzing the customer's opinion shows the customer's actual feelings about the product [43]. Taking into account the problem of gripping, an online survey was prepared to match the situation faced by the reviewers to the people of Thailand, This online survey was widely disseminated among students, product design researchers, and some members of the local community. The survey's findings revealed that the reviewer's and local people's problems were similar. The questionnaires with respective responses are listed below.

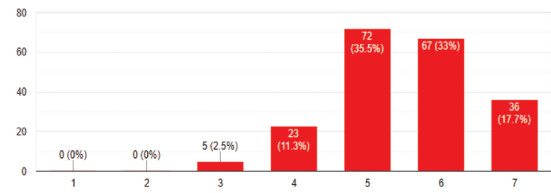
1. Gender



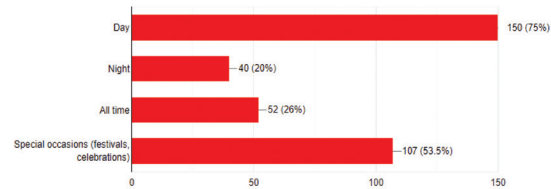
2. Age Group



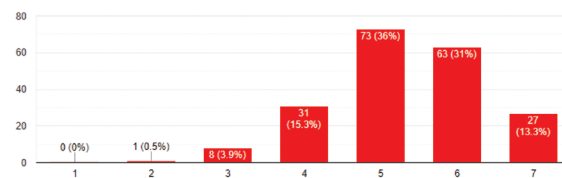
3. In your daily life, how important is perfume? (1=Not Important 7=Highly Important)



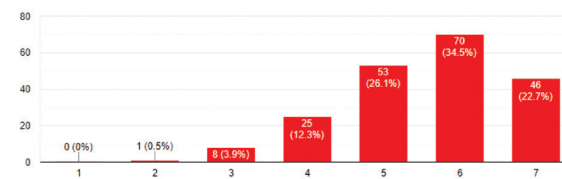
4. When do you like to put perfume on?



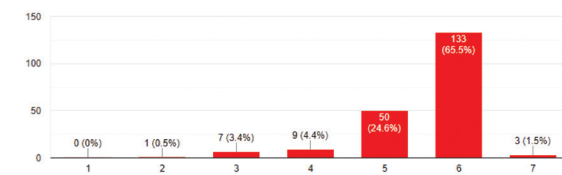
5. How likely are you impressed by perfume bottle design? (1=Very Unlikely 7=Very likely)



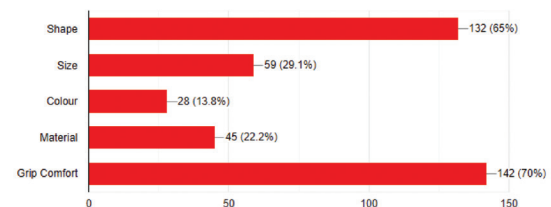
6. How vital is it to you that a design is user-friendly? (1=Not Vital, 7=Highly Vital)



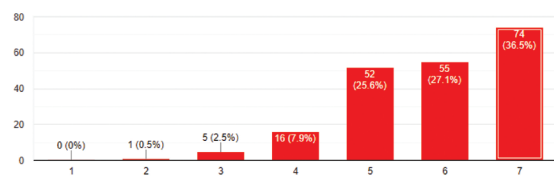
7. How much do you agree the design should be user-centered? (1=Not Agree 7=Highly Agree)



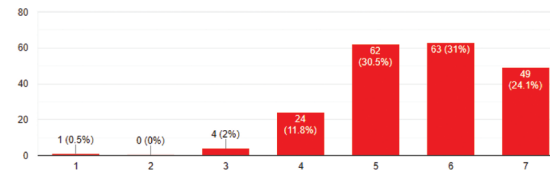
8. What aspects of the perfume container fascinate you the most in terms of ergonomics?



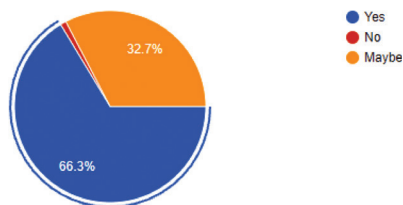
9. How crucial is it for you to be able to spray with ease?



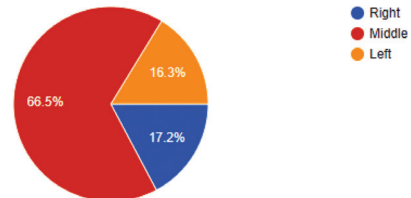
15. How much is the need of comfort of hand/wrist to you while gripping bottle?



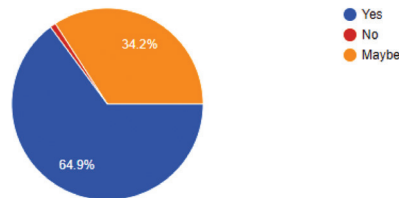
10. Have you ever had difficulty with gripping to spray in perfume bottles?



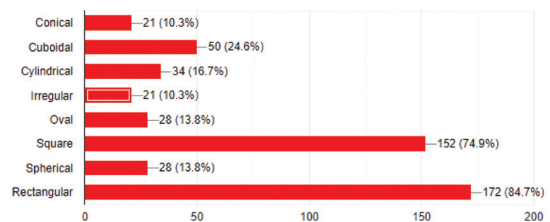
16. What location would you like the spray top to be?



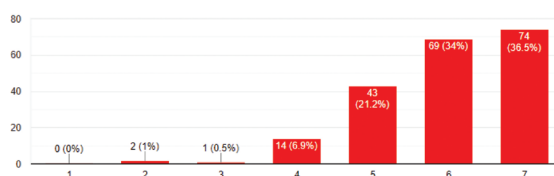
11. Do you believe that poor ergonomics in gripping to reach the spray caused by the incorrect form and size of the perfume bottle may create health problems in the finger or hand?



17. What are your go-to perfume container shapes?

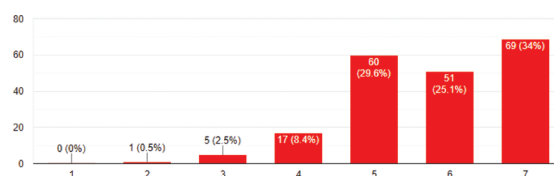


12. How significant is the sense of comfort you get when you hold the perfume bottle in your hands?

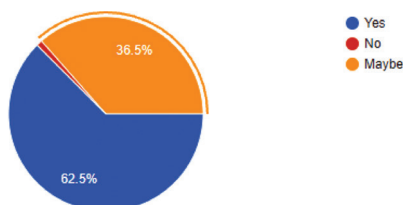


A total of 203 persons took part in the survey. According to the survey's findings, around 69.5% of men and 30% of women replied. 90% of the respondents were in the 20-29 year-old age bracket. Perfume appeared to play a significant role in the lives of the respondents. Respondents appeared to wear perfume primarily throughout the day, on special occasions, and at night. The design of the perfume bottle seems likely to have charmed a long number of users. The users seemed to place a high value on a user-friendly design. Almost 67% of respondents said the design should be centered on the user. Shape and grip comfort was discovered to be the most fascinating aspects of the perfume bottle in terms of ergonomics. Spraying convenience appears to be important to users. The difficulty of gripping has also been reported by respondents. Poor ergonomics in gripping to reach the spray caused by the inappropriate form and size of the perfume bottle, according to 65% of respondents, may cause health problems in the finger or hand, while 35% believe it may happen. The ability to grip the bottle comfortably while avoiding damage appears to be a highly desired feature among the respondents. It was also confirmed that a perfume bottle with a wider width and length is more difficult to grasp and spray. While gripping

13. To you, how essential is safety in perfume bottle design (i.e., protection against injury caused by frequent gripping due to inappropriate dimension design)?



14. Do you believe that a perfume bottle with a longer breadth and length will be more difficult to handle and spray?



the perfume bottle, hand-to-wrist comfort was also required. About 66.5% chose the middle position for the spray, while 17.3% chose Left and 16.3% opted Right. The respondent seems to prefer square and rectangular shapes. This selection could potentially be based on the respondents' ergonomic perceptions. Minitab 19 software was used for item analysis to ensure the internal consistency of the number of reviews received. The *Cronbach's alpha* can be calculated using the formula:

$$(\alpha) = \frac{k}{k-1} \left( 1 - \frac{\sum_{i=1}^k \sigma_{y_i}^2}{\sigma_x^2} \right) \quad (1)$$

$K$  is the total number of factors.

$\sigma_{y_i}^2$  is the variance for the current sample of respondents.

$\sigma_x^2$  is the variance for the sum of all respondents.

**Cronbach's Alpha:**

$$\frac{\text{Alpha}}{0.8297}$$

The Cronbach's Alpha value of 0.8297 indicates that the survey has strong internal consistency [44].

#### Methods Applied for Design Optimization

Gtilay Hasdoan et al. [45] attempted to throw some light on how user models might be used in product design and development to satisfy customers' expectations. The designer's assumption that various product attributes will be incorporated may not meet the requirements of the user. This happens when customers do not grasp how to use the product or when there are unforeseen accidents with the product in a certain context, causing a mismatch between the designer's prediction and the customer's actual use. Optimized the lat bar design for pull-down training stations using Taguchi design and a neural network for muscle responsiveness, proving that the method is appropriate for product optimization [46]. Lin et al. used grey relational analysis, grey prediction, and the Technique for Order of Preference by Similarity to Ideal Solution to produce new perfume bottle designs based on client preferences [13]. Sutono et al. employed a hybrid strategy that integrated Taguchi with grey connection analysis and principal component analysis to show that the hybrid method was capable of optimizing car design while meeting the multi-Kansei needs of the client [47]. Li et al. used fuzzy logic and Taguchi design to optimize the car body, with the results indicating an optimized product [48]. Based on customer feedback, the outcome revealed an upgraded and optimized product. Employed Kansei engineering to translate a customer request into a better design for eyeglasses [49]

Hybrid approaches are widely employed for product design optimizations, according to many researchers. In this study, the Taguchi method was used to create the experiment in this study, which was then combined with grey relational analysis and Kansei engineering. Chaiwat et al. discovered that this strategy is especially effective for shape parameter optimization of a wine bottle, using Kansei engineering and Taguchi-based Grey Relational analysis [50].

#### IV. RESEARCH CONCEPT

After the survey confirmed the gripping problem, the recommended design was chosen for further investigation. The favored shape dimensions were gathered from the market, and the Taguchi method was utilized to create the experiment. The 3D perfume model was built using a 3D printer, and the Grey-Relation analysis was integrated with Kansei engineering to determine the user's grip comfort based on their feeling. The diagram (Fig. 1) depicts the flowchart of this research.

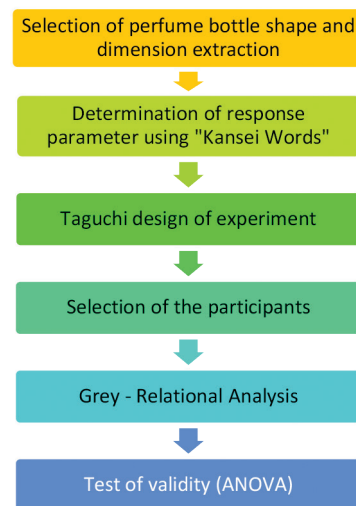


Fig. 1. Methodology

##### A. Selection of Perfume Bottle Shape and Dimension Extraction

The rectangular shape of 100 ml was chosen for this investigation since it received the highest rating on the survey questionnaire. The potential dimensions of the perfume bottles were extracted, and a range was determined for use in the experiment design. Dimensions were gathered from numerous sources on the internet like [51] as well as from store-bought bottles show in Fig. 2(a) and 2(b).

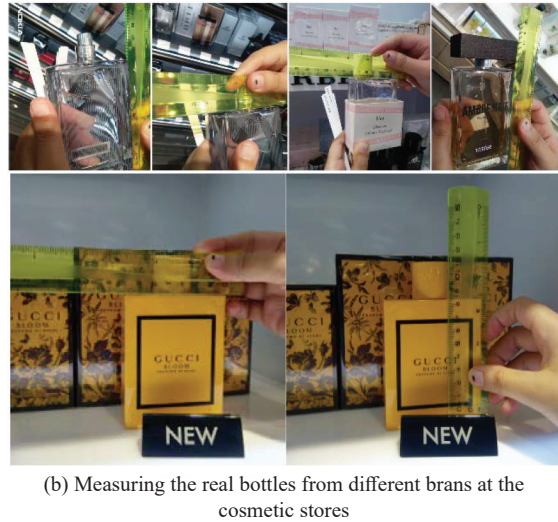
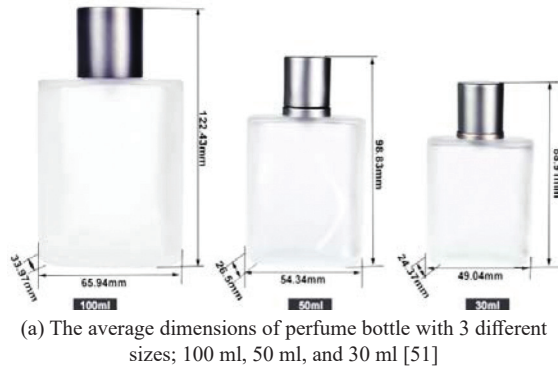


Fig. 2. Dimension extraction of perfume bottle

Many concepts have been applied in this study for obtaining clean and clear results where the designs of the perfume bottle can be introduced to support users in different categories [51]-[58]. Total Height is obtained from the sum of height from bottom to neck and height from neck to top. Table III shows the extracted dimension for carrying out the design of the experiment. Fig. 3 depicts the parameters for the perfume bottle study.

TABLE III  
THE EXTRACTED DIMENSIONS

Length	Width	Height bottom to Neck	Neck to top Height	Position of Spray
(A)	(B)	(C)	(D)	(E)
55	30	90	30	Left
65	33	96	35	Middle
70	36	105	39	Right

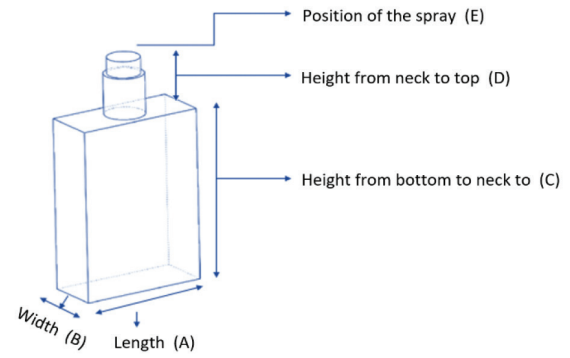


Fig. 3. The main components of perfume bottle

**B. Determination of Response Parameter Using Kansei Words**

Kansei is a Japanese word that refers to a customer’s feelings and emotions. Kansei engineering blends human emotions and feelings to design fields in order to build a product that reflects consumer feelings and maximizes customer delight. Kansei words shown in Table IV are primarily chosen to elicit a customer’s emotion to the product. To apply Kansei to the realm of design, qualitative data must be quantified [52]. The user’s feelings toward product characteristics were quantified using a semantics scale of 1-7.

TABLE IV  
SELECTION OF KANSEI WORDS

Product Characteristics	Descriptions
Hand/ Wrist Comfort	Wrist and hand motion are both relaxing while using the product
Overall Comfort	While utilizing the product, comfort is felt in the palm, finger joints, and virtually everything else in the human hand.
Safety	Condition of Protection from injury
User-friendly	Easy to use operate and understand

**C. Design of Experiment**

The Taguchi method is mostly used to build the experimental design for this project. Taguchi Design is a statistical method for planning and assessing trials aimed at improving product quality [50], [53]. To examine the process, the original data is converted to a signal-to-noise (S/N) ratio, which is the ratio of the mean to the standard deviation. Lower-the-better, higher-the-better, and nominal-the-better [50], [54] are the three types of S/N ratios.

For, this study higher the better (S/N) is preferred, and the following equation was used for Higher-the-better (S/N):

$$\frac{s}{N} \text{ ratio} = -10 \log \left( \frac{1}{n} \sum_{i=1}^n \frac{1}{Z_{ij}^2} \right) \quad (2)$$

Where,

- n = number of replicates
- Z<sub>ij</sub> = response observed value at i<sup>th</sup> replication of j<sup>th</sup> response
- i = 1, 2, ..., n
- j = 1, 2, ..., k

#### D. Fabricating Perfume Prototype

Once the experiment was developed, the perfume bottles were printed according to their run. The perfume bottle was created utilizing ABS (Acrylonitrile Butadiene Styrene) material and XYZ 3D Printer with different views as shown below (Fig. 4) to get responses from the users. Illustrated in Fig. 5 are the perfume bottle samples that were fabricated by using rapid prototyping (RP) - 3D Printing process where the physical parameters were obtained from the above experimental design. Three classic styles of the nozzle-head pressing set are introduced; the left RP model presents the pressing set on the left-hand side of the bottle, the middle RP model shows the middle area of pressing activity, and the right RP model provides the nozzle-head set at the right-hand side of the bottle.

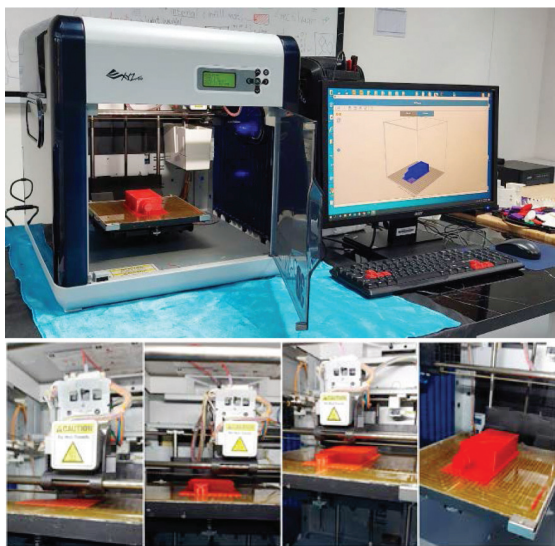


Fig. 4. 3D printing machine with different views during fabricating sample models of the perfume bottles

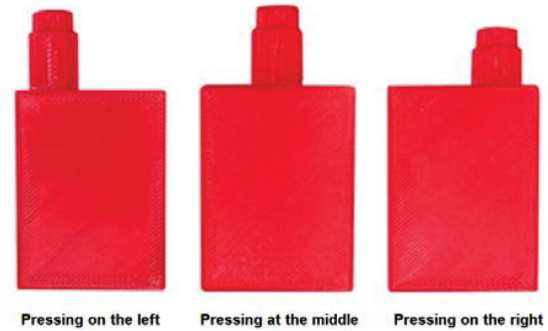


Fig. 5. Three styles of printed perfume bottle samples

#### E. Selection of Participants

The study included thirty participants (15 men and 15 women) with an average age of 22.6 years and a standard deviation of 3.2 years. A university dormitory population was used to choose all of the participants. They were all right-handed and in good health, with no musculoskeletal issues in their wrists. Individuals with a variety of hand lengths, including short, medium, and long-handed, were enlisted. Every participant signed a consent form and was compensated for their time. The experimental protocol was approved by the local institutional review board. Short (177.5 mm, 30th % ile), medium (177.6-180.3 mm, 45th-55th % ile), and long (120.3 mm, 70th and greater % ile) were the three categories for men’s hand length. Short (165.7 mm, 30th % ile), medium (167.6-170.5 mm, 45th-55th % ile), and long (190.5 mm, 70th% ile and greater) were the three categories for female hand length. Previous research has revealed a similar measurement [57]. Participants were requested to offer their response by gripping the bottle in their hand and expressing the relevant semantic number with reference to Kansei words.

#### F. Grey Relational Analysis

Grey Relational analysis is a useful method for supporting decision-making in ambiguous circumstances and situations with varying quality by evaluating the similarity of variables in each alternative to the best choice [55]. Taguchi mainly fails for optimizing the multi- objective problems thus grey relational analysis was selected which has ability for multi-objective optimization mainly by exploring the relationship between the variables and the responses [50], [56]. The steps involved in Grey Relation Analysis are given below as:

**Step 1.** Normalization of signal to noise ratio as  $P_{ij}$  ( $0 < P < 1$ ) given by Eq. (3)  
 For “Higher-the-better”

$$P_{ij} = \frac{Q_{ij} - (Q_{ij})_{\min}}{(Q_{ij})_{\max} - (Q_{ij})_{\min}} \quad (3)$$

Where,

- $P_{ij}$  = the noramalized value
- $Q_{ij} \min$  refers to the minimum value max
- $Q_{ij} \max$  refers to the maximum value at i th replicate of j th response
- $i$  = 1,2,...,n
- $j$  = 1,2,...,k

**Step 2.** Calculation of the deviation sequence Eq. (4).

$$\Delta_{ij} = |Q_0 - Q_{ij}| \quad (4)$$

$Q_{oj}$  = optimum performance value of the j th response

**Step 3.** Calculation of Grey relational coefficient from the deviation sequence from the given equation:

$$GRC_{ij} = \frac{\Delta_{\min} + \delta \Delta_{\max}}{\Delta_{ij} + \delta \Delta_{\max}} \quad (5)$$

Where,

- $GRC_{ij}$  the grey relational coefficient for the i th replicate of j the response
- $\Delta_{ij}$  = the deviation sequence
- $\Delta_{\min}$  = minimum value of delta
- $\Delta_{\max}$  = maximum value of delta
- $\delta$  distinguishing coefficient which is defined in the range  $0 \leq \delta \leq 1$

**Step 4.** Using the average of the grey relational coefficient, the grey relational grade is calculated by the given equation as:

$$G_i = \frac{1}{k} \sum_{j=1}^k G C_{ij} \quad (6)$$

Where,

- $G_i$  = grey relational grad for the i th replicate
- $k$  = the number of responses

*G. Analysis of Variance*

The hypothesis that the means of two or more populations are equal is tested using analysis of variance (ANOVA). ANOVA compares the response variable means at different factor levels to determine the importance of one or more factors [58].

V. RESULT AND DISCUSSION

A. Taguchi Experimental Design and Result

The Taguchi design was mostly used in this study. For five factors and three levels, the L 27 orthogonal array was employed. The users’ semantic replies for Kansei words were collected and averaged. The higher the better the S/N ratio was employed. Minitab 19 was used for the experiment design and signal-to-noise ratio analyses. Table V depicts the experimental design.

TABLE V  
TAGUCHI DESIGN OF EXPERIMENT

No. of Iteration	Bottle Design parameters				
	Length (A)	Width (B)	Height from Bottom to Neck (C)	Neck to top Height (D)	Position of Spray (E)
1	55	30	90	30	Left
2	55	30	90	30	Middle
3	55	30	90	30	Right
4	55	33	96	35	Left
5	55	33	96	35	Middle
6	55	33	96	35	Right
7	55	36	105	39	Left
8	55	36	105	39	Middle
9	55	36	105	39	Right
10	65	30	96	39	Left
11	65	30	96	39	Middle
12	65	30	96	39	Right
13	65	33	105	30	Left
14	65	33	105	30	Middle
15	65	33	105	30	Right
16	65	36	90	35	Left
17	65	36	90	35	Middle
18	65	36	90	35	Right
19	70	30	105	35	Left
20	70	30	105	35	Middle
21	70	30	105	35	Right
22	70	33	90	39	Left
23	70	33	90	39	Middle
24	70	33	90	39	Right
25	70	36	96	30	Left
26	70	36	96	30	Middle
27	70	36	96	30	Right

In practice, the ways to identify the size of the hands (for both left and right ones) are quite subjective and difficult, therefore, in this research, the customer perceptions and experiences were very



useful and crucial for classifying dimensions of hands into three categories: short, medium, and long hands. The responses of participants with short, medium, and long-size hands are converted to signal to noise ratio.

The “Higher- the better” S/N ratios for each of the participant feelings were determined using Eq. (2). Table VI to VIII show the S/N ratio of participants with three sizes of hands: short, medium, and long, respectively.

TABLE VI  
S/N RATIO FOR SHORT-SIZE HANDS

No. of Iteration	S/N Hand to Wrist Comfort	S/N Overall Comfort	S/N Safety	S/N User Friendliness
1	13.1515	13.1318	13.1115	13.0908
2	13.6166	13.6082	13.5995	13.5493
3	13.4504	13.4799	13.4682	13.4142
4	13.4922	13.5225	13.4701	13.4161
5	13.6166	13.6082	13.5582	13.5898
6	13.6985	13.7328	13.7271	13.7618
7	13.4083	13.3949	13.3387	13.2809
8	13.2380	13.1772	13.2013	13.2689
9	13.6985	13.6920	13.6445	13.5955
10	13.6985	13.7328	13.7676	13.7628
11	13.0643	13.0862	13.1085	13.1747
12	12.9316	12.9952	13.0597	13.1252
13	14.2131	14.1799	14.2228	14.2283
14	13.9001	13.8583	13.8955	13.8536
15	14.2131	14.2184	14.1852	14.2283
16	14.1359	14.1394	14.2202	14.3020
17	13.9398	13.8992	13.8574	13.8546
18	13.2380	13.2204	13.2454	13.2280
19	14.2515	14.2192	14.1861	14.1522
20	13.8601	13.8574	13.8946	13.9720
21	12.9761	12.9962	13.0607	13.0825
22	13.1949	13.1762	13.1570	13.0938
23	13.4504	13.5216	13.5938	13.6261
24	13.6985	13.7733	13.7685	13.8041
25	13.7797	13.8155	13.8918	13.9296
26	13.4922	13.4808	13.5109	13.5416
27	13.1949	13.1328	13.1125	13.1788

TABLE VII  
S/N RATIO FOR MEDIUM-SIZE HANDS

No. of Iteration	S/N Hand to Wrist Comfort	S/N Overall Comfort	S/N Safety	S/N User Friendliness
1	13.2236	12.3958	13.0643	13.3801
2	13.2236	13.0643	12.9019	11.8583
3	13.6849	12.7364	12.9019	13.9794
4	13.6849	13.2236	12.7364	13.0643
5	13.0643	12.7364	14.5400	13.2236
6	12.5678	13.6849	12.7364	13.0643
7	12.0412	12.5678	13.6849	13.0643
8	12.0412	13.0643	12.7364	11.8583
9	13.6849	13.6849	13.8334	13.2236
10	13.3801	13.8334	12.3958	12.9019
11	12.5678	13.2236	12.9019	12.9019
12	13.9794	13.3801	13.0643	13.3801
13	13.5339	12.7364	12.9019	13.3801
14	13.8334	13.2236	13.3801	13.3801
15	13.6849	13.3801	12.7364	13.2236
16	14.8073	13.9794	14.1230	14.1230
17	14.4032	14.8073	14.2642	14.8073
18	13.9794	13.6849	13.5339	13.0643
19	13.9794	12.9019	13.0643	12.3958
20	12.9019	12.9019	12.0412	11.6715
21	13.0643	13.5339	13.5339	11.0857
22	12.3958	11.4806	12.0412	12.3958
23	13.0643	13.0643	13.2236	11.4806
24	13.3801	13.5339	12.5678	11.8583
25	13.2236	13.3801	12.3958	12.7364
26	12.7364	13.2236	12.7364	11.8583
27	12.0412	13.6849	12.0412	12.0412

TABLE VIII  
S/N RATIO FOR LONG-SIZE HANDS

No. of Iteration	S/N Hand to Wrist Comfort	S/N Overall Comfort	S/N Safety	S/N User Friendliness
1	12.2203	12.4273	12.2203	12.7364
2	12.3958	12.6141	12.9019	12.5678
3	11.2854	12.6141	13.5339	13.8334
4	11.2854	13.8200	13.3801	13.8334
5	12.7364	13.4922	13.2236	13.3801
6	13.0643	12.7970	12.7364	13.0643
7	12.2203	12.7970	12.7364	12.7364
8	13.2236	13.4922	12.0412	12.2203
9	11.8583	12.9761	13.2236	13.2236
10	12.9019	13.6577	11.8583	12.0412
11	12.5678	12.4273	13.3801	12.7364
12	12.9019	12.9761	13.8334	14.1230
13	12.0412	13.3235	13.2236	13.3801
14	12.2203	13.3235	13.6849	13.9794
15	12.9019	13.6577	11.6715	12.5678
16	12.9019	14.1359	13.5339	13.0643
17	13.6849	14.8787	12.9019	13.2236
18	12.7364	13.4922	13.5339	12.3958
19	12.3958	12.9761	13.0643	12.9019
20	12.5678	14.1359	11.6715	13.2236
21	12.3958	14.2896	13.2236	12.5678
22	12.2203	13.4922	12.9019	13.8334
23	11.8583	12.7970	12.5678	12.7364
24	11.2854	12.6141	12.2203	13.2236
25	12.3958	13.3235	13.5339	14.1230
26	12.5678	12.9761	13.3801	13.6849
27	12.3958	13.1515	11.6715	13.5339

*B. Grey Relation Analysis Result*

This section will discuss how to identify the proper conditions and physical characteristics of a perfume design where Eq. (3) was used to normalize the “Higher-the-better” S/N ratio, and Eq. (4) was used to compute the deviation sequence value utilizing the normalized value. The deviation sequence value was used to calculate the grey relational coefficient

by using Eq. (5), and the grey relational coefficient was then used to calculate the grey relational grade by using Eq. (6).

Finally, using their grade values, the grey relational average grade for each level of parameters for the respective hand was calculated to obtain the ideal perfume bottle model. Tables IX to XI shows the grey relation coefficient and grade for short-size hands, medium-sized hands, and long-size hands.

TABLE IX  
GREY RELATIONAL COEFFICIENT AND GRADE (SHORT-SIZE HANDS)

No. of Iteration	Grey Relational Coefficient (Short-size Hands)				Grade	Rank
	Hand to Wrist Comfort	Overall Comfort	Safety	User Friendliness		
1	0.3750	0.3601	0.3435	0.3348	0.3534	24
2	0.5097	0.5004	0.4827	0.4475	0.4851	13
3	0.4517	0.4529	0.4352	0.4071	0.4367	18
4	0.4650	0.4676	0.4359	0.4077	0.4440	17
5	0.5097	0.5004	0.4667	0.4612	0.4845	14
6	0.5441	0.5571	0.5398	0.5302	0.5428	11
7	0.4390	0.4261	0.3968	0.3739	0.4089	19
8	0.3944	0.3700	0.3628	0.3712	0.3746	21
9	0.5441	0.5372	0.5014	0.4633	0.5115	12
10	0.5441	0.5571	0.5609	0.5307	0.5482	10
11	0.3573	0.3507	0.3429	0.3510	0.3505	25
12	0.3333	0.3333	0.3333	0.3413	0.3353	27
13	0.9451	0.9396	1.0000	0.8922	0.9442	1
14	0.6525	0.6291	0.6399	0.5762	0.6244	7
15	0.9451	0.9986	0.9393	0.8922	0.9438	2
16	0.8510	0.8847	0.9955	1.0000	0.9328	4
17	0.6792	0.6566	0.6141	0.5768	0.6317	6
18	0.3944	0.3799	0.3730	0.3621	0.3774	20
19	1.0000	1.0000	0.9406	0.8027	0.9358	3
20	0.6277	0.6285	0.6392	0.6489	0.6361	5
21	0.3410	0.3335	0.3335	0.3333	0.3353	26
22	0.3845	0.3698	0.3530	0.3354	0.3607	22
23	0.4517	0.4673	0.4804	0.4743	0.4684	15
24	0.5441	0.5785	0.5614	0.5505	0.5586	9
25	0.5831	0.6025	0.6373	0.6208	0.6109	8
26	0.4650	0.4532	0.4496	0.4450	0.4532	16
27	0.3845	0.3603	0.3437	0.3519	0.3601	23

TABLE X  
GREY RELATIONAL COEFFICIENT AND GRADE  
(MEDIUM-SIZE HANDS)

No. of Iteration	Grey Relational Coefficient (Med.-size Hands)				Grade	Rank
	Hand to Wrist Comfort	Overall Comfort	Safety	User Friendliness		
1	0.4662	0.4082	0.4585	0.5659	0.4747	15
2	0.4662	0.4883	0.4327	0.3869	0.4435	22
3	0.5520	0.4454	0.4327	0.6921	0.5306	8
4	0.5520	0.5123	0.4092	0.5163	0.4975	10
5	0.4424	0.4454	1.0000	0.5402	0.6070	3
6	0.3818	0.5971	0.4092	0.5163	0.4761	14
7	0.3333	0.4262	0.5937	0.5163	0.4674	17
8	0.3333	0.4883	0.4092	0.3869	0.4044	25
9	0.5520	0.5971	0.6388	0.5402	0.5820	4
10	0.4922	0.6307	0.3682	0.4941	0.4963	12
11	0.3818	0.5123	0.4327	0.4941	0.4552	20
12	0.6256	0.5382	0.4585	0.5659	0.5470	6
13	0.5206	0.4454	0.4327	0.5659	0.4912	13
14	0.5868	0.5123	0.5186	0.5659	0.5459	7
15	0.5520	0.5382	0.4092	0.5402	0.5099	9
16	1.0000	0.6677	0.7498	0.7311	0.7871	2
17	0.7739	1.0000	0.8192	1.0000	0.8983	1
18	0.6256	0.5971	0.5539	0.5163	0.5732	5
19	0.6256	0.4661	0.4585	0.4355	0.4964	11
20	0.4206	0.4661	0.3333	0.3724	0.3981	26
21	0.4424	0.5664	0.5539	0.3333	0.4740	16
22	0.3645	0.3333	0.3333	0.4355	0.3667	27
23	0.4424	0.4883	0.4870	0.3587	0.4441	21
24	0.4922	0.5664	0.3878	0.3869	0.4583	19
25	0.4662	0.5382	0.3682	0.4733	0.4615	18
26	0.4004	0.5123	0.4092	0.3869	0.4272	23
27	0.3333	0.5971	0.3333	0.4022	0.4165	24

TABLE XI  
GREY RELATIONAL COEFFICIENT AND GRADE

No. of Iteration	Grey Relational Coefficient (Long-size Hands)				Grade	Rank
	Hand to Wrist Comfort	Overall Comfort	Safety	User Friendliness		
1	0.4503	0.3333	0.4012	0.4288	0.4034	27
2	0.4820	0.3512	0.5371	0.4009	0.4428	23
3	0.3333	0.3512	0.7830	0.7824	0.5625	9
4	0.3333	0.5366	0.7046	0.7824	0.5892	6
5	0.5585	0.4692	0.6393	0.5835	0.5626	8
6	0.6590	0.3706	0.4963	0.4958	0.5054	14
7	0.4503	0.3706	0.4963	0.4288	0.4365	24
8	0.7223	0.4692	0.3762	0.3536	0.4803	18
9	0.3964	0.3918	0.6393	0.5365	0.4910	17
10	0.6051	0.5009	0.3537	0.3333	0.4483	22
11	0.5178	0.3333	0.7046	0.4288	0.4961	16
12	0.6051	0.3918	1.0000	1.0000	0.7492	2
13	0.4219	0.4408	0.6393	0.5835	0.5214	13
14	0.4503	0.4408	0.8792	0.8788	0.6623	4
15	0.6051	0.5009	0.3333	0.4009	0.4601	21
16	0.6051	0.6226	0.7830	0.4958	0.6266	5
17	1.0000	1.0000	0.5371	0.5365	0.7684	1

No. of Iteration	Grey Relational Coefficient (Long-size Hands)				Grade	Rank
	Hand to Wrist Comfort	Overall Comfort	Safety	User Friendliness		
18	0.5585	0.4692	0.7830	0.3760	0.5467	12
19	0.4820	0.3918	0.5843	0.4602	0.4796	19
20	0.5178	0.6226	0.3333	0.5365	0.5026	15
21	0.4820	0.6754	0.6393	0.4009	0.5494	11
22	0.4503	0.4692	0.5371	0.7824	0.5597	10
23	0.3964	0.3706	0.4606	0.4288	0.4141	25
24	0.3333	0.3512	0.4012	0.5365	0.4056	26
25	0.4820	0.4408	0.7830	1.0000	0.6765	3
26	0.5178	0.3918	0.7046	0.7038	0.5795	7
27	0.4820	0.4151	0.3333	0.6386	0.4673	20

The optimal model of the perfume bottle that could contain values of participants' emotions and feelings was determined and listed into Table XII to XIV.

For the "short-size hands", the suggestions were shown as: the length (65 mm) at level 2, width (33 mm) at level 2, height bottom to neck (90 mm) at level 1, height from neck to top (35 mm) at level 2, and position of spray at left at level 1, as listed in Table XII

TABLE XII  
GREY RELATIONAL AVERAGE GRADE FOR EACH LEVEL OF PARAMETERS (SHORT-SIZE HANDS)

Level	Length (A)	Width (B)	Height bottom to Neck (C)	Neck to top Height (D)	Position of Spray (E)
1	0.4491	0.4907	0.5116	0.5791	0.5313
2	0.6320	0.5968	0.4014	0.5912	0.5009
3	0.5244	0.5179	0.4014	0.4352	0.4352
Delta	0.1830	0.1061	0.1103	0.1560	0.0961
Rank	1	4	3	2	5

The optimum design of perfume bottles for short-hand users is depicted in the figure below (Fig. 6) as;

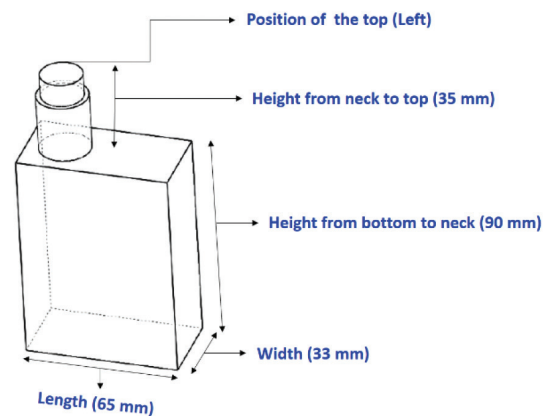


Fig. 6. Optimum perfume bottle design for "short-size hand" users

For the “medium-size hands”, the suggestions were shown as the length (65 mm) at level 2, width (36 mm) at level 3, the height bottom to neck (90 mm) at level 1, the height from neck to top (35 mm) at level 2 and the position of spray in middle at level 2 as presented in Table XIII and Fig. 7.

TABLE XIII  
GREY RELATIONAL AVERAGE GRADE FOR EACH LEVEL OF PARAMETERS (MEDIUM-SIZE HANDS)

Level	Length (A)	Width (B)	Height bottom to Neck (C)	Neck to top Height (D)	Position of Spray (E)
1	0.4982	0.4698	0.5530	0.4779	0.5043
2	0.5894	0.4886	0.4871	0.5786	0.5130
3	0.4381	0.5575	0.4855	0.4691	0.5075
Delta	0.1513	0.0877	0.0675	0.1096	0.0087
Rank	1	3	4	2	5

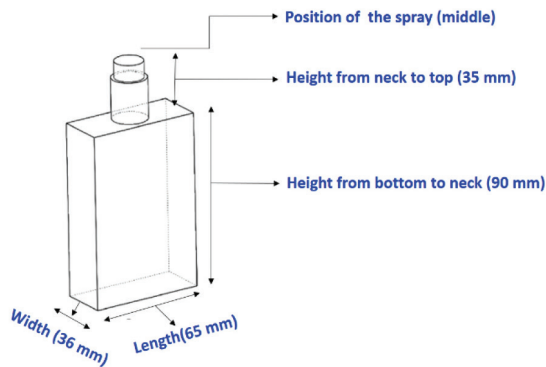


Fig. 7. Optimum perfume bottle design for “medium-size hand” users

For the “long-size hands”, the suggestions were shown as the length (65 mm) at level 2, width (33 mm) at level 2, the height bottom to the neck (96 mm) at level 2, the height from neck to top (35 mm) at level 2 and the position of spray in middle at level 2 as presented in Table XIV and Fig. 8.

TABLE XIV  
GREY RELATIONAL AVERAGE GRADE FOR EACH LEVEL OF PARAMETERS (LONG-SIZE HANDS)

Level	Length (A)	Width (B)	Height bottom to Neck (C)	Neck to top Height (D)	Position of Spray (E)
1	0.4971	0.5200	0.5255	0.5306	0.5268
2	0.5866	0.5636	0.5638	0.5701	0.5454
3	0.1521	0.5200	0.5092	0.4979	0.5263
Delta	0.4345	0.0436	0.0546	0.0722	0.0191
Rank	1	4	3	2	5

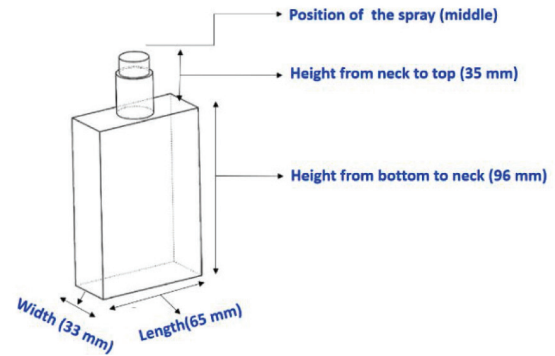


Fig. 8. Optimum perfume bottle design for “long-size hand” users

C. ANOVA for the Grey Relational Grade

The percentage contribution of each shape parameter in the response variable is attributed using ANOVA to determine which of the shape parameters are significant and influence the consumer emotions and experiences. Fig. 9 to Fig. 11 are the ANOVA results to support the perfume design of “short, medium, and long-size-hand” users.

• Analysis of Variance – (Short-Size Hands)

Source	DF	Adj SS	Adj MS	F-Value	P-Value	Contribution
Length	2	0.1522	0.0761	2.9	0.084	24%
Width	2	0.0547	0.0273	1.04	0.375	9%
Height from Bottom to Neck	2	0.147	0.0735	2.81	0.09	23%
Neck to top Height	2	0.1355	0.0678	2.59	0.106	22%
Position of Spray	2	0.0877	0.0438	1.67	0.219	14%
Error	16	0.4193	0.0262			8%
Total	26	0.9964				100%

Fig. 9. ANOVA results to support the perfume design of “short-size hand” users

None of the parameters appear to be significant in the ANOVA for “short-size hand users” based on this table. With contributions of 24%, 23%, and 22%, respectively, bottle length (A), height from bottom to the neck (C), and height from neck to top (D) supplied the most variability, while width (B) and spray position (E) (14%) contributed the least.

• Analysis of Variance – (Medium-Size Hands)

Source	DF	Adj SS	Adj MS	F-Value	P-Value	Contribution
Length	2	0.1044	0.0522	8.26	0.003	43%
Width	2	0.0328	0.0164	2.59	0.106	13%
Height from Bottom to Neck	2	0.0266	0.0133	2.11	0.154	11%
Neck to top Height	2	0.0667	0.0334	5.27	0.017	27%
Position of Spray	2	0.0004	0.0002	0.03	0.968	0%
Error	16	0.1012	0.0063			5%
Total	26	0.3322				100%

Fig. 10. ANOVA results to support the perfume design of “medium-size hand” users

Only the length (A) and neck-to-top height (D) were significant in influencing the grey relational grade values, accounting for 43% and 27% of total variability, respectively. As a result, the length (A) and neck-to-top height (D) were the most important factors influencing client sentiments and feelings. The remaining variables, such as height from bottom to the neck (C), width (B), and spray position (E), were found to be insignificant, and their effects were minimal.

#### • Analysis of Variance – (Long-Size Hands)

Source	DF	Adj SS	Adj MS	F-Value	P-Value	Contribution
Length	2	0.0404	0.0202	2.08	0.158	36%
Width	2	0.0129	0.0065	0.66	0.528	11%
Height from Bottom to Neck	2	0.0141	0.0071	0.73	0.499	13%
Neck to top Height	2	0.0235	0.0118	1.21	0.324	21%
Position of Spray	2	0.0021	0.0011	0.11	0.897	2%
Error	16	0.1554	0.0097			17%
Total	26	0.2485				100%

Fig. 11. ANOVA results to support the perfume design of “long-size hand” users

None of the parameters for long-hand users appear to be significant in the ANOVA based on this table. With 36%, 13%, and 21% contributions, respectively, bottle length (A), height from bottom to neck the (C), and height from neck to top (D) offered the most variability, whereas width (B) with 11% and spray position (E) with (14 %) gave the least.

## VI. CONCLUSION

This study mostly relied on customer feedback to identify a gripping problem in a perfume bottle caused by inappropriate dimensions. This challenge was solved by using the Taguchi method to create an experimental design, using Kansei words to elicit user sentiment about grip comfort, and using grey relational analysis to find the best combination of perfume bottle dimensions. For users with short, medium, and long hands, three optimum parameters for bottle design were discovered. The length (65 mm), breadth (33 mm), height from bottom to neck (90 mm), height from neck to top (35 mm), and position of spray at left was the recommended design of perfume bottle for small hand users that could store values of participants’ emotions and sentiments. The length (65 mm), width (36 mm), height from bottom to the neck (90 mm), height from neck to top (35 mm), and the position of spray in the middle at was the

optimal design model of rectangular perfume bottles that could carry values of consumer emotions and feelings for medium hand users. The ideal design model of the rectangular perfume bottle that could hold values of customer emotions and sentiments for long-hand users was the length (65 mm), width (33 mm), height bottom to the neck (96 mm), height from neck to top (35 mm), and the position of spray in the middle. The length (65 mm), width range (33-36 mm), height from bottom to neck (90-96 mm), height from neck to top (35 mm), and position of spray in the middle could be considered the ideal design framework for rectangular perfume bottles for users of all sizes of hands that can store values of participants’ emotions and sentiments. In the case of short long-hand users, none of the dimension factors were shown to be significant in rectangular perfume bottle design. In the case of medium-hand users, length and height from neck to top factors were determined to be significant in the dimensional design of perfume bottles. In all cases, length, height from the bottom to the neck, and height from the neck to the top contributed the most to the variation, while width and spray position contributed the least. This study aims to demonstrate the importance of gripping comfort, which appears to be overlooked in perfume bottle design. This research also addresses the issue of gripping comfort by determining the right dimensions of rectangular perfume bottles using a hybrid optimization technique based on the emotion of the customer. The analysis of customer emotions was primarily used to boost customer willingness to buy. Other perfume bottle shapes could be subjected to a similar investigation.

## VII. LIMITATIONS OF THIS STUDY

This research was carried out in Thailand. In this study, only right-handed university students were used as participants. The study was based on customer emotion and feelings in order to determine the appropriate size of the perfume bottle enhancing purchase willingness. This study did not include any musculoskeletal examination for grip comfort.

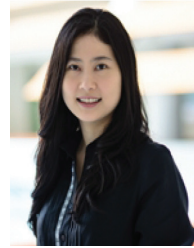
## ACKNOWLEDGEMENT

This research study is supported by School of Manufacturing Systems and Mechanical Engineering, Sirindhorn International Institute of Technology, Thammasat University, Thailand.

## REFERENCES

- [1] W. Tien-You, "Incorporating Customer Preference in Perfume Bottle Design," *International Journal of Scientific and Research Publications*, vol. 2, no. 9, pp. 1-5, Sep 2012.
- [2] C. Pei, "The Study of Perfume's Purchase Criteria Comparing Irregular and Regular Users of Customers in Bangkok," Independent Study (M.B.A), Graduate School, Bangkok Univ., Bangkok, Thailand, 2019.
- [3] Grand View Research. (2021, Jul. 11). *Perfume Market Size, Share & Trends Analysis Report*. [Online]. Available: <https://www.grandviewresearch.com/industryanalysis/perfume-market>
- [4] Statista. (2021, Jul. 2). *Fragrances*. [Online]. Available: <https://bit.ly/3nqk4fz>
- [5] D. Elango and V. Thansupatpu, "The Factors Affecting Local Brand Perfume Packaging on Consumers Purchase Decision in Bangkok," *Journal of Management, Economics, and Industrial Organization*, vol. 4, no. 2, pp. 59-76, May. 2020.
- [6] M. Sivagnanasundaram, "Effect of Packaging on Perfume Purchase Decision of Consumers", *Journal of Management Research and Analysis*, vol. 6, no. 1, pp. 6-20, Mar. 2019.
- [7] R. Al Saed, M. Abu-Salih, A. H. Hussien et al, "The Impact of Perfume Packaging on Consumer Buying Behavior of Jordanian Female," *International Journal of Business Excellence*, vol. 1, no. 1, pp. 1, May. 2020.
- [8] M. Z. Salem, "Effects of Perfume Packaging on Basque Female Consumers Purchase Decision in Spain. Management Decision," *Management Decision*, vol. 56, no. 8, Jul. 2018.
- [9] A. S. Abusrour, "Factors Affecting Consumers' Choice of Perfume Products: The Case of Famagusta-North Cyprus," M.S. thesis, Eastern Mediterranean University-Doğu Akdeniz Üniversitesi, Famagusta, Turkey, 2016.
- [10] K. E. Neuschildkamp, "Effects of Design Aspects in Advertising on Odour Perception of Consumers," M.S. thesis, University of Twente, Enschede, Netherlands, 2012.
- [11] Y. C. Lin, C. C. Wei, and Y. T. Chen, "Emotional Design: A Multisensory Evaluation to Visual and Olfactory Perceptions of Consumers," in *Proc. IEEE CASI*, 2018, pp. 1292-1295.
- [12] H. Y. Chen, H. C. Chang, and C. I. Huang, "Potential Dimensions of Consumers Affective Responses to Perfume Bottle Form," *Journal of Design Research*, vol. 16, no. 1, pp. 47-63, Jul. 2017.
- [13] Y. C. Lin and C. C. Wei, "A Hybrid Consumer-Oriented Model for Product Affective Design: An Aspect of Visual Ergonomics," *Human Factors and Ergonomics in Manufacturing and Service Industries*, vol. 27, no. 1, pp. 17-29, Sep. 2016.
- [14] A. S. Abusrour, "Factors Affecting Consumers' Choice of Perfume Products: The Case of Famagusta-North Cyprus," M.S. thesis, Eastern Mediterranean Univ. North Cyprus, Turkey, 2016.
- [15] K. E. Neuschildkamp, "Effects of Design Aspects in Advertising on Odour Perception of Consumers," M.S. thesis, University of Twente, Enschede, Netherlands, 2012.
- [16] T. Y. Lee and E. T. Bradlow, "Automated Marketing Research using Online Customer Reviews," *Journal of Marketing Research*, vol. 48, no. 5, pp. 881-894, Oct. 2011.
- [17] P. D. Turney, "Thumbs up or Thumbs Down? Semantic Orientation Applied to Unsupervised Classification of Reviews," in *Proc. The 40th Annual Meeting of the Association for Computational Linguistics*, 2002, pp. 417-424.
- [18] T. Nasukawa and J. Yi, "Sentiment Analysis: Capturing Favorability using Natural Language Processing," in *Proc. The 2nd International Conference on Knowledge Capture*, 2003, pp. 70-77.
- [19] B. Jeong, J. Yoon, and J. M. Lee, "Social Media Mining for Product Planning: A Product Opportunity Mining Approach Based on Topic Modeling and Sentiment Analysis," *International Journal of Information Management*, vol. 48, pp. 280-290, Oct. 2019.
- [20] Fragrantica. (2021, Jul. 11). *Fragrantion Reviewer*. [Online]. Available: <https://www.fragrantica.com>
- [21] S. L. Johnson, "Ergonomic Design of Handheld Tools to Prevent Trauma to the Hand and Upper Extremity," *Journal of Hand Therapy*, vol. 3, no. 2, pp. 86-93, Apr. 1990.
- [22] H. Y. Chen, and H. C. Chang, "Extraction of Potential Dimensions for Consumers' Psychological Perceptions Regarding Perfume Bottle Form," *Journal of Design Research*, vol. 16, no. 1, pp. 47-6, Apr. 2018.
- [23] C. C. Wei, M. Y. Ma, and Y. C. Lin, "Applying Kansei Engineering to Decision Making in Fragrance form Design," in *Proc. Intelligent Decision Technologies*, Springer, Berlin, Heidelberg. 2011, pp. 85-94.
- [24] Y. Chen and J. Xie, "Online Consumer Review: Word-of-Mouth as a New Element of Marketing Communication Mix," *Management Science*, vol. 54, no. 3, pp. 477-491, Mar. 2008.
- [25] S. M. Mudambi and D. Schuff, "Research Note: What Makes a Helpful Online Review? A Study of Customer Reviews on Amazon. Com," *MIS Quarterly*, vol. 35, no. 1, pp. 185-200, Mar. 2010.
- [26] G. Askalidis and C. Malthouse, "The Value of Online Customer Reviews," in *Proc. The 10th ACM Conference on Recommender Systems*, 2016, pp. 155-158.
- [27] H. S. Kim and Y. Noh, "Elicitation of Design Factors through Big Data Analysis of Online Customer Reviews for Washing Machines," *Journal of Mechanical Science and Technology*, vol. 33, no. 6, pp. 2785-2795, Jun. 2019.
- [28] S. Rianmora, K. Poulpanich, J. Rattanagosol et al., "JMM Gimbal Stabilizer," *International Scientific Journal of Engineering and Technology*, vol. 3, no. 1, pp. 31-40, Jun. 2019.
- [29] S. Rianmora, D. Padnoi, T. Rattanopas et al., "Alternative Design for Salad Spinner-Sallatë," *International Scientific Journal of Engineering and Technology*, vol. 3, no. 2, pp. 1-14, Dec. 2019.
- [30] J. H. Kim, Z. T. Bae, and S. H. Kang, "The Role of Online Brand Community in New Product Development: Case Studies on Digital Product Manufacturers in Korea," *International Journal of Innovation Management*, vol. 12, no. 3, pp. 357-376, 2008.
- [31] Fragrantica. (2021, Jul. 11). *Cologne Bottle Ergonomics*. [Online]. Available: <https://bit.ly/3Bet6kO>
- [32] Fragrantica. (2021, Jul. 11). *Hard-to-Hold Bottles*. [Online]. Available: <https://bit.ly/3vH2ZC7>
- [33] Fragrantica. (2021, Sep. 11). *What Size Bottles do You Normally Buy?* [Online]. Available: <https://bit.ly/3BcOBCB>
- [34] Fragrantica. (2021, Jul. 11). *Bottle Sizes?* [Online]. Available: <https://bit.ly/3m77faM>
- [35] Fragrantica. (2021, Jul. 11). *What Size of Perfume Bottle do You Usually Buy?* [Online]. Available: <https://bit.ly/3B9AJcq>
- [36] Fragrantica. (2021, Jul. 11). *Size of Perfume Bottles?* [Online]. Available: <https://bit.ly/3Cche4e>
- [37] N. G. Gilal and J. G. Gilal, "The Four-Factor Model of Product Design: Scale Development and Validation," *Journal of Product & Brand Management*, vol. 27, no. 6, pp. 684-700, Dec. 2018.
- [38] P. H. Bloch, "Product Design and Marketing: Reflections After Fifteen Years," *Journal of Product Innovation Management*, vol. 28, no. 3, pp. 378-380, Mar. 2011.
- [39] H. Moon, J. Park, and S. Kim, "The importance of an Innovative Product Design on Customer Behavior: Development and Validation of a Scale," *Journal of Product Innovation Management*, vol. 32, no.2, pp. 224-232, Mar. 2015.
- [40] S. Rianmora, G. Nak Da, and M. Phlernjai, "Let-It-Cold Design Concept for Supporting Temperature-Sensitive Products," *International Scientific Journal of Engineering and Technology*, vol. 5, no. 1, pp. 41-57, Jun. 2021.
- [41] R. P. Jindal, K. R. Sarangee, R. Echambadi et al., "Designed to Succeed: Dimensions of Product Design and their Impact on Market Share," *Journal of Marketing*, vol. 80, no. 4, pp. 72-89, Jul. 2016.

- [42] E. Norman, "The Nature of Technology for Design," *International Journal of Technology and Design Education*, vol. 8, no. 1, pp. 67-87, Jan. 1998.
- [43] M. Hu and B. Liu, "Mining Opinion Features in Customer Reviews," in *Proc. AAAI*, 2004, pp. 755-760.
- [44] K. S. Taber, "The use of Cronbach's Alpha when Developing and Reporting Research Instruments in Science Education," *Research in Science Education*, vol. 48, no. 6, pp. 1273-1296, Dec. 2018.
- [45] G. Hasdoğan, "The Role of User Models in Product Design for Assessment of User Needs," *Design Studies*, vol. 17, no.1, pp. 19-33, Jan. 1996.
- [46] M. C. Lin, G. P. Qiu, X. H. Zhou et al., "Using Taguchi and Neural Network Approaches in the Optimum Design of Product Development Process," *International Journal of Computer Integrated Manufacturing*, vol. 33, no. 4, pp. 343-359, Apr. 2020.
- [47] S. B. Sutono, S. H. Abdul-Rashid, Z. Taha, Subagyo et al., "Integration of Grey-Based Taguchi Method and Principal Component Analysis for Multi-Response Decision-Making in Kansei Engineering," *European Journal of Industrial Engineering*, vol. 11, no. 2, pp. 205-227, Mar. 2017.
- [48] Y. Li and L. Zhu, "Optimisation of Product form Design Using Fuzzy Integral-Based Taguchi Method," *Journal of Engineering Design*, vol. 28, no.7-9, pp. 480-504, Jun. 2017.
- [49] S. Rianmora and S. Werawatganon, "Applying Quality Function Deployment in Open Innovation Engineering," *Journal of Open Innovation: Technology, Market, and Complexity*, vol. 7, no. 1, pp. 26, Jan. 2021.
- [50] K. Chaiwat, "Applications of Kansei Engineering for Shape Design and Material Selection of Products," Ph.D. Dissertation, Nagaoka Univ. Technol., Nagaoka, Japan, 2017.
- [51] Marvel Packaging. (2021, Jul. 19). *What Are Perfume Bottle Sizes?* [Online]. Available: <https://bit.ly/3Ebj5H3>
- [52] Handbook of Human Factors and Ergonomics Methods, CRC Press, Florida, USA. 2004. pp. 794-799.
- [53] V. Ganta and D. Chakradhar, "Multi Objective Optimization of Hot Machining of 15-5PH Stainless Steel Using Grey Relation Analysis," *Procedia Materials Science*, vol. 5, pp. 1810-1818, Jan. 2014.
- [54] S. Dewangana, C.K. Biswasb, and S. Gangopadhyayc, "Optimization of the Surface Integrity Characteristics of EDM Process using PCA Based Grey Relation Investigation," *Procedia Materials Science*, vol. 6, pp. 1091-1096, Jan. 2014.
- [55] L. Y. Zhai, L. P. Khoo, and Z. W. Zhong, "Design Concept Evaluation in Product Development Using Rough Sets and Grey Relation Analysis," *Expert Systems with Applications*, vol. 36, no. 3, pp. 7072-7079, Apr. 2009.
- [56] P. K. Sahu and S. Pal, "Multi-Response Optimization of Process Parameters in Friction Stir Welded AM20 Magnesium Alloy by Taguchi Grey Relational Analysis," *Journal of Magnesium and Alloys*, vol. 3, pp. 36-46, Mar. 2015.
- [57] J. Klamklay, A. Sungkhaopong, N. Yodpijit et al., "Anthropometry of the Southern Thai Population," *International Journal of Industrial Ergonomics*, vol. 38, no.1, pp. 111-118, Jan. 2008
- [58] Minitab. (2021, Jul. 19) *What is ANOVA?* [Online]. Available: <https://bit.ly/3EeRHrQ>



**Suchada Rianmora** is a lecturer in the School of Manufacturing Systems and Mechanical Engineering, Sirindhorn International Institute of Technology, Thammasat University, Thailand. She received her D.Eng from the Asian Institute of Technology, Thailand. Her research interests are reverse engineering, rapid prototyping, design and development, and manufacturing processes.



**Pervez Alam Khan** received his Bachelor of Technology in Mechanical Engineering, India 2019. Nowadays, is a full time Master degree student in Logistics Supply Chain System Engineering at Sirindhorn International Institute of Technology, Pathum Thani, Thailand. His research interests are product design and development, and manufacturing processes, supply chain and marketing strategy.

# Fluke Eggs Detection and Classification Using Deep Convolution Neural Network

Natthaphon Hongcharoen<sup>1</sup>, Parinya Sanguansat<sup>2</sup>, and Sanparith Marukatat<sup>3</sup>

<sup>1,2</sup>Panyapiwat Institute of Management, Engineering and Technology, Nonthaburi, Thailand

<sup>3</sup>NECTEC, AI Research Group, Pathumthani, Thailand

E-mail: 627210108@stu.pim.ac.th, parinyasan@pim.ac.th, sanparith.marukatat@nectec.or.th

Received: October 14, 2021 / Revised: December 19, 2021 / Accepted: January 27, 2022

**Abstract**—We present the experimental results of utilizing object detection to solve the problem of detecting and also classifying the parasite eggs in the fecal slides. We experimented with different detection techniques and different sizes of the backbone part. The trained models were evaluated using standard mean Average Precision (mAP) on the results from labeled data collected from the closed environment and also manual evaluation on the results from field data collected from actual medical diagnoses that do not have accurate labels. On the lab data, VFNet achieved a very good 0.897 mAP at the Intersection over Union (IoU) of 0.7 thresholds but performed rather poorly in the classification part on the field data. The relatively older technique Cascade Faster R-CNN had a little below average result in the lab data but had a very good classification accuracy on the field data. The backbone part also had conflicting results on the lab data and field data. The smaller backbones performed better in the lab data but lost to the bigger backbones on the field data.

**Index Terms**—Deep Learning, Microscopic Images, Object Detection

## I. INTRODUCTION

According to World Health Organization (WHO), liver cancer is the fourth leading cause of cancer death in 2018 [1]. With liver fluke or *Opisthorchis Vivertini* (OV) being one of the causes of liver cancer and one of the causes of OV infection is raw fish consumption which is common in the north-eastern region of Thailand. The accumulation of OV will eventually lead to liver cancer in advanced age if not treated properly.

Parasite infection in humans can be detected by analyzing the fecal slide but OV is not the only type of parasite eggs found in human feces. Minute Intestinal Flukes (MIF) are in fact very similar to OV as shown

in Fig. 1 but they infect different organs, OV infects livers whereas MIF infects small intestines.

While finding the parasite eggs in the fecal slide is achievable, it is very difficult to distinguish them and would need experts to do the job.

This paper aims to utilize the object detection methods and create models that can accurately detect and classify the types of parasite eggs in the fecal slides which would free up the experts for other tasks. And without the need for experts, the diagnosis can be done on a larger scale easily as medical students, nurses or clinicians can perform the task as well.

## II. RELATED WORK

Bruun et al. [2] used an elliptic filter to detect the eggs to detect the eggs. The filters were designed using the average size of the eggs and manually selected rotation angles. Yang et al. [3] used the classic artificial neural network (also known as multi-layer perceptron) to classify the parasite eggs. Two models were used in this work, one for determining whether or not the object is a parasite egg and another one for classification. Akintayo et al. [4] used a convolutional autoencoder for the localization and classification of microscopic nematode eggs.

## III. DATA

### A. Training Data

To train an object detection model, the images and corresponding annotations of the objects inside the images are needed. We used the data obtained from a medical laboratory and the two types of parasites (OV and MIF) that were cultivated in a closed environment. Then the eggs were added to the fecal slides; one type per slide either OV or MIF. This ensured that all the eggs in the images were correctly classified and reduced the problems with incorrect labeling.



The fecal slides were then passed through the Kato-Katz method. The images were taken from the microscope with about 40 times magnification using hand-held digital cameras and smartphone cameras. This increased the variation of the obtained images to some extent. The locations of the eggs in these images were then manually tagged by domain experts from the Department of Disease Control (DDC), Ministry of Public Health.

In total, there were 1,684 MIF images and 1,553 OV images with 2,439 MIF eggs and 3,510 OV eggs. These images were then separated into 2,465 training images and 772 validation images. The examples of the data are shown in Fig. 1.

### B. Field Data

We also used real images obtained from actual medical diagnoses. As it is possible that the images gathered from the closed environments using cultivated parasites may not represent the real-world problem well enough. But with the difficulty of classifying the eggs resulted in many incorrect labeling and conflicting classification of the images from the same slides from multiple sources, we used them only as test data instead. The examples of the field data are shown in Fig. 2.

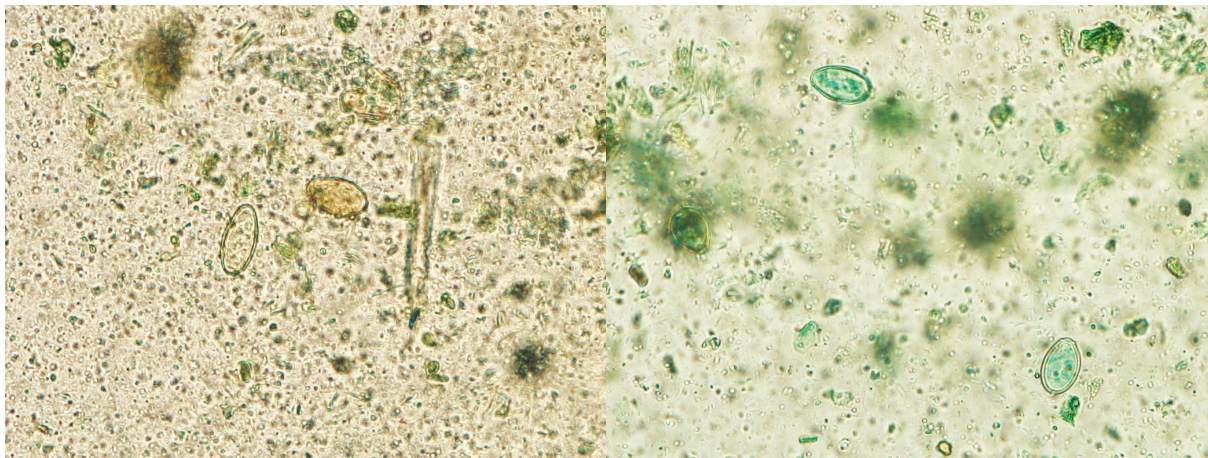


Fig. 1. Example images from the lab data, with MIF on the left and OV on the right. Note that the color difference is per slice basis and cannot be used to distinguish the eggs in the picture.

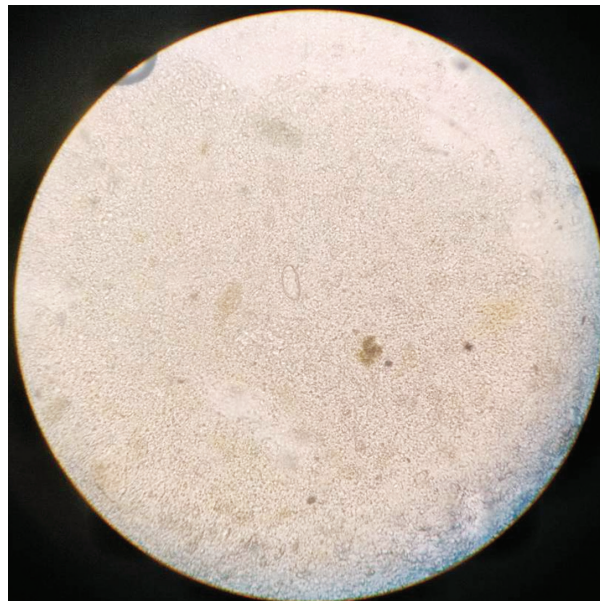


Fig. 2. Example images from the field data. With MIF on the left and OV on the right.

## IV. EXPERIMENT

We experimented with standard object detection, having the detectors do both localizing and classifying the objects. The option of using object detection to only locate the objects and use sophisticated classification models is also considered but we choose not to use it because that would require near-perfect object localization for the models to be accurate.

We compared different object detection algorithms in terms of performance and speed. The performance of the algorithms was measured using mean Average Precision (mAP) and measure the speed with how many images can the algorithms process in one second during the inference phase.

We chose to standardize on one single framework that contained many algorithms in order to reduce the differences between each experiment to only the differences in the algorithms as much as possible. MMDetection [5] was chosen for this.

All techniques except the YoloV3 used the same data augmentation in the training phase. Each input image was resized to have a smaller size equal to 800 pixels and keep the aspect ratio after resizing the bigger size was not bigger than 1333 pixels, if it was bigger, we center cropped it to 1333 pixels. Then the images were randomly flipped with 0.5 probability both vertically and horizontally. The input images were then normalized using MSCOCO [6] mean and standard deviation. And as the images needed to be stacked as batches for training, we pad the smaller images with zero to make the size equal to the biggest image in each batch, if that particular model needed the input to be divisible by 32 then we padded all images further to meet that requirement.

The optimizer and learning rate schedule for each model was configured similarly to the original paper. Except with a smaller learning rate as we used smaller batch sizes for our smaller GPUs.

TABLE I  
MEAN AVERAGE PRECISION AND COMPUTATION TIME OF EACH TECHNIQUE.

Technique	Backbone	Mean Average Precision (mAP)				Speed (frames/sec)
		0.3	0.5	0.7	0.9	
Deformable DETR	ResNet 50	0.847	0.814	0.517	0.001	4.519
YoloV3	DarkNet 53	0.845	0.835	0.723	0.097	8.364
RetinaNet	ResNet 101	0.875	0.838	0.737	0.402	4.898
Faster R-CNN	ResNet 101	0.873	0.853	0.751	0.426	4.666
<b>Cascade Faster R-CNN</b>	<b>ResNet 101</b>	<b>0.860</b>	<b>0.830</b>	<b>0.752</b>	<b>0.462</b>	<b>4.040</b>
RetinaNet	ResNet 50	0.888	0.857	0.755	0.433	5.660
Cascade Faster R-CNN	ResNet 50	0.870	0.836	0.765	0.482	4.681
GFL	ResNeXt 101 DCN	0.919	0.880	0.773	0.366	3.858
DETR	ResNet 50	0.916	0.898	0.800	0.096	5.996
Faster R-CNN	ResNet 50	0.912	0.885	0.807	0.457	5.474
VFNet	ResNet 50	0.944	0.927	0.840	0.565	5.313
GFL	ResNet 101 DCN	0.941	0.935	0.875	0.533	4.409
VFNet	ResNeXt 101 DCN	0.945	0.937	0.878	0.611	2.506
GFL	ResNet 50	0.945	0.941	0.882	0.518	5.770
VFNet	ResNet 50 DCN	0.953	0.944	0.897	0.597	4.729

The table is sorted by mAP at IOU 0.7.

TABLE II  
SENSITIVITY AND SPECIFICITY SCORE OF EACH TECHNIQUE

Technique	Backbone	MIF		OV	
		Sensitivity	Specificity	Sensitivity	Specificity
<b>Cascade Faster R-CNN</b>	<b>ResNet 101</b>	<b>0.931</b>	<b>0.981</b>	<b>0.848</b>	<b>0.912</b>
Cascade Faster R-CNN	ResNet 50	0.933	0.993	0.851	0.903
DETR	ResNet 50	0.961	0.971	0.908	0.667
RetinaNet	ResNet 50	0.931	0.978	0.833	0.893
RetinaNet	ResNet 101	0.924	0.976	0.837	0.889
Faster R-CNN	ResNet 101	0.933	0.993	0.840	0.893
Faster R-CNN	ResNet 50	0.963	0.993	0.890	0.922
YoloV3	DarkNet 53	0.939	0.967	0.862	0.936
Deformable DETR	ResNet 50	0.818	0.999	0.816	0.934
GFL	ResNet 50	0.984	0.983	0.915	0.897
GFL	ResNet 50	0.984	0.988	0.936	0.893
GFL	ResNet 101 DCN	0.99	0.965	0.915	0.854
GFL	ResNeXt 101 DCN	0.951	0.977	0.787	0.807
VFNet	ResNet 50 DCN	0.984	0.990	0.911	0.893
VFNet	ResNet 50 DCN	0.984	0.988	0.915	0.914

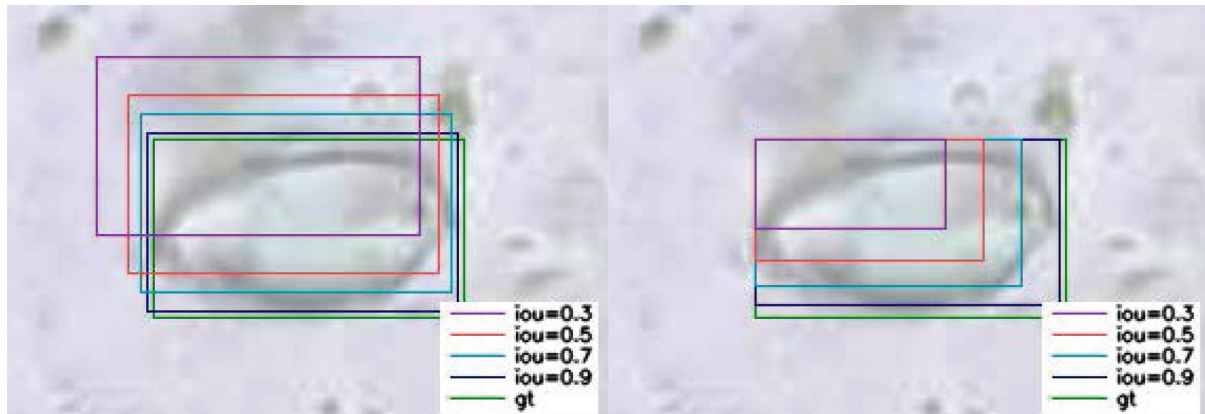


Fig. 3. A comparison of the 4 chosen IOU. IOU 0.3 is purple, 0.5 is red, 0.7 is yellow, and 0.9 is blue compared to the ground truth (green). The left image shows similar bounding boxes in different locations while the right image shows different bounding boxes with the same starting points.

We also experimented with the effectiveness of using bigger feature extractors as part of the algorithms (also known as backbones). As backbones like ResNet [7] can be made more accurate by simply adding more layers but this would increase processing time and thus reduce the speed. We intended to see whether or not using a bigger backbone helps increase performance in measurable metrics and how much the speed decreases. The ResNet 50 [4], ResNet 101 [4], and ResNeXt 101 [8] are chosen. With ResNet 50 as the baseline, ResNet 101 is twice the depth of ResNet 50, and ResNeXt is 101 a larger version of ResNet 101. We also trained some models using Deformable Convolution [6] layers in the detection stage.

We then measure the inference speed of each technique using an Nvidia GTX 1080 GPU with a batch size of 1 and the same resizing as the training stage.

#### A. RetinaNet

RetinaNet introduces Focal Loss. A method to reduce the imbalanced data problem where there are too many background objects in the ground-truth compare to the foreground objects by reducing the contribution of score from the background class [10]. Two models were trained. One with ResNet 50 as the backbone and one with ResNet 101. Both models were trained for 24 epochs with a batch size of 2. We used Stochastic Gradient Descent as the optimizer with a base learning rate of 0.01, the a momentum of 0.9, and a weight decay of 0.0001. The warm-up procedure was by using a 0.00001 initial learning rate and linearly increased by 0.000002 after every batch until it reached the base learning rate (500 batches). The learning rate was then reduced by a factor of 0.1 at epochs 16 and 22.

#### B. YOLO v3

Yolo v3 predicts the center point of each foreground object and uses a set of handcrafted anchor boxes to help determines the object boxes' width and height. Then classify the objects on the same output head as the bounding boxes head [11].

The Yolo v3 was trained with a different pre-processing procedure than other models as it is the only model that was trained using square input in the original paper. And with our expected performance of Yolo being a fast model with some accuracy compromise, we decided to use the square resizing as well and also used Yolo's unique backbone DarkNet 53. The input images were randomly cropped to the minimum of 30% of the original size while keeping the center of all the bounding boxes. The images were then center-cropped with randomized sizes between 320x320 and 608x608.

The model was trained using Stochastic Gradient Descent (SGD) as the optimizer with a base learning rate of 0.00025 and momentum of 0.9. The learning rate was warm up by starting at 0.000025 and linearly increase to the base value after 2000 batches. The model was trained for 100 epochs and the learning rate was reduced by a factor of 0.1 at epoch 80 and 90.

#### C. Faster R-CNN

Faster R-CNN is a two-stage network. An improved version of R-CNN and Fast R-CNN. It utilizes Region Proposal Network (RPN) to predict regions of interest after the backbone stage. Then uses the Region of Interest Pooling network (ROI Pooling) to choose the relevant boxes and then predict the bounding boxes and classify the objects [12].

Two models were trained with one using ResNet 50 and one with ResNet 101 as backbones. The models were trained using SGD with a base learning rate of 0.005, a momentum of 0.9, and the a weight decay of 0.0001. The warm-up train phase was using an initial learning rate of 0.000005 and linearly increased to the base learning rate at 500 batches. Training for a total of 24 epochs with a batch size of 2. The learning rate was reduced by a factor of 0.1 at epochs 16 and 22.

#### D. Cascade Faster R-CNN

An improved version of Faster R-CNN. It is designed to solve the problem of positive samples vanishing when increasing the IOU threshold and when the testing phase uses a different IOU than during the training phase [13].

The training configurations were the same as the ones that were used to train Faster R-CNN.

#### E. DETR

DETR [14] utilizes the Transformer [15] for the prediction stage in order to get away with the hand-crafted knowledge such as anchor boxes and Non-Maximum Suppression.

The Decoupled Weight Decay Regularization version of the Adam (AdamW) optimizer was used with an initial learning rate of  $1e-4$  and weight decay of  $1e-4$ . The input images were heuristically resized to have the a larger size equal to 1333 pixels and then random cropped to have a smaller size between 480 to 800 pixels. The batch size was 2. The model trained for 24 epochs and the learning rate was divided by 10 at epochs 16 and 22.

#### F. Deformable DETR

A proposed improved version of DETR to increase the convergence speed and feature spatial resolution [16].

The model was trained using AdamW like DETR and similar other setups. In addition to using a smaller learning rate with 0.1 factor at the backbone, sampling offsets, and reference points.

#### G. Generalized Focal Loss

An improved version of RetinaNet and its Focal Loss. Instead of calculating the IOU score on the bounding box head separate from both the bounding box and classification and then perform Non-Maximum Suppression on the joined value of all three. GFL combines the IOU and classification score and NMS suppression over this value not on the bounding box [17].

As it is being an improved version of RetinaNet, we trained GFL using the same configuration. With the exception of an additional ResNeXt 101 backbone and using DCN [6] on both ResNet 101 and ResNeXt.

#### H. VarifocalNet

As the name implies, VarifocalNet or VFNet is another variation of Focal Loss [7] similar to the GFL combines the star-shaped bounding boxes. The VFNet replaces the classification score of the ground-truth class with the IOU score between predicted boxes and ground-truth boxes [18]. Very similar in concept to the GFL but with the difference is being that GFL combines both bounding boxes and classification scores together whereas VFNet keeps them separated like the original Focal Loss.

VFNet was trained using the same configuration as RetinaNet and GFL. With the backbone being ResNet 50, ResNet 50 DCN, and ResNeXt 101 DCN. In order to measure the performance of DCN, we trained VFNet with ResNet 50 and ResNet 50 DCN two separate models each.

## VI. COMPARATIVE RESULTS

### A. Lab Data

We evaluate the models on the validation dataset using the Mean Average Precision (mAP) metric. The score was calculated by computing the intersection over union (IOU) between the predicted bounding box and ground truth. The IOU threshold was set at 0.3, 0.5, 0.7, and 0.9. The predicted bounding box with over the chosen IOU score compared to a ground-truth bounding box was considered as matched. Precision was the ratio between the correctly predicted bounding boxes over the total number of predicted bounding boxes.

Table I shows the mAP for the five detectors sorted by mAP at IOU 0.7. VFNet models outperformed everything in terms of precision while YOLO v3 was significantly faster than other models. The scores of VFNet with ResNet 50 and ResNet 50 DCN are the average of the two models of each backbone.

To visualize the differences between the IOU numbers, Fig. 3 shows bounding boxes with IOU 0.3 to IOU 0.9 compare to ground truth. While the bounding boxes with IOU 0.9 were very similar to the ground truth but we decided that boxes with IOU 0.7 are good enough for our usage, which as shown in Table I faster models had a significant drop in precision at IOU 0.9 compared to IOU 0.7.

We then measure each technique's specificity and sensitivity performance. The specificity score was calculated by the number of pictures without the eggs from the specific class and the models did not predict any object over the total number of pictures without the eggs from the specific class. The sensitivity score was calculated by the number of pictures with eggs from each class and the model correctly detected over the total number of pictures with eggs from the specific class. Because the specificity test did not need

any label, we included the field data along with using the data from the different classes. The results are shown in Table II.

### B. Field Data

Without the usable labels as stated in section III-B, we only had the models predict these images and manually verify the bounding boxes' precision and classification accuracy on some images with known classes.

We selected a small portion of images that contains eggs from only one class. The results are as shown in Fig. 4 to Fig. 9. Contradicted to the lab data and

mAP table, GFL performed worse than other hi-mAP models by tending to not predict anything like Fig. 7. The best performing in this test is Cascade Faster R-CNN with its remarkable classification accuracy on top of good detection as well. The most surprising result of this test would be Yolo v3, considering its performance in the lab data it did very well in the field data, especially in classification. Every model tested was capable of reliably detecting most of the eggs but often fail to classify them and predict everything as OV. This suggests there should be some kind of biases in the training data.

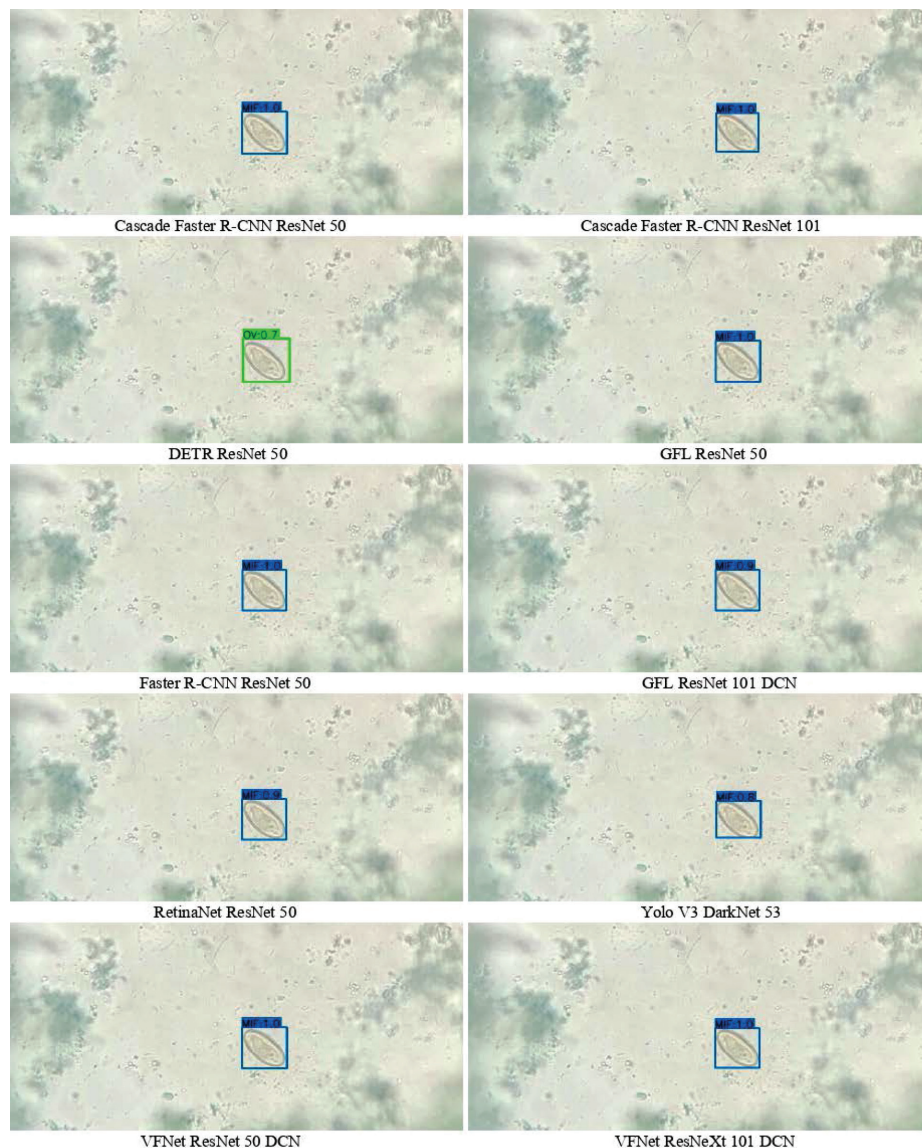


Fig. 4. Example result of an image with a MIF egg from the field data

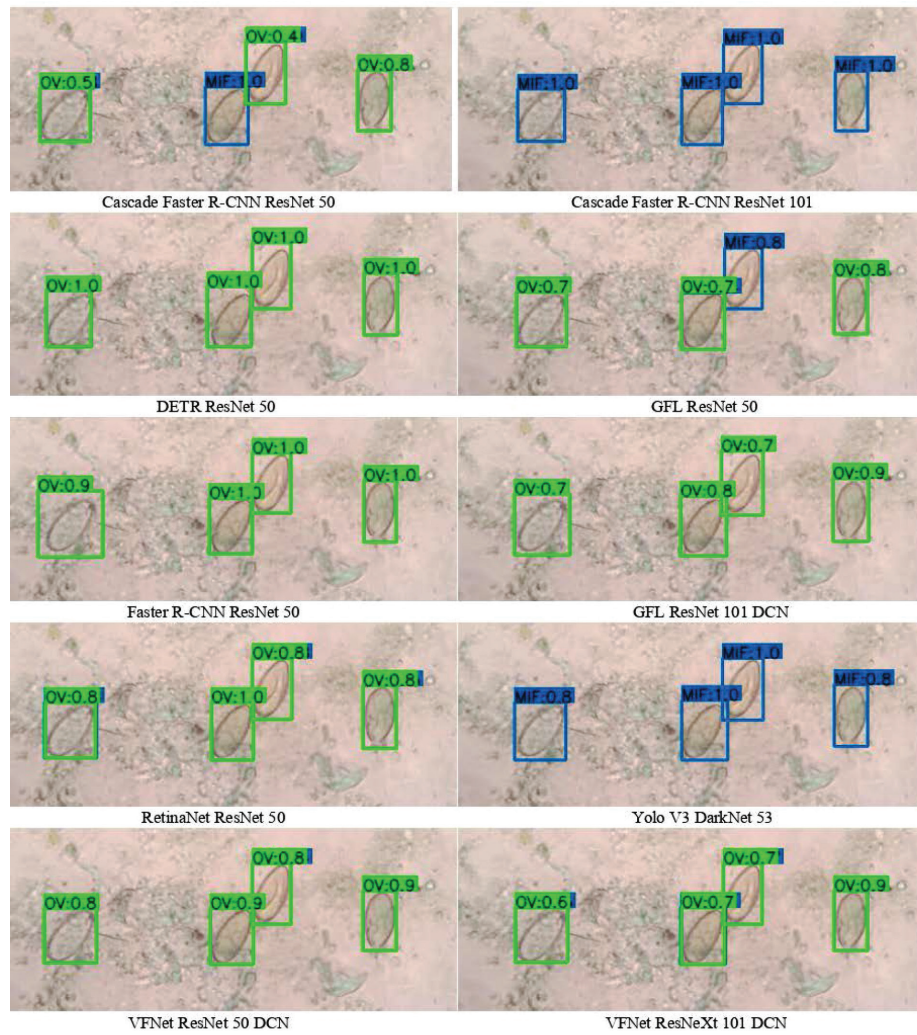


Fig. 5. Example result of an image with a MIF egg from the field data

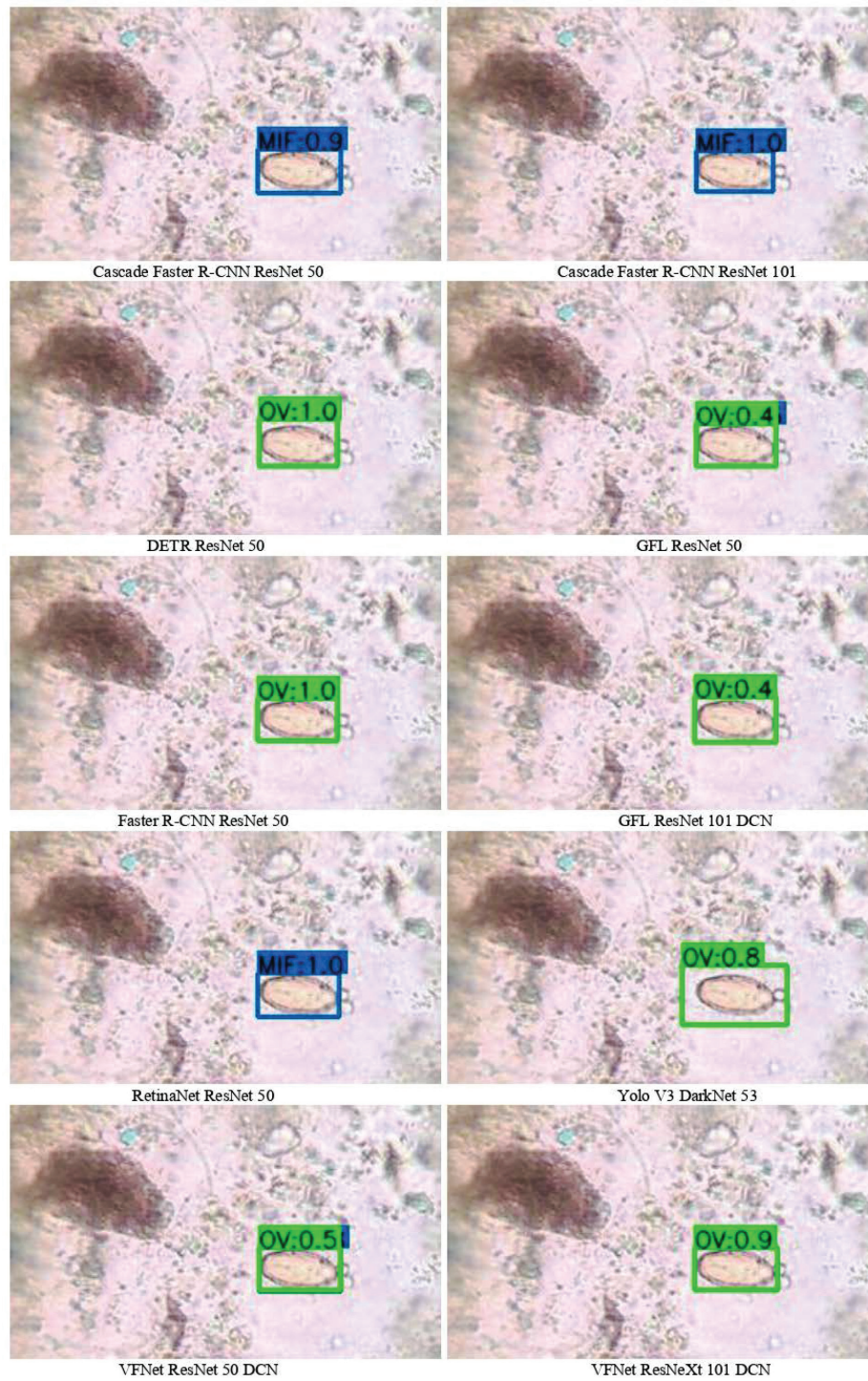


Fig. 6. Example result of an image with a MIF egg from the field data

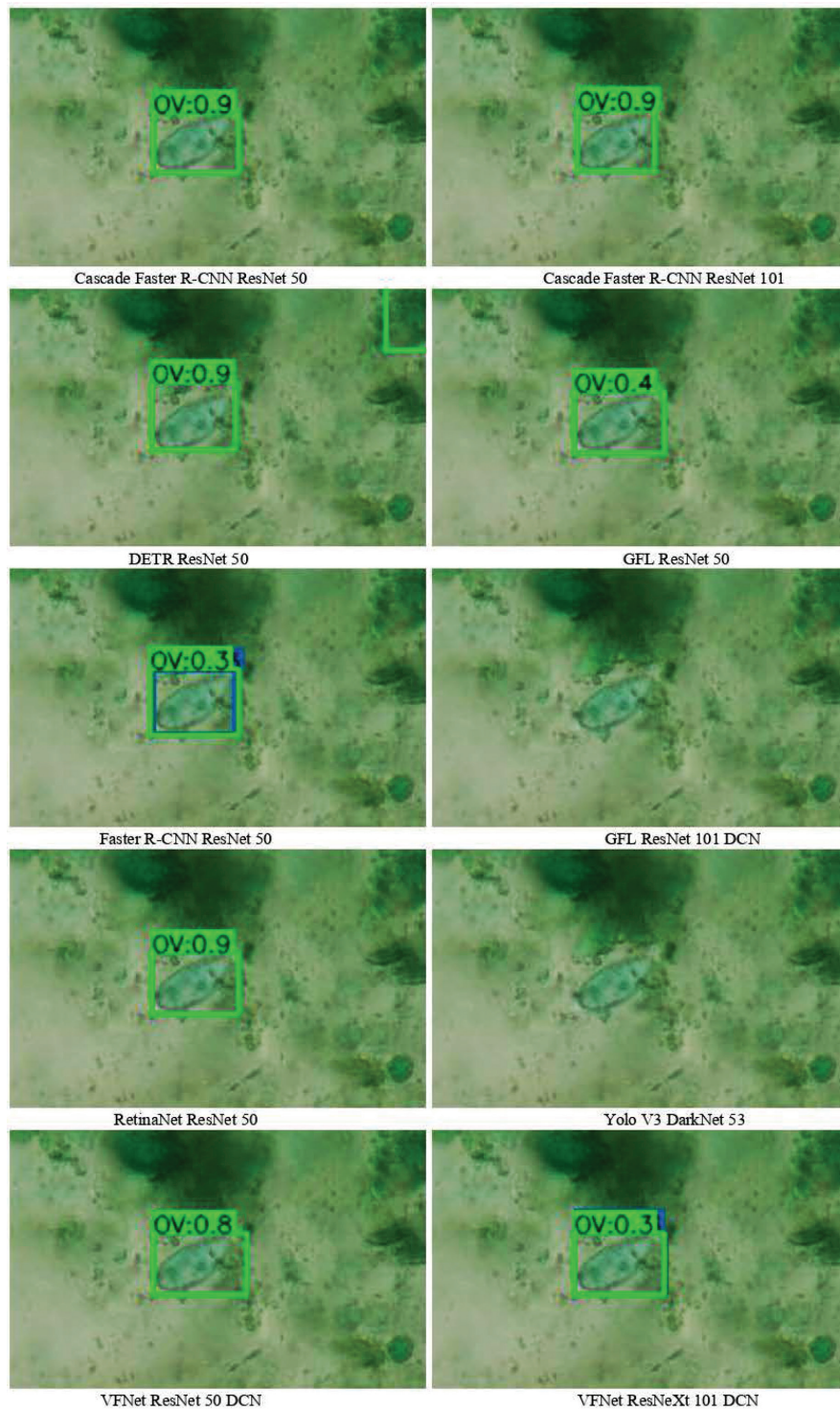


Fig. 7. Example result of an image with an OV egg from the field data



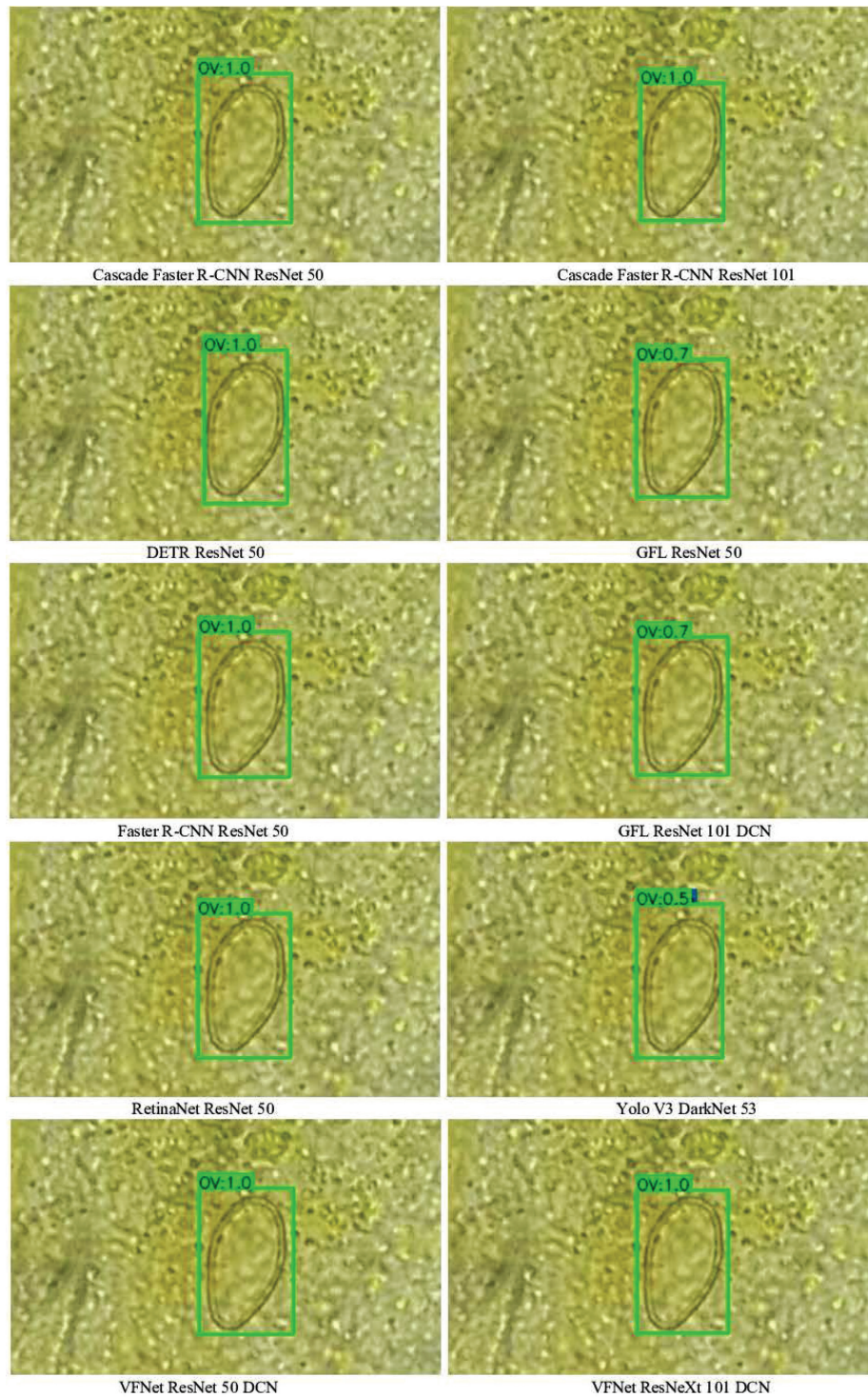


Fig. 8. Example result of an image with an OV egg from the field data

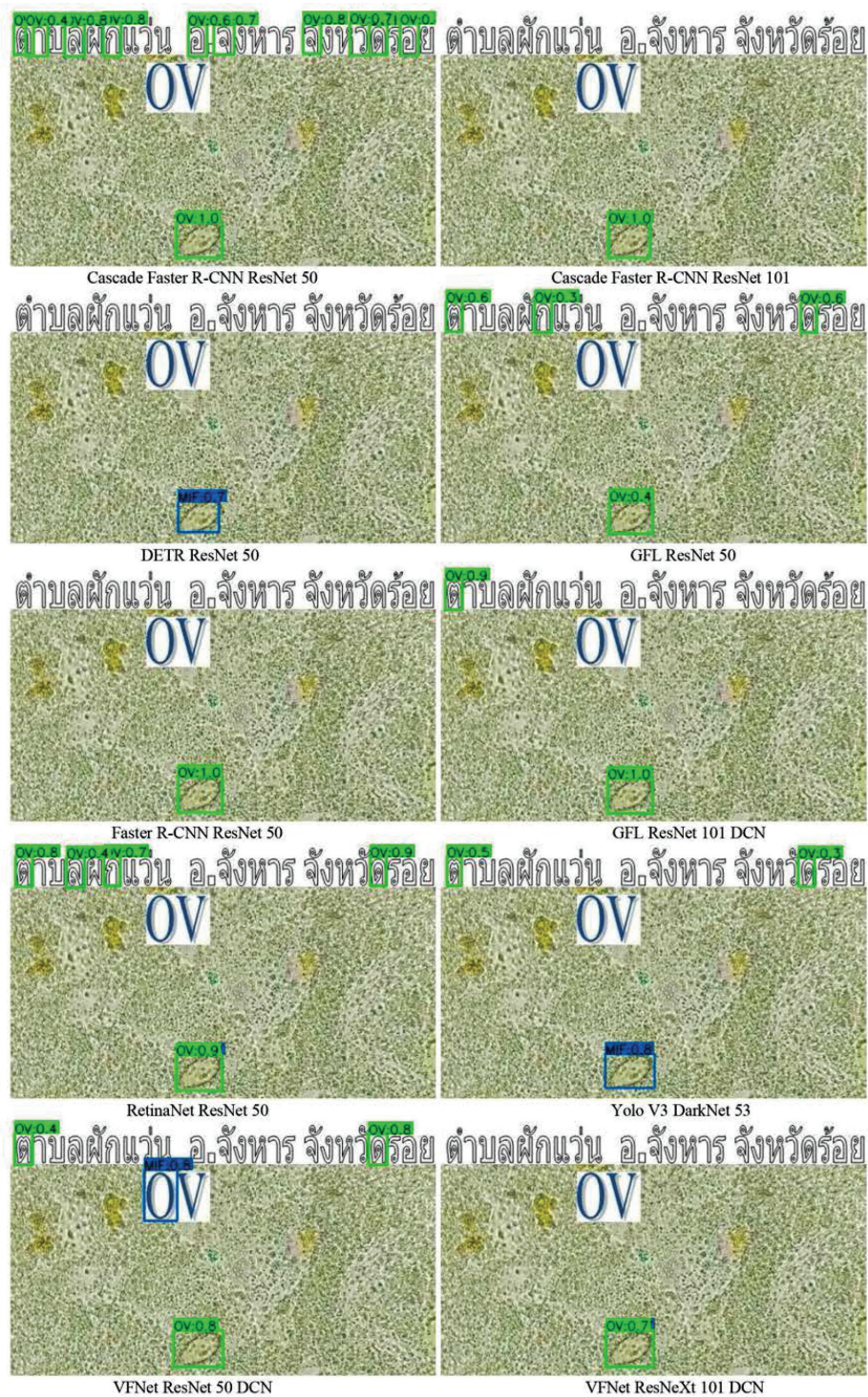


Fig. 9. Example result of an image with an OV egg and unrelated noises in the forms of overlay characters

C. Backbone Comparison

In the lab data, the smaller backbone performs significantly better than the bigger ones, with the baseline ResNet 50 outperforming other backbones in all techniques except VFNet in which the best is still ResNet 50 but with DCN.

In the field data, however, the results are somewhat different. The bigger backbone in Cascade Faster R-CNN performed noticeably better than the

smaller counterpart in terms of classification. Also, for most models, the ones with a bigger backbone are less likely to predict false positives, especially on noises that are not in the training data such as overlay characters as shown in Fig. 9.

The DCN showed good results in the Lab data as in Table 1 but no noticeable difference in the field data. The side-by-side comparisons of VFNet with ResNet 50 with and without DCN are shown in Fig. 10 and Fig. 11.

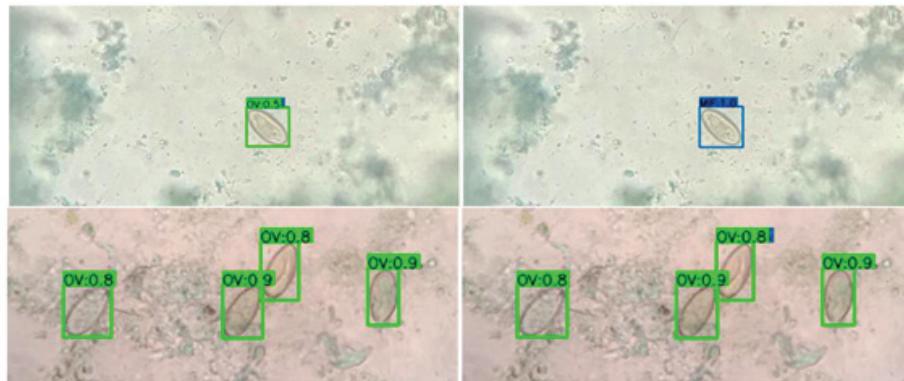


Fig. 10. Side-by-side comparison between base ResNet 50 and ResNet 50 DCN using VFNet technique on MIF images

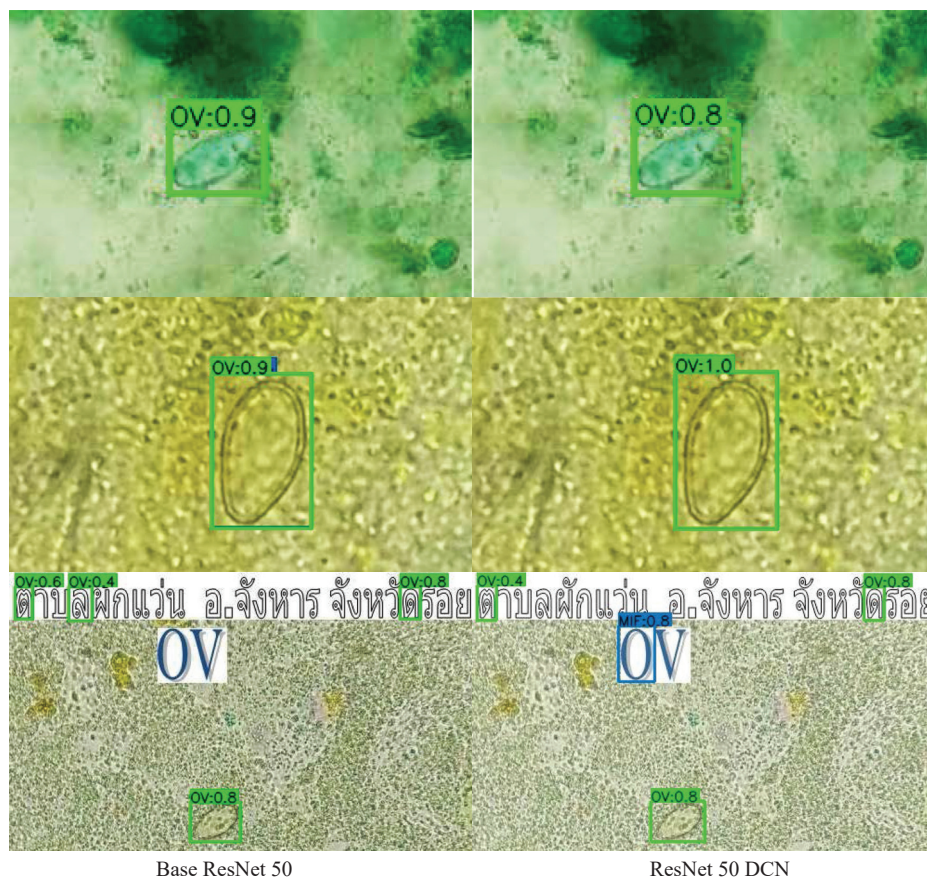


Fig. 11. Side-by-side comparison between base ResNet 50 and ResNet 50 DCN using VFNet technique on OV images

## CONCLUSION

The task of detecting and classifying parasite eggs is certainly possible using object detection techniques. The performance of each technique however may be different from the usual object detection task like COCO, possibly due to the training data we had been different from the real data used for evaluation. We determined that Cascade Faster R-CNN [10] is the best-performing technique for this task primarily because of its classification accuracy in test data. The bigger backbones showed worse results than the smaller counterpart in the lab data but with manual evaluations on the test dataset, some techniques like Cascade Faster R-CNN and RetinaNet had better results with bigger backbones. DCN showed satisfactory results on evaluation data but no noticeable difference in the test data. These points may need further prove with fully labeled test data.

The improved versions of Focal Loss on GFL [14] and VFNet [15] had significantly improved performance over the original RetinaNet [7]. The Deformable DETR on the other hand did not work very well on our task even when compared to the original DETR. The Transformer based DETR [11] tended to predict the noises and also had poor classification accuracy resulting in a rather poor specificity score. We suspected that the model had to be fine-tuned on some unseen data first.

## ACKNOWLEDGMENT

Scholarship received from Thailand Graduate Institute of Science and Technology (TGIST) of the National Science and Technology Development Agency (NSTDA). Scholarship ID SCA-CO-2562-9836-TH.

## REFERENCES

- [1] F. Bray, J. Ferlay, I. Soerjomataram et al., "Global Cancer Statistics 2018: Globocan Estimates of Incidence and Mortality Worldwide for 36 Cancers in 185 Countries," *CA: A Cancer Journal for Clinicians*, vol. 68, no. 6, pp. 394–424, Sep. 2018.
- [2] J. M. Bruun, C. M. Kapel, and J. M. Carstensen. (2012, Jun. 21). *Detection and Classification of Parasite Eggs for Use in Helminthic Therapy*. [Online]. Available: <https://ieeexplore.ieee.org/document/6235888>
- [3] Y. S. Yang, D. K. Park, H. C. Kim et al. (2001, Jun. 2). *Automatic Identification of Human Helminth Eggs on Microscopic Fecal Specimens Using Digital Image Processing and an Artificial Neural Network*. [Online]. Available: <https://pubmed.ncbi.nlm.nih.gov/11396601/>
- [4] A. Akintayo, G. L. Tylka, A. K. Singh et al. (2021, Jul. 2). *A Deep Learning Framework to Discern and Count Microscopic Nematode Eggs*. [Online]. Available: <https://www.nature.com/articles/s41598-018-27272-w>
- [5] K. Chen, J. Wang, J. Pang et al. (2019, Jun. 15). *MMDetection: Open MMLab Detection Toolbox and Benchmark*. [Online]. Available: <https://arxiv.org/abs/1906.07155>
- [6] T. Y. Lin, M. Maire, S. Belongie et al. (2015, Jun. 15). *Microsoft Coco: Common Objects in Context*. [Online]. Available: <https://cocodataset.org>
- [7] K. He, X. Zhang, S. Ren et al. (2015, Jun. 15). *Deep Residual Learning for Image Recognition*. [Online]. Available: <https://arxiv.org/abs/1512.03385>
- [8] S. Xie, R. Girshick, P. Dollár et al. (2017, Jun. 20). *Aggregated Residual Transformations for Deep Neural Networks*. [Online]. Available: <https://arxiv.org/abs/1611.05431>
- [9] X. Zhu, H. Hu, S. Lin et al. (2018, Jun.21). *Deformable Convnets V2: More Deformable, Better Results*. [Online]. Available: <https://arxiv.org/abs/1811.11168>
- [10] T. Y. Lin, P. Goyal, R. Girshick et al. (2018). *Focal Loss for Dense Object Detection*. [Online]. Available: <https://arxiv.org/abs/1708.02002>
- [11] J. Redmon and A. Farhadi. (2021, Jun. 20). *Yolov3: An Incremental Improvement*. [Online]. Available: <https://arxiv.org/abs/1804.02767>
- [12] S. Ren, K. He, R. Girshick et al. (2021, Jun. 20). *Faster R-CNN: Towards Real-Time Object Detection with Region Proposal Networks*. [Online]. Available: <https://arxiv.org/abs/1506.01497>
- [13] Z. Cai and N. Vasconcelos. (2021, Jun. 21). *Cascade R-CNN: High Quality Object Detection and Instance Segmentation*. [Online]. Available: <http://dx.doi.org/10.1109/tpami.2019.2956516>
- [14] N. Carion, F. Massa, G. Synnaeve et al. (2021, Jun. 20). *End-to-end Object Detection with Transformers*. [Online]. Available: <https://arxiv.org/abs/2005.12872>
- [15] A. Vaswani, N. Shazeer, N. Parmar et al. (2021, Jun. 2). *Attention is All You Need*. [Online]. Available: <https://arxiv.org/abs/1706.03762>
- [16] X. Zhu, W. Su, L. Lu et al. (2021, Jun. 21). *Deformable Detr: Deformable Transformers for End-to-End Object Detection*. [Online]. Available: <https://arxiv.org/abs/2010.04159>
- [17] X. Li, W. Wang, L. Wu et al. (2021, Jul. 2). *Generalized Focal Loss: Learning Qualified and Distributed Bounding Boxes for Dense Object Detection*. [Online]. Available: <https://arxiv.org/abs/2006.04388>
- [18] H. Zhang, Y. Wang, F. Dayoub et al. (2021, Mar. 4). *VarifocalNet: An IoU-aware Dense Object Detector*. [Online]. Available: <https://arxiv.org/abs/2008.13367>

**Natthaphon Hongcharoen**

received his B. Eng. degree from the Department of Computer Engineering, Faculty of Engineering and Technology, Panyapiwat Institute of Management in 2019. He has experience in internships at the National Electronics and Computer Technology Center (NECTEC), and the National Science and Technology Development Agency (NSTDA) in the Image Technology Research Laboratory. And won a gold medal at Super AI Engineer Camp season 1 by the Artificial Intelligence Association of Thailand (AIAT). His research areas include Machine Learning, Image processing, and Computer Vision.



**Parinya Sanguansat** is an Associate Professor in Electrical Engineering and head of Computer Engineering and Artificial Intelligence at Panyapiwat Institute of Management (PIM), Thailand. He graduated B.Eng., M.Eng.

and Ph.D. in Electrical Engineering from Chulalongkorn University. His research areas include Machine Learning, Image processing, and Computer Vision. He got many research grants from both private and public organizations. He has written several books about Machine Learning and MATLAB programming.



**Sanparith Marukatat** graduated in computer science in 1998 from the University of Franche-Comté, Besançon, France. In 2004, he has completed the doctoral thesis on online handwriting recognition at University Paris 6, France.

Currently, he is Principal Researcher in the AI Research Group at the National Electronics and Computer Technology Center (NECTEC). Dr. Marukatat's research interests include machine learning, pattern recognition using statistical tools, and deep learning.

# Identifying ATM Fraud Transactions in Thailand using Outlier Detection with Location-Based Grouping and Behavior Feature

Natsuda Kaothanthong<sup>1</sup> and Roongtawan Laimek<sup>2</sup>

<sup>1,2</sup>Sirindhorn International Institute of Technology, Thammasat University,  
Pathumthani, Thailand  
Email: natsuda@siit.tu.ac.th, amabird@live.com

Received: October 27, 2021 / Revised: January 31, 2022 / Accepted: February 21, 2022

**Abstract**—Financial fraud causes a major loss to a bank. The challenge of classifying fraud is a high true positive rate while keeping the number of false positives as low as possible. One difficulty is the unbalanced size of the labeled data which causes a low detection rate and a high false-positive rate. We present a method to sample the data to cope with the unbalance problem in the fraud detection problem. The location feature is applied to separate accounts into ‘local-only’ and ‘has-abroad’. The proposed feature extraction can separate many fraud transactions from legitimate transactions. To differentiate fraud from legitimate transactions, fraud can be considered an outlier. Transformation functions, deviation, risk, and probability features are applied in this work to both numeric and non-numeric features. The experimental result shows that the location-based separation together with the proposed features achieves higher TRP and lower FPR than not dividing the group. It achieves a true positive rate of 75.00% for ‘local-only’ and 100% for ‘has-abroad’. The lowest false positive rate is 8.23% for ‘has-abroad’. Comparing the efficiency of the proposed features with the classification using an isolation forest, the true positive rate is improved from 56.25% to 75.00% and the false positive rate is increased from 2.47% to 28.02%.

**Index Terms**—ATM Fraud, Outlier Detection

## I. INTRODUCTION

Bank fraud is a deceptive activity for monetary gain. Frauds involve many forms of complicated financial transactions depending on the tools that a fraudster is targeting. According to a survey by [1], 23% of respondents in Thailand encountered fraud in 2016. An Automatic Teller Machine (ATM) is widely used for many purposes, i.e., withdrawing,

transferring, and making bill payments. In addition, a credit card and a debit card can be used for withdrawing money from an ATM, which can be targeted by fraudsters. A skimming technique can be used to steal card information and duplicate it into white fake cards, to be used as an identification of the account for a cash withdrawal.

Fraud detection is implemented to identify a suspicious transaction, to prevent losses to the bank. Although machine learning has extensively been studied for credit card fraud detection, the prediction model cannot directly be implemented for an ATM because the channel of transactions affects the different fraud behaviors. Formerly, it was manually performed by fraud analysts. Each ATM transaction was inspected by rule-based software and the suspicious transactions were notified to the analyst. The fraud investigation was taken manually by making a phone call to the account’s owner for a confirmation of the transaction. As the number of transactions has increased extensively and many false-positive transactions were reported by the rule-based software, such a method becomes unfeasible. Machine learning utilizes previously known fraud transactions to construct a model to predict a new transaction. The suspicious transaction can then be notified automatically.

The ATM fraud detection models can be summarized into three categories: (1) Aggregation [2]-[4], (2) Binary Classification [5]-[11], and (3) Outlier Detection [12], [13], [14]. The aggregation method extracts the pattern of transactions. The numeric features in a fixed period are aggregated to represent a normal behavior [4]. In addition, [3] defined the behavior pattern using non-numeric values such as point-of-sale terminals and type of transactions to define the risk of the transaction. The usage of a credit card was identified as a sequence of operations [2]. The relationship among the transactions is extracted using a neural network for defining the confidence of

the new transactions. Recently, [15] used an automatic deep learning-based feature extraction to represent each transaction using 200 detailed features. The model was able to reduce 54% of the false positives predicted by the traditional model.

The binary classification applies a machine learning technique to predict whether a transaction is a fraud. The detection model is trained with labeled transactions. Dorrnsoro et al. [5] applied a Multi-Layer Perceptron (MLP), which can perform real-time fraud detection. A system called CardWatch [6]; applied a feed-forward MLP of three-layers architecture. The proposed architecture can detect 85% of fraudulent transactions. The difficulty of the binary classification method is unbalanced of the labeled data between frauds and non-fraud transactions, which results in the classification of the non-fraud cases rather than the fraud cases. In the credit scoring domain, research has mainly focused on features that represent the behavior to be utilized in the prediction models. The performance for the minority class decreases significantly as the imbalance ratio increases [16], [17]. However, only a few works have addressed the design solutions for unbalanced credit data sets [18]. In addition, extracting good features that are able to separate fraud from legitimate transactions plays an important role.

Abnormal behavior can be considered an outlier. It as a transaction with characteristics that significantly deviated from the characteristics of inlier transactions as a fraud [14]. Applied a graph-based method for anomaly detection for determining financial frauds in money laundering on transactions [12]. Wu et al. Applied a convolutional algorithm that defined the boundary between normal and abnormal transactions, to detect frauds in an Automated Banking Machine (ABM) [11]. Applied a probabilistic model to compare the features of previously known transactions to find outliers [13]. Detected fraud transactions using the aggregated features to define the boundary of normal behavior for each account. Any transactions that are outside the boundary are considered fraudulent transactions [14]. There are many adoptions of deep neural networks in fraud detection using graph-based anomaly detection [18], [19]. Since transactions can be considered as sequential data, that are many methods that apply a Long Short-Term Memory (LSTM) network for fraud detection [20], [21]. One limitation of applying time series credit card detection is a lack of consistent patterns due to a limitation of proper data labeling of the huge dataset. Deep Anomaly Detection (DAD) was proposed [22] to track the customer's profile

and usage behavior.

To measure the efficiency of the prediction model: the True Positive Rate (TPR), False-Positive Rate (FPR), and True Negative Rate (TNR) are considered. TPR measures the efficiency that correctly identifies fraudulent transactions. In contrast, TNR measures the efficiency of correctly identifying legitimate transactions as non-fraud. Lastly, FPR shows the proportion of legitimate transactions that are incorrectly identified as fraud. Due to an extremely low number of known fraud transactions, a prediction model can correctly predict one of the two classes. For example, many transactions are predicted as fraud, while they are non-fraud cases and overlook fraud cases, creating losses to the bank. In this work, a high number of TPR with a low FPR is preferred for prediction. The consequence of a false positive is the cost of investigating the transaction.

Two problems are being considered in this work. The first problem is unbalanced of the dataset. The previous research of our companion paper of [24] reported that the ratio of ATM fraud transactions from a bank in Thailand is less than 0.0002 of the total transactions. Sampling methods such as under and over-sampling were applied, but the accuracy is low. The second problem is the features representing customer behavior. Since many machine learning algorithms use numeric values for constructing models, non-numeric features were excluded.

In this work, we present a feature-based account-grouping method to cope with the unbalanced dataset problem. Also, the transformation functions are utilized for extracting numeric and non-numeric features. A descriptive analysis shows that the proposed features can separate suspicious transactions from normal transactions. Outlier detection methods, such as isolation forests and local outlier factors, are used to classify the frauds.

The experiments of the proposed methods are conducted on both supervised and unsupervised learning models. The results show that the proposed grouping method achieves higher TPR for both supervised and unsupervised methods. The FPR for the unsupervised methods is lower. Similarly, the proposed features achieve higher TPR.

The rest of this paper is organized as follows. Section 2 presents the result of a preliminary study and the previous works. Section 3 explains the data preprocessing. Section 4 presents the details of the feature extractions. Section 5 presents the feature-based sampling. The experimental result and the discussion are in Section 6. The conclusion is in Section 7.

## II. PRELIMINARY STUDY AND PREVIOUS WORKS

### A. Data Sampling

The popular sampling strategies for data consist of applying different forms of resampling to change the class distribution of the data. This can be done by either over-sampling the minority class or under-sampling the majority class until both classes are approximately equally represented [23].

Over-sampling is the simplest strategy that increases the amount of data in the minority class. It is a non-heuristic method that balances the class distribution through the random replication of positive examples. The drawback of the oversampling method is the original class distribution since it is artificially altered. In contrast, an under-sampling method may result in throwing out useful information about the majority class by randomly removing data. Despite its simplicity, it has empirically been shown to be one of the most effective resampling methods. However, the major problem with this technique is that potentially important data may be discarded in the prediction process. The study of [23] reported that an over-sampling method called SMOTE (Synthetic Minority Over-sampling TEchnique) proposed by [25] outperformed other sampling methods. It generates artificial examples from the minority class by interpolating the existing instances.

In this work, achieving a high true positive rate while keeping the number of false-positive lows is being focused on. The preliminary results for the no-sampling, under-sampling, and over-sampling methods are shown in Table I.

TABLE I  
PREDICTION RESULT USING  
DIFFERENT SAMPLING METHODS

Sampling Method	Classifier	TPR	FPR	TNR
No Sampling	Neural Network	0.00%	0.00%	100.00%
	Random Forest	5.88%	0.00%	99.99%
	Isolation Forest	56.25%	2.47%	97.52%
	Overall	20.71%	0.82%	99.17%
Under-Sampling	Neural Network	90.63%	47.04%	52.95%
	Random Forest	56.25%	1.15%	98.84%
	Isolation Forest	0.00%	0.67%	99.32%
	Overall	48.96%	16.29%	83.71%
Over-Sampling	Neural Network	90.63%	47.14%	52.85%
	Random Forest	0.00%	0.14%	99.85%
	Isolation Forest	12.50%	4.72%	95.27%
	Overall	34.37%	17.34%	82.66%

Without sampling, the model only predicted the transactions as non-fraud. Therefore, the TNR of the three models was high which are 100.00%, 99.99%, and 97.52% for the neural network, random forest, and isolation forest, respectively. Comparing the over-sampling to the under-sampling, the under-sampling using random forest achieved the best result which that was 56.25% TPR and 1.15% FPR. Although the TPR of the random forest is lower than the neural network, the false positive rate shows that the random forest performed better.

The overall performance is computed from the average true positive, false positive, false negative, and true negative of the three models for each sampling technique. The overall result shows that applying the sampling technique either an under-sampling or over-sampling technique achieved a better true positive rate. From the preliminary result, we can conclude that utilizing a sampling technique can improve the performance of the prediction model, to achieve a high true-positive rate while keeping a low false-positive rate.

In our preliminary study in [24], there were 227 fraud transactions, where 35 took place locally in Thailand and 192 were from abroad. The ratio of frauds, when compared to the total number of transactions in one year was 0.0033% for local transactions and 18.69% for abroad transactions. The transactions that took place abroad have a higher chance of being fraud, as shown in Fig. 1. In this way, utilizing a location feature can be used to separate the dataset.

### B. Outlier Detection Methods

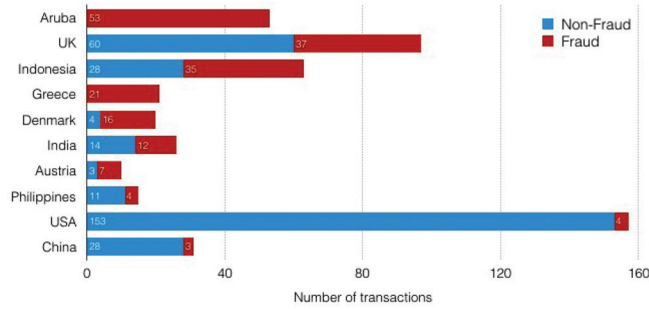
Many outlier detection methods were proposed to identify data points that do not conform to the normal characteristics by measuring distances or densities.

The Isolation Forest algorithm presented in [26] constructs a binary search tree to isolate outliers. It isolates data points in each tree level by selecting features and splitting values of the majority points to differentiate a common range of features from the uncommon. Fig. 2 illustrates the partition of a data point denoted by a rectangular point. If a data point is an outlier (as shown in Fig. 2 (b)), it is distinguishable in early partitioning. In other words, the number of partitions for the observation is less, as compared to the partition of Fig. 2 (a). Isolation Forest is an algorithm with low time and space complexity. It also has the ability to deal with high-dimensional data with irrelevant attributes. To get more accurate partitioning, Isolation Forest constructs multiple trees and averages the distances from the root node

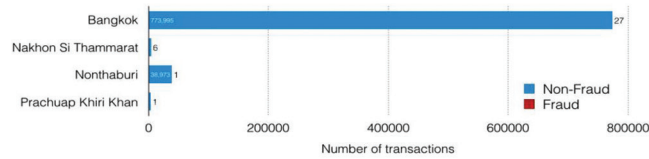


to each leaf node (an isolated node). The number of samples and features that are picked for partitioning are random and different for each tree. In this way, the distance from the root node to each isolated node is

different in each tree. The isolated nodes that are far from other nodes are isolated, to be nearby the root nodes of every tree.



(a) Number of legitimate and fraudulent transactions in different countries



(b) Number of legitimate and fraudulent transactions in Thailand

Fig. 1. Percentages of frauds and non-frauds in different locations

The Local Outlier Factor (LOF) presented in [27] is a density-based method that employs a  $k$ -nearest neighbors search. Each data point is scored by comparing the local density of the point, denoted by  $A$  in Fig. 3, with the local densities of its neighbors, denoted by  $B$ . The local density of  $A$  is the average reachable distance of  $A$  from its  $k$  neighbors. The reachable distance from  $A$  is defined by the maximum distance from  $A$  to  $B$  and  $B$  to the other neighbors such as  $c$ . In Fig. 3, the reachable distance from  $A$  is the distance from  $A$  to  $B$ .

The degree of being an outlier is the reachable distance from  $A$  to its nearest neighbors and from a neighbor  $B$  to its neighbors. For every neighbor  $B$  of  $A$ , the local density is the average reachable distance with each  $k$ -nearest neighbor's average reachable distance. If the average reachable distance is approximately equal to 1, the density of  $A$  is similar to its neighbor [28]. On the other hand,  $A$  is an inlier if the average reachable distance is less than 1. Otherwise, it is an outlier. In Fig. 3, the average reachable distance of  $A$  is greater than 1, therefore,  $A$  is considered as an outlier.

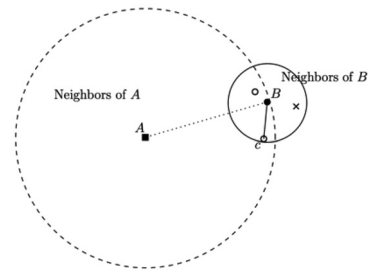


Fig. 3. An illustration of the local density of observation  $A$  to one of its  $k$ -nearest neighbors  $B$

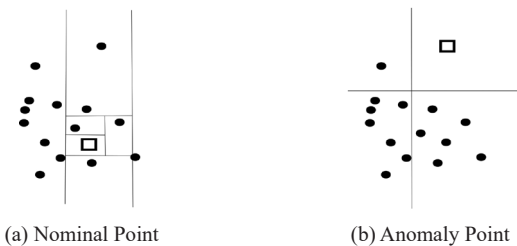


Fig. 2. (a) Partitions of a normal point. (b) Partitions of an anomaly point

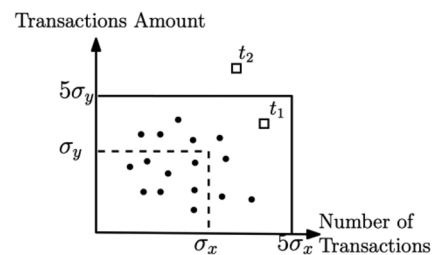


Fig. 4. Example of the normal behavior of an account within a fixed period

### C. Aggregated Features

The normal pattern of transactions was extracted by aggregating numeric features extracted from the previous transaction during a fixed period to summarize the account behavior. In [4], the normal behavior was represented using the mean value of the numeric features such as the transaction amount and the number of transactions per day, which are

defined as  $\mu_x$  and  $\mu_y$  in Fig. 4. To identify fraud using the previous transactions, normal behavior was defined using  $\mu_x$  and  $\mu_y$  by defining a boundary from  $(0,0)$  to  $(5\mu_x,0)$  and from  $(0,0)$  to  $(0,5\mu_y)$ . For an aggregate transaction, denoted by  $t$ , it is identified as a normal behavior if  $t$  lies within the solid boundary. See transaction  $t_1$  in Fig. 4 for an illustration. The aggregated transactions of day  $t_2$  are defined as fraud since it lies outside the solid boundary.

### III. PREPROCESSING

#### A. ATM Transactions and Feature Selection

The ATM transactional data was obtained from a bank in Thailand. Due to the non-disclosure agreement, the name of the financial institution is omitted in this work. The ATM transactions were collected from 1/01/2017 to 31/12/2017. The number of transactions is 1,317,717.

For each transaction, there are 14 features, in which 2 features are numeric and the remaining 12 features are non-numeric values. The detail of each numeric feature is described below:

- Trans\_Amnt: Amount of money in a transaction
- Fee\_Amnt: Amount of fee, applied in a transaction

The detail of each non-numeric feature is described below:

- Card\_No: Identification number of an ATM card
- Account\_ID: Identification number of a bank account
- Trans\_Date: Date of transaction
- Trans\_Time: Time of transaction
- Service\_Type: Service such as ATM, Account Setting, etc.
- Trans\_Type: Transactions such as withdraw, deposit, etc.
- Trans\_CD: Result of a transaction, e.g. success, failure, or rejection
- Trans\_Reason: Reason for the response transaction
- Terminal\_ID: Identification number of an ATM terminal
- Terminal\_Bank: Owner of the ATM terminal
- Dest\_Account\_ID: Destination account number of the transaction
- Flag: Fraud label. For example, 'False' indicates a legitimate transaction.

In this work, behavior features of withdrawal transactions through an ATM are aggregated daily.

Therefore, the non-numeric features, which are 'Service\_Type', 'Trans\_Time', 'Trans\_Reason', and 'Dest\_Account ID' are omitted and 10 raw features are used in this research.

#### B. Preprocessing

From the obtained data of 1,317,717 transactions, only withdrawal transactions, where the terminal country can be retrieved and the amount is greater than zero, are used. Therefore, 1,045,847 transactions are used, whereas 227 transactions of 43 accounts are frauds. The preprocessed features of each transaction that are used as input in this work are shown in Table II.

To represent the behavior of each account, features of 'date of the month' and 'day of the week' are derived from the 'Trans Date' feature. In addition, the location of the terminal ID is replaced with the corresponding coordinates.

In our preliminary study in [24], fraud transactions frequently took place abroad as shown in the descriptive analysis in Fig.1. Two new features, i.e. the 'distance' and the 'velocity' between the two consecutive transactions of each account are extracted. The intuition is the location of the two consecutive transactions should be varied to the interval between the transactions. Therefore, the latency of the two transactions in different countries or provinces should not be too close.

Let  $\mathcal{T} = \{T_1, \dots, T_n\}$  be a set of transactions of  $n$  accounts in the dataset. For each account  $i$ , let  $T_i$  be a set of  $k$  transactions, where  $T_i = \{t_1, \dots, t_p, \dots, t_k\}$ . Each transaction  $t_j$  is a set of features as shown in TABLE II. The transaction  $t_j$  is defined as  $t_j = \{t_{acc}, t_{card}, t_{date}, t_{dom}, t_{dow}, t_{amt}, t_{cd}, t_{type}, t_{terID}, t_{terBank}, t_{loc}, t_{flag}\}$

Let  $dist(t_{j-1}, t_j)$  be the  $L_1$  distance between the two consecutive transactions, i.e. and it is defined as follows:

$$dist(t_{j-1}, t_j) = |t_{j-1}^{loc} - t_j^{loc}| \quad (1)$$

where is the coordinates of the location where the transaction  $t_j$  took place. Let  $velocity(t_{j-1}, t_j)$  be a latency between the two transactions. It is defined as the ratio of the distance to the number of days of the two consecutive transactions. It is defined as:

$$velocity(t_{j-1}, t_j) = \frac{dist(t_{j-1}, t_j)}{days(t_{j-1}^{date}, t_j^{date})} \quad (2)$$

where  $dist(t_{j-1}, t_j)$  is the distance as defined in (1) and  $days(t_{j-1}, t_j)$  is the number of days between the transactions  $t_{j-1}$  and  $t_j$ .

TABLE II  
DESCRIPTION OF 14 FEATURES BEING USED IN THIS WORK

Features	Notation	Description
Account ID	$t^{acc}$	Account number of ATM card number.
Card No	$t^{card}$	Card number that was inserted.
Trans Date	$t^{date}$	Date of transaction.
Trans DOM	$t^{dom}$	Date of month.
Trans DOW	$t^{dow}$	Day of week.
Trans Amt	$t^{amt}$	Amount of money in the transaction.
Trans CD	$t^{cd}$	Result of the transaction.
Trans Type	$t^{type}$	Type of the transaction.
Terminal ID	$t^{terID}$	ID of ATM terminal.
Bank	$t^{terBank}$	Bank owner of the ATM terminal.
Location	$t^{loc}$	Coordinate of a terminal's location.
Flag	$t^{flag}$	Flag indicating non-fraud (0) or fraud (1).
Distance	$dist$	Distance from the previous transaction.
Velocity	$velocity$	Latency of the previous transaction.

From the obtained 10 raw features, each transaction is transformed to find the distance and the velocity of the two consecutive transactions. Therefore, the features of the transaction  $t_j$  become:  
 $t_j = \{t^{acc}, t^{card}, t^{date}, t^{dom}, t^{dow}, t^{amt}, t^{cd}, t^{type}, t^{terID}, t^{terBank}, t^{loc}, t^{flag}, dist, velocity\}$ .

The details of the features being utilized in this work can be found in Table II.

#### IV. BEHAVIOR FEATURE EXTRACTION

Given a set of transactions  $\mathcal{T} = \{T_1, \dots, T_n\}$  on  $n$  accounts, the transactions of each account  $T_i$  are preprocessed. An ATM transaction  $t_j \in T_i$  of each account  $i$  has 14 features as explained in Section III, which are

$$t_j = \{t^{acc}, t^{card}, t^{date}, t^{dom}, t^{dow}, t^{amt}, t^{cd}, t^{type}, t^{terID}, t^{terBank}, t^{loc}, t^{flag}, dist, velocity\}$$

The 14 features show the details of each transaction. To represent whether the transaction is consistent with the normal behavior of the account or likely the result of a fraudster, four transformation functions, which are 'Normal Behavior', 'Deviation of Normal Behavior', 'Risk Value', and 'Probability', are derived. Each function is denoted by  $g(f, i)$ ,  $c(f, j, i)$ ,  $r(\hat{f}_x)$ , and  $p(\hat{f}_x, i)$ , respectively, where  $f$  is a feature with a numeric value and  $\hat{f}_x$  is a non-numeric value in a transaction  $t_j$  of an account  $i$ . The summary of the transformed features that are used in this work is summarized in Table III. The details of each function are described in the following subsections.

TABLE III  
SUMMARY OF THE DERIVED FEATURES OF A SET OF TRANSACTIONS  $T_i$  OF AN ACCOUNT  $I$

Features	Description
$c(t^{amt}, i)$	Deviation from the average transaction amount
$c(t^{terBank}, i)$	Deviation from the average transaction amount of a bank
$p(t^{terBank}, i)$	Probability of using this bank
$r(t^{terBank})$	A risk score of this bank
$c(t^{terID}, i)$	Deviation from the average amount of a terminal
$p(t^{terID}, i)$	Probability of using this terminal
$r(t^{terID})$	A risk score of this terminal
$c(t^{loc}, i)$	Deviation from the average amount for a country
$p(t^{loc}, i)$	Probability of using this country
$r(t^{loc})$	A risk score of this country
$c(dist, i)$	Distance deviation from the average distance between consecutive transactions
$c(velocity, i)$	Velocity deviation from average velocity between consecutive transactions. (m/day)
$c(t^{dow}, i)$	A number of days that deviate from the average day of the week
$c(t^{dom}, i)$	A number of days that deviate from the average day of the month

### A. Normal Behavior Value

To obtain normal behavior, only normal transactions are considered to characterize the normal behavior of each account. In other words, the transactions  $t_j \in T_i$  in which  $t_j^{lag} = 1$  are excluded from the normal behavior computation.

Given a set of normal transactions  $T_i$  of an account  $i$ , where  $T_i = \{t_1, \dots, t_j, \dots, t_k\}$  and  $t_j^{lag} = 0$  for  $1 \leq j \leq k$ , let  $g(f, i)$  be an average value of a numeric feature  $f$  such as  $t_j^{amt}$  of account  $i$ , which is defined as follows:

$$g(f, i) = \frac{1}{|T_i|} \sum_{j \in T_i} f_i \quad (3)$$

where  $f_j$  is a numeric feature value of a transaction  $j$ .

The non-numeric features are transformed into numerical values by aggregating the transaction amount that occurred with the non-numeric values. For example, 10 transactions took place in Bangkok. The total amount of those transactions was 12,000. The non-numeric value of  $t^{loc} = \text{Bangkok}$  is 12000/10. Therefore,  $g(\widehat{f}_x)$  where  $x = \text{Bangkok}$  becomes 1200.

Let  $g(\widehat{f}_x, i)$  be the average transaction amount of a non-numeric feature  $\widehat{f}_x$  of value equal  $x$  such as 'Bangkok' for 'Terminal Location'. It can be defined using the following equation:

$$g(\widehat{f}_x, i) = \frac{1}{k} \sum_{j \in T_i(\widehat{f})} t_j^{amt} \quad (4)$$

where  $k$  is the number of transactions such that  $f \in T_i$  and  $= x$ .

In this paper, the normal behavior model of an account consists of aggregated features derived from  $t^{amt}$ ,  $dist$ ,  $velocity$ ,  $t^{dom}$ ,  $t^{dow}$ ,  $t^{terID}$ ,  $t^{terBank}$ , and  $t^{loc}$ . Only  $t^{amt}$ ,  $dist$ , and  $velocity$ , which are numeric values, are aggregated using  $g(f, i)$ . The remaining features apply  $g(\widehat{f}_x, i)$ .

### B. Deviation from Normal Behavior Value

The deviation from the normal behavior value considers all the transactions of each account, including both legitimate and fraud. To represent the variation of each transaction  $t_j$  to the normal behavior of account  $i$ , a confidence value is computed using the normal behavior value to determine the deviation from the current transaction.

Let  $c(f, j, i)$  be the confidence on the value of feature  $f$  for each transaction  $t_j \in T_i$  in an account  $i$ . It is defined as follows:

$$c(f, j, i) = \frac{f - g(f, i)}{g(f, i)} \quad (5)$$

where  $g(f, i)$  is the normal behavior value of the feature  $f$  as defined in (3). A non-numeric feature, such as the terminal location, is defined using  $g(\widehat{f}, i)$ , as defined in (4). The value of  $\widehat{f}$  is the transaction amount occurring with the value of the non-numeric feature.

The confidence value  $c(f, j, i)$  is computed for  $t^{amt}$ ,  $velocity$ ,  $dist$ ,  $t^{dom}$ ,  $t^{dow}$ ,  $t^{terID}$ ,  $t^{terBank}$ , and  $t^{loc}$ .

### C. Risk Value

The risk value is the ratio of the total number of known fraudulent transactions to the total number of every transaction that occurred with the non-numeric feature  $\widehat{f}_x$ . It is determined from all transactions in the training dataset that are associated with all the non-numeric feature  $\widehat{f}_x$  with a value  $x$ .

Let  $r(\widehat{f}_x)$  be the risk value for the feature  $\widehat{f}$ , with a value of  $x$ . Let  $\mathcal{F}$  be the set of all fraudulent transactions and let  $\mathcal{T}$  be a set of all transactions. The risk value is defined as follows:

$$r(\widehat{f}_x) = \frac{\sum_{l=1}^{|\mathcal{F}|} h(\mathcal{F}, \widehat{f}_x, t_l)}{\sum_{l=1}^{|\mathcal{T}|} h(\mathcal{T}, \widehat{f}_x, t_l)} \quad (6)$$

where,  $h(\mathcal{F}, \widehat{f}_x, t_l)$  is the total number of known fraudulent transactions in  $\mathcal{F}$  associated with the value of the feature  $\widehat{f}_x$ , and  $h(\mathcal{T}, \widehat{f}_x, t_l)$  is the number of all transactions in  $\mathcal{T}$  with the feature.

The number of fraud transactions  $h(\mathcal{F}, \widehat{f}_x, t_l)$  is obtained using the following condition:

$$h(\mathcal{F}, \widehat{f}_x, t_l) = \begin{cases} 1 & \text{if } t_l^f == x \\ 0 & \text{otherwise} \end{cases}$$

The value of  $h(\mathcal{T}, \widehat{f}_x, t_l)$  can be obtained analogously using all transactions in  $\mathcal{T}$ .

For example, if  $\widehat{f} = \text{'location'}$  and  $x = \text{'Bangkok'}$ . There are 10 transactions in in 'Bangkok', where 90 are legitimate and 10 are fraudulent transactions. The risk value of the of 'location' = 'Bangkok' is 0.1. The risk values are determined for non-numeric value  $\widehat{f}_x$  of  $t^{terID}$ ,  $t^{terBank}$ , and  $t^{loc}$ .

### D. Probability

A probability feature shows how likely the account  $i$  will complete the transaction  $t_j$  regarding to the non-numeric feature  $\widehat{f}_x$  of a value  $x$ .

Given a set of transactions  $T_i$  of the account  $i$ , a probability is a ratio of the number of transactions  $t_j \in T_i$  that has the feature  $\widehat{f} = x$  to the total number of transactions of  $T_i$ . Since fraud transaction is rare, the number of legitimate transactions that occurred with  $\widehat{f}_x$  should be larger. In this way, the probability of a normal transaction is higher than fraud. The probability is defined as follows.

$$p(\widehat{f}_x, i) = \frac{\sum_{l=1}^{|T_i|} h(T_i, \widehat{f}_x, t_l)}{|T_i|} \quad (7)$$

where,

$$h(T_i, \widehat{f}_x, t_l) = \begin{cases} 1 & \text{if } t_l^f == x \\ 0 & \text{otherwise} \end{cases}$$

The probabilities are computed for non-numeric values, i.e.,  $\widehat{f}_x$  of  $t^{terID}$ ,  $t^{terBank}$ , and  $t^{loc}$ .

## V. FEATURE-BASED DATA GROUPING

To achieve a high true positive rate while keeping the false positive rate as low as possible, accounts are separated into ‘local-only’ and ‘has-abroad’ groups based on the location feature,  $t_j^{loc}$ .

Given a set of transactions  $T_i$  of an account  $i$  and  $T_i \in \mathcal{T}$ , all transactions  $t_j \in T_i$  is assigned to the ‘has-abroad’ group if there is a transaction  $t_j$  such that the location  $t_j^{loc}$  is not in Thailand. Otherwise, they are assigned to the ‘local-only’ group.

The number of transactions in the ‘local-only’ group is 1,025,216, where 16 transactions are frauds and the rest are legitimate transactions. For the ‘has-abroad’ group, there are 16,330 transactions, where 16 transactions are frauds and the rest are legitimate transactions.

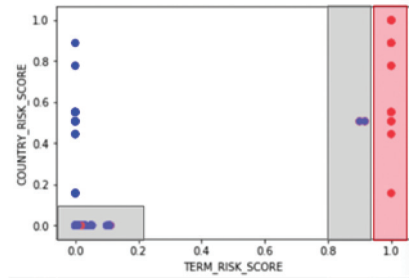
### A. Analysis: Behavior Features and Data Grouping

To visualize the performance of the features in identifying fraud, a two-dimensional scatter plot of ATM transactions for terminal risk score and country risk score features is shown in Fig. 5(a). The frauds are in red and the normal transactions are in blue. From the graph, the transactions with a terminal risk score of 1 are frauds. However, there are some frauds whose feature values are close to the legitimate transactions that are depicted in Fig. 5(b). From the figure, it can be concluded that the separation between normal and fraudulent transactions is hard to be defined.

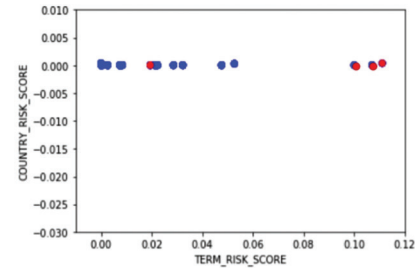
A plot of the country and the terminal risk scores of transactions in the ‘has-abroad’ group is shown in Fig. 6(a). Compared to the plot in Fig. 5(b), the fraud transactions in Fig. 6(a) can be separated. Using the other derived features such as the deviation from the average amount of a country and the terminal’s risk score, the fraud transactions can also be separated as depicted in Fig. 6(b).

## VI. EXPERIMENT

The ATM transactional data from 1/01/2017 to 31/12/2017 were obtained from a bank in Thailand. Due to the nondisclosure agreement, the name of the bank cannot be given. The objective of this work is to effectively detect fraud transactions while keeping a low number of false positives. The true positive rate (TPR), the false positive rate (FPR), and the true negative rate (TNR) are used to show the efficiency of the model.

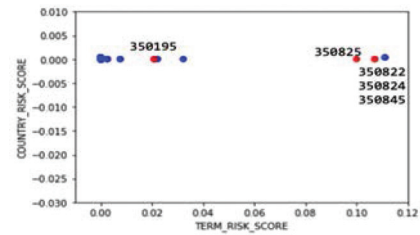


(a) Labeled ATM transactions of terminal risk score and country risk score.

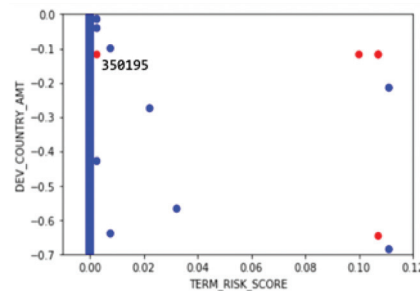


(b) The points in the lower-left shaded area of Fig. 5(a)

Fig. 5. Examples of fraud transactions (red) that are similar to legitimate transactions (blue).



(a) The transactions in the has-abroad group in the lower-left shaded area of Fig. 5(a)



(b) The transactions in the has-abroad account group with the terminal risk and deviation amount.

Fig. 6 Effects of the proposed risk score features for separating fraud transactions

Only withdrawal transactions, where the terminal country is known and the amount is greater than zero, are used. The total number of transactions in the experiment is 1,045,847. They are separated into the training and the testing sets. The training set contains the transactions from 01/01/2017 to 30/09/2017.

The transactions in the testing set of each account are transformed using the same functions. They are used to compare the result of the prediction model and the label assigned by the fraud investigators.

The testing set is the transactions from 01/10/2017 to 31/12/2017. The performance of the proposed features, the grouping using location-based features, and the classifiers including an outlier detection are being studied. Three patterns of the data grouping, i.e., 'no-grouping', 'local-only', and 'has-abroad' are used. In 'no-grouping', all the 1,045,847 transactions are used, where 790,984 (75.63%) transactions are for training and 254,863 (24.37%) are for testing. The 735,865 (71.77%) transactions in 'local-only' group are for developing a model and 289,351 (28.23%) are for testing. Among the testing transactions, 16 transactions were identified as frauds and confirmed by the bank. The 12,939 (79.23%) transactions in

'has-abroad' are for model development; 3,391 (20.77%) are for testing where 16 were identified as frauds by the bank.

Two outlier detection models: Local Outlier Factor (LOF) and Isolation Forest (IF) are employed. The two models are available in SciKit-Learn library [29]. Each model requires different parameters. LOF utilizes two parameters which are the number of neighbors and the contamination. The former parameter is the minimum number of  $k$ -nearest neighbors of each transaction required to classify the transaction as normal, while the latter is the estimated ratio of frauds in the population, which can be set between 0 and 0.5. IF requires three parameters. The first one is maximum number of samples for constructing each tree. The second is the maximum number of features to be used for each tree. Lastly, the contamination parameter is the ratio of fraud in the data set. In addition to the outlier detection methods, two binary classification models based on the artificial neural network (ANN) and Random Forest (RF) are employed. parameters settings for each experiment are in TABLE IV.

TABLE IV  
PARAMETER SETTINGS FOR ATM FRAUD DETECTION

Model	Tuning Parameters		
	Local-Only	Has-Aboard	No grouping
LOF	n neighbors = 8, contamination = 0.1	n neighbors = 3, contamination = 0.4	n neighbors = 4, contamination = 0.5
IF	max samples = 1000, max features = 12, contamination = 0.045	max samples = 320, max features = 15, contamination = 0.0145	max samples = 1000, max features = 15, contamination = 0.0125
ANN	hidden layer size = 40, 20, 10, 10	hidden layer size = 40, 20, 10, 10	hidden layer size = 40, 20, 10, 10
RF	maximal depth=10, number of trees=10	maximal depth=10, number of trees=10	maximal depth=10, number of trees=10

TABLE V  
CONFUSION MATRIX FOR FRAUD DETECTION

		Predicted	
		Fraud	Not Fraud
Actual	Fraud	TP	FN
	Not Fraud	FP	TN

The classified result can be decomposed using a confusion matrix for fraud detection as shown in TABLE V. True Positive (TP) outcome occurs when a fraud transaction (positive) is correctly classified as a fraudulent transaction. A False Positive (FP) occurs when a non-fraudulent transaction (negative) is incorrectly identified as a fraudulent transaction. A False Negative (FN) occurs when a fraud transaction (positive) is incorrectly identified as a non-fraudulent transaction (negative). Lastly, a True Negative (TN) outcome occurs when a non-fraudulent transaction (negative) is correctly identified as a non-fraudulent transaction (negative).

The overall performance measures are true positive rate (TPR), false-positive rate (FPR), and accuracy. TPR is a ratio of the number of correctly classified as fraud transactions to the total number of transactions that are actually a fraud. It can be calculated as follow:

$$TPR = \frac{TP}{TP + FN}$$

FPR is a ratio between the number of not fraud transactions that are wrongly classified as fraud and the total number of actual 'not fraud' transactions. It can be calculated as follow:

$$FPR = \frac{FP}{FP + TN}$$

Accuracy is a ratio of the correctly classified transaction to the total number of transactions. It can be calculated as follow:

$$Accuracy = \frac{TP + TN}{TP + TN + FP + FN}$$

A. Performance of the Sampling Methods

The results shown in Table VI are from the parameters settings of each model in Table IV. The binary classifier, the ANN, cannot detect any fraud transactions. In other words, every transaction is predicted as a legitimate transaction.

For the ‘local-only’ sampling method, the RF achieves 62.5% for detecting fraud, while the IF achieves a higher TPR of 75%. Comparing the false positive rate, IF is better than RF. However, the LOF obtains a lower FPR but it can correctly detect less than half of the fraud transactions.

For the ‘has-abroad’ sampling method, the IF can correctly detect all fraud transactions while the RF cannot detect any frauds. The IF can also achieve a low FPR of 8.23% that is lower than the LOF.

Table VII shows the confusion matrix of the IF classifier for detecting the fraud in the ‘has-abroad’ group. The result shows that it can correctly detect all 16 fraud transactions, while incorrectly detecting 278 normal transactions as frauds. The false-positive rate is 8.23%. The LOF detects 9 out of 16 fraud transactions but incorrectly detects 1,251 normal transactions as frauds.

Table VIII shows the confusion matrix of the IF for detecting the fraud in the ‘local-only’ group. It can detect 12 fraudulent transactions out of 16 transactions. However, 81,077 normal transactions are incorrectly detected as frauds, which results in 28.02% false-positive rate. The LOF model detects 7 out of 16 frauds and incorrectly detects 39,530 normal transactions.

TABLE VI  
COMPARISON OF PERFORMANCE OF THE ATM FRAUD DETECTION MODEL OF ‘LOCAL-ONLY’ AND ‘HAS-ABROAD’

Model	Local-Only		
	TPR	FPR	TNR
LOF	43.75%	13.66%	86.33%
IF	75.00%	28.02%	71.97%
ANN	0.00%	0.00%	100.00%
RF	62.50%	35.84%	64.15%
Model	Has-Aboard		
	TPR	FPR	TNR
LOF	56.25%	37.07%	62.93%
IF	100.00%	8.23%	91.76%
ANN	0.00%	0.00%	100.00%
RF	0.00%	1.30%	98.69%

TABLE VII  
CONFUSION MATRIX OF ISOLATION FOREST (IF) FOR THE ‘HAS-ABROAD’ ACCOUNT GROUP

		Predicted	
		Fraud	Not Fraud
Actual	Fraud	16	0
	Not Fraud	278	3,097

TABLE VIII  
CONFUSION MATRIX OF ISOLATION FOREST FOR ‘LOCAL-ONLY’ ACCOUNT GROUP

		Predicted	
		Fraud	Not Fraud
Actual	Fraud	12	4
	Not Fraud	81,077	208,258

TABLE IX  
CONFUSION MATRIX OF ISOLATION FOREST FOR ‘NO-GROUPING’ ACCOUNT GROUP

		Predicted	
		Fraud	Not Fraud
Actual	Fraud	24	8
	Not Fraud	32,172	260,538

Table IX shows the confusion matrix of the IF with ‘no-grouping’ transactions. The IF detects 24 out of 32 fraud transactions. However, it incorrectly detects 32,172 normal transactions as frauds, which results in a 10.99% false-positive rate.

The overall result of the proposed sampling method is compared with a method that does not apply any grouping. The average of the prediction result in the confusion matrix for true positive, false positive, false negative, and true negative of the ‘local-only’ and the ‘has-abroad’ groups of each model are computed. The result is shown as the average of two sampling methods in Table X.

The result shows that utilizing the proposed sampling method achieves better TPR for the IF of 87.50% and the false positive rate is 27.98%. The false-positive rate of the proposed grouping methods is higher than ‘no-grouping’, but the true positive rate is better. It can be concluded from the result that the proposed method is effective for the accounts that have transactions abroad.

TABLE X  
COMPARISON OF PERFORMANCE OF THE AVERAGE OF THE ‘LOCAL-ONLY’ AND THE ‘HAS-ABROAD’ GROUPS WITH ‘NO-GROUPING’

Model	‘Local-Only’ And ‘Has-Abroad’		
	TPR	FPR	TNR
LOF	50.00%	13.93%	86.06%
IF	87.50%	27.98%	72.21%
ANN	0.00%	0.00%	100.00%
RF	31.25%	35.44%	64.55%
Model	No Grouping		
	TPR	FPR	TNR
LOF	31.25%	5.21%	94.78%
IF	75.00%	10.99%	89.00%
ANN	0.00%	0.00%	99.99%
RF	6.25%	5.31%	94.69%

TABLE XI  
COMPARISON OF PERFORMANCE OF RAW FEATURES AND  
THE PROPOSED FEATURE EXTRACTION

Features	Classifier	TPR	FPR	TNR
Raw	ANN	0.00%	0.00%	100.00%
	RF	5.88%	0.00%	99.99%
	IF	56.25%	2.47%	97.52%
Proposed Feature	ANN	0.00%	0.00%	99.99%
	RF	6.25%	5.31%	94.69%
	IF	75.00%	10.99%	89.00%

### B. Performance of Feature Extraction

The performance of the proposed feature extraction is compared using ‘no-grouping’. Comparing ‘no-sampling’ with the raw feature is shown in Table XI. The proposed feature, applied with the IF, can detect 75.00% TPR and 10.99% FPR. Although the false-positive rate of the proposed feature is higher than using the raw feature, the performance for directly detecting fraud transactions correctly is much better.

### C. Analysis

The experimental results show that the IF outperforms the other models. To identify an outlier, the IF looks through every tree and computes the average path length from the root to the isolation node. If the average path length of the observation is shorter than the average path length of a normal transaction, the observation is identified as an outlier. A fraud transaction as in Fig. 6 (a) is not located at the bottom of the tree. Apart from selecting the country and the terminal risk scores as the features, it selects the terminal amount deviation and the terminal risk scores features, as shown in Fig. 6 (a), in the other trees. Using these features, a fraud transaction is separated from normal transactions.

The LOF reports an outlier using the density of an observation and its  $k$ -nearest neighbors. From Fig. 6(b), the average density of the fraud transaction to its  $k$ -nearest neighbors is close to one. Therefore, it could not detect 350,195 transactions as fraud.

Comparing our behavior features to the previous work in credit card fraud [3], the proposed method requires transactions of one account owner for a longer period than the previous work that utilized only 7 days. This limitation is caused by the number of transactions of ATM being lower than the credit card one card owner may have many cards but only a few accounts are owned by the same customer.

## VII. CONCLUSION

Three features: the deviation, the risk, and the probability features for both numeric and non-numeric values are presented. The proposed features can separate legitimate transactions from frauds. The accounts are separated into two groups depending on the location of the previous transactions, which are ‘local-only’ and ‘has-abroad’ groups. The experimental result shows that the ‘has-abroad’ group can improve the true positive rate of detecting fraud from 75% to 100% TPR when applying the isolation forest outlier detection method. Moreover, the false positive rate is 8.23%.

From the experimental result, the proposed features and the location-based grouping is performed well on the transaction that occurred abroad. Compare to the previous research on fraud detection, the proposed location-based grouping extracts the behavior features of the accounts in the same group, while the previous works use the behavior of every account or credit card. To improve the performance of the transactions that occurred locally, like in Thailand, finer details of the location should be mentioned such as a place with many tourists or an isolation location of the ATMs.

## ACKNOWLEDGEMENTS

This work was supported by an SIIT Young Researcher Grant, under contract no. SIIT 2017-YRG-NK04. The authors would like to thank Prof. Dr. Thanaruk Theeramunkong, Dr. Thepchai Supnithi, and Assoc. Prof. Dr. Nobuhiko Sugino for their fruitful advice and comments.

## REFERENCES

- [1] Ben Knieff, “2016 Global Customer Card Fraud: Where Card Fraud is Coming From,” Aite Group LLC., Boston, USA, Jul. 2016.
- [2] T. Guo and G.-Y. Li, “Neural Data Mining for Credit Card Fraud Detection,” in *Proc. 2008 International Conference on Machine Learning and Cybernetics*, 2008, pp. 3630-3634.
- [3] C. Whitrow, D. J. Hand, P. Juszczak et al., “Transaction Aggregation as a Strategy for Credit Card Fraud Detection,” *Data Mining and Knowledge Discovery*, vol. 18, no. 1, pp. 30-55, Feb. 2009.
- [4] M. Krivko, “A Hybrid Model for Plastic Card Fraud Detection Systems,” *Expert Systems with Applications*, vol. 37, no. 8, pp. 6070-6076, Aug. 2010.
- [5] J. R. Dorronsoro, F. Ginel, C. Sgnchez et al., “Neural Fraud Detection in Credit Card Operations,” *IEEE Transactions on Neural Networks*, vol. 8, no. 4, pp. 827-834, Jul. 1997.



- [6] E. Aleskerov, B. Freisleben, and B. Rao, "Cardwatch: A Neural Network Based Database Mining System for Credit Card Fraud Detection," in *Proc. The IEEE/IAFE 1997 Computational Intelligence for Financial Engineering*, 1997, pp. 220-226.
- [7] K. K. Sherly and R. Nedunchezian, "Boat Adaptive Credit Card Fraud Detection System," in *Proc. 2010 IEEE International Conference on Computational Intelligence and Computing Research*, 2010, pp. 1-7.
- [8] J. Gehrke, V. Ganti, R. Ramakrishnan et al., "Boat—Optimistic Decision Tree Construction," *SIGMOD Rec.*, vol. 28, no. 2, pp. 169-180, Jun. 1999.
- [9] E. Kirkos, C. Spathis, and Y. Manolopoulos, "Data Mining Techniques for the Detection of Fraudulent Financial Statements," *Expert Systems with Applications*, vol. 32, no. 4, pp. 995-1003, May. 2007.
- [10] E. Ngai, Y. Hu, Y. Wong et al., "The application of Data Mining Techniques in Financial Fraud Detection: A Classification Framework and An Academic Review of Literature," *Decision Support Systems*, vol. 50, no. 3, pp. 559-569, Feb. 2011.
- [11] S. X. Wu and W. Banzhaf, "Combating Financial Fraud: A Coevolutionary Anomaly Detection Approach," in *Proc. The 10th Annual Conference on Genetic and Evolutionary Computation*, SER. GECCO '08, 2008, pp. 1673-1680.
- [12] D. Huang, D. Mu, L. Yang et al., "Codetect: Financial Fraud Detection with Anomaly Feature Detection," *IEEE Access*, vol. 6, pp. 19161-19174, Mar. 2018.
- [13] K. Yamanishi, J. I. Takeuchi, G. Williams et al., "On-Line Unsupervised Outlier Detection Using Finite Mixtures with Discounting Learning Algorithms," *Data Mining and Knowledge Discovery*, vol. 8, no. 3, pp. 275-300, May. 2004.
- [14] V. Chandola, A. Banerjee, and V. Kumar, "Anomaly Detection: A Survey," *ACM Comput. Surv.*, vol. 41, no. 3, pp. 15:1-15:58, Jul. 2009.
- [15] MIT. (2018, Oct. 2). *Reducing False Positives in Credit Card Fraud Detection*. [Online]. Available: <https://www.sciencedaily.com/releases/2018/09/180920131513.htm>
- [16] D. J. Hand and V. Vinciotti, "Choosing K for Two-Class Nearest Neighbour Classifiers with Unbalanced Classes," *Pattern Recognition Letters*, vol. 24, no. 9, pp. 1555-1562, 2003.
- [17] S. Bhattacharyya, S. Jha, K. Tharakunnel et al., "Data mining for Credit Card Fraud: A Comparative Study," *Decision Support Systems*, vol. 50, no. 3, pp. 602-613, Feb. 2011.
- [18] S. Branka, J. B. K. Hofer-Schmitz, K. Nahrgang et al., "Follow the Trail: Machine Learning for Fraud Detection in Fintech Applications," *Sensors*, vol. 21, no. 5, pp. 1594, Feb. 2021.
- [19] T. Pourhabibi, K. L. Ongb, B. H. Kama et al., "Fraud Detection: A Systematic Literature Review of Graph-Based Anomaly Detection Approaches," *Decis. Support System*, vol. 133, pp. 113303, Jun. 2020.
- [20] W. Bao, J. Yue, and Y. Rao, "A Deep Learning Framework for Financial Time Series Using Stacked Autoencoders and Long-Short Term Memory," *PLoS ONE*, vol. 12, pp. e0180944, Jul. 2017.
- [21] A. Singh, "Anomaly Detection for Temporal Data Using Long Short-Term Memory (LSTM)," *IFAC-Papers Online* vol. 52, pp. 2408-2412, Jan. 2017.
- [22] C. R. Chawla, "Deep Learning for Anomaly Detection: A Survey," *arXiv:1901.03407*, Jan. 2019.
- [23] A. I. Marques, V. Garcia, and J. S. Sanchez, "On the Suitability of Resampling Techniques for the Class Imbalance Problem in Credit Scoring," *Journal of the Operational Research Society*, vol. 64, no. 7, pp. 1060-1070, Jul. 2013.
- [24] R. Laimek and N. Kaothanthong, "Atm Fraud Detection Using Outlier Detection," in *Proc. IDEAL, 2018*, pp. 539-547.
- [25] N. V. Chawla, K. W. Bowyer, L. O. Hall et al., "Smote: Synthetic Minority Over-Sampling Technique," *Journal of Artificial Intelligence Research*, vol. 16, pp. 321-357, Jun. 2002.
- [26] F. T. Liu, K. M. Ting, and Z.-H. Zhou, "Isolation-Based Anomaly Detection," *ACM Trans. Knowl. Discov. Data*, vol. 6, no. 1, pp. 3:1-3:39, Mar. 2012.
- [27] M. M. Breunig, H. P. Kriegel, R. T. Ng et al., "Lof: Identifying Density-Based Local Outliers," *SIGMOD Rec.*, vol. 29, no. 2, pp. 93-104, May. 2000.
- [28] M. Elahi, K. Li, W. Nisar, X. Lv et al., "Detection of Local Outlier Over Dynamic Data Streams Using Efficient Partitioning Method," in *Proc. 2009 WRI World Congress on Computer Science and Information Engineering*, 2009, pp. 76-81.



**Natsuda Kaothanthong** received a Ph.D. in Information Science from Graduate School of Information Sciences, Tohoku University. She is an Assistant Professor in School of Management Technology at Sirindhorn International Institute of Technology, Thammasat University. Her research interests are machine learning, artificial intelligence, image processing, and medical images processing.



**Roongtawan Laimek** received a master degree in engineering from Thailand Advanced Institute of Science and Technology and Tokyo Institute of Technology.

# Reverse Logistics Network Design for Infected Medical Waste Management in Epidemic Outbreaks under Uncertainty: A Case Study of COVID-19 in Pathum Thani, Thailand

Pornpawee Supsermpol<sup>1</sup>, Sun Olapiriyakul<sup>2</sup>, and Navee Chiadamrong<sup>3</sup>

<sup>1,2,3</sup>School of Manufacturing Systems and Mechanical Engineering, Sirindhorn International Institute of Technology, Thammasat University, Pathum Thani, Thailand  
E-mail: p.supsermpol@gmail.com, suno@siit.tu.ac.th, navee@siit.tu.ac.th

Received: January 24, 2022 / Revised: February 15, 2022 / Accepted: February 28, 2022

**Abstract**— Disease outbreaks cause disruption in the economy and threaten human life. This study proposes a Fuzzy Multi-Objective Multi-Period Mixed-Integer Linear Programming (FMOMILP) model for effective IMW management in outbreaks under uncertain environments considering financial and risk aspects. The strategic decision is to determine optimal locations and suitable capacity levels of temporary facilities, including temporary storage centers and temporary treatment centers, as well as optimal transportation strategies. To solve the proposed FMOMILP model, an integrated interactive fuzzy approach is employed. First, an equivalent auxiliary crisp model is used to handle the uncertainties by the feasibility degree ( $\alpha$ ) concept. The problem is solved using Fuzzy Goal Programming (FGP). A case study of the COVID-19 outbreak in Pathum Thani province in Thailand was carried out to demonstrate the proposed model's performance. The proposed method yields solutions with varying feasibility degrees and allowed percentage deviations, providing alternatives for the decision-makers. The contribution of this study helps identify the optimal setting of temporary facilities in appropriate locations and seizes and improves the performance of IMW management subject to the uncertainty of data by trading off between conflicting objectives. A comparison of the results with (optimal solution) and without (actual solution) temporary facilities is also presented.

**Index Terms**—Epidemic Logistics, Fuzzy Goal Programming, Medical Wastes, Multi-Objective Fuzzy Programming, Operational Risks, Reverse Logistics

## I. INTRODUCTION

The amount of Infected Medical Waste (IMW) increases drastically as the number of infected people exponentially increases. This leads to one important challenge in outbreaks situation, which is effective reverse logistics to manage IMW. An effective reverse logistics plan of IMW is crucial in controlling the spreading of the disease since improper collection and treatment can hugely create risk for the medical staff, patients, and communities around hospitals and treatment centers.

Coronavirus disease (COVID-19) is the most recent pandemic transmitted by human-to-human caused by a newly discovered coronavirus. On 31st December 2019, the first case was reported in Wuhan, China, and later developed into a global crisis [1]. The situation in Thailand might not be as critical as in some other countries. However, a surge in the number of infected people generates an increasing amount of IMW, which should be treated properly in a timely manner to control the risk of spreading the disease. Since the number of IMW rapidly increases, as well as the existing treatment centers' capacity is not sufficient, the decision the establishment of temporary facilities is significant in designing effective reverse logistics of IMW.

Considering the actual outbreak situation, the availability and accuracy of collected information are always problems. These uncertainties cause ineffectiveness in designing each network since the problems are no longer purely deterministic. Thus, the inclusion of the uncertainty assumptions should be effectively applied when considering such problems where a great deal of unknown and uncertain parameters exists.

In this study, considering a real situation in a province in Thailand, Pathum Thani, a Fuzzy Multi-Objective Multi-Period Mixed-Integer Linear Programming (FMOMILP) model is developed for the reverse logistics network design of IMW management in outbreaks with the purpose of improving the decisions of establishing temporary facilities with optimal locations and sizes, and determining the transportation strategies under uncertain environment.

The remainder of this paper is arranged as follows. Section 2 presents a literature review on relevant topics. Section 3 contains the problem description and mathematical formulation. Section 4 proposes an integrated interactive fuzzy programming approach. Section 5 validates the proposed model and approach via a case study of COVID-19 in Pathum Thani province, Thailand. Section 6 discusses and analyses the results. Lastly, Section 7 concludes the study and states limitations and further research directions.

## II. LITERATURE REVIEW

Our literature review would be focused on three related topics, i.e., (1) Risks in the supply chain, (2) Multi-objective fuzzy programming, and (3) Reverse logistics network model for IMW management.

### A. Risks in Supply Chain

Risks in the supply chain are classified into 2 types: operational risks and disruptive risks [2]. Operational risks are concerned with risks from uncertain internal processes or external events, for example, demand uncertainties and cost uncertainties. Disruptive risks, on the other hand, are concerned with natural disasters, e.g., earthquakes, or man-made disasters. Epidemic outbreaks are one of the special cases of supply chain disruptive risk, which has dynamic nature over many regions, i.e., SARS, Ebola, and the latest one, which is COVID-19.

Risk is an abstract concept that is hard to evaluate accurately. Cheng and Yu [3] proposed a fuzzy comprehensive evaluation with the Delphi method to evaluate and assign weight to the risks in emergency logistics. Sherali et al. [4] developed a branch-and-bound framework to minimize weighted and mitigate risks arising from the post-disaster. Considering multi-objective problems, Nolz et al. [5] presented a post-disaster problem considering transportation risk and location risk as one of the objectives. Three approaches to measuring risks were analyzed and the unreachability approach turned out to be the most suitable one for this problem. Abkowitz and Cheng [6] proposed a methodology for estimating costs and risks in hazardous waste transportation optimization. Several causes of accidents and their consequences were used in evaluating the risk.

### B. Multi-Objective Fuzzy Programming

In a real situation, data are not always known or accurately obtained since there might be all kinds of unpredictable impacts from both environmental uncertainty and system uncertainty. As the outbreak nature is dynamic and there are several unpredictable conditions, uncertainties arise in various parameters such as disease transmission rate and recovery rate. As a result, Linear Programming (LP) based on crisp values is no longer capable to solve such problems. So, the fuzzy theory has been introduced to deal with problems containing uncertainties.

In addition, real-world problems are quite complex and usually contain more than one objective. Conflicting among objectives is a common problem in many cases, so there is no ideal outcome, which can improve all objectives concurrently [7], [8]. To solve these conflictive multi-objective programming problems, several approaches have been proposed based on the flexibility and ability to play with the degree of satisfaction among objectives of fuzzy programming approaches. Fuzzy programming approaches can start from preliminary methods such as weighted max-min, weighted additive, and Zimmermann methods. However, the solutions generated by these methods might not be efficient or practical [9]. Thus, several methods have been developed to generate more effective results. Interactive Fuzzy Linear Programming (i-FLP) is one of the methods developed to consider efficiency and user dependency in generating satisfactory outcomes. The i-FLP has the advantage of assisting decision-makers in obtaining preferable solutions at various levels of feasibility. To make the method interactive, different approaches have been implemented such as Torabi and Hassini (TH) method, Selim and Ozkarahan (SO) method, and the Jimenez approach. Each method has its own advantages and disadvantages subject to its application in each situation.

Goal Programming (GP) is a part of linear programming that can solve multiple objectives. It was first introduced by Charnes et al. [10]. Charnes and Cooper [11] later provided a more precise definition. Because of its effectiveness, it has been widely used in a variety of research [12]. Traditional goal programming requires precise determination of aspiration levels and weights in order to minimize deviations. However, due to incomplete information and uncertain natures, it is difficult to determine these values precisely in practice. Therefore, Fuzzy Goal Programming (FGP) was developed to deal with fuzziness in the aspiration levels. Several FGP approaches were developed. For example, Narasimhan [13] developed an FGP approach considering both fuzziness in aspiration levels and weights. Later, Rubin and Narasimhan [14] proposed

a nested hierarchy approach to assign the priorities of each goal. Then, Arora and Gupta [15] developed a bilevel interactive FGP that incorporates the concept of tolerance.

### *C. Reverse Logistics Network Model for IMW Management*

Recently, medical waste management during epidemic outbreaks has become more popular among researchers. This medical waste management is vital in designing effective waste management since it can help in controlling the spreading of diseases. The first known concept of Reverse Logistics (RL) was proposed by Stock [16] as the backward flow with the role of managing materials, recycling materials, and disposing of wastes. In another word, reverse logistics considers the flow starting from End-of-Use (EOU) products to the recovery of those products. Fleischmann et al. [17] analyzed the impact of the return flow and developed a Mixed-Integer Linear Programming (MILP) model, which was commonly used in further Closed-Loop Supply Chains (CLSC) problems.

The very first research of multi-objective reverse logistics associated with waste management was proposed by Shih and Lin [18] where the developed MILP and a dynamic programming model were employed to determine optimal routing and scheduling in managing IMW in Taiwan. Their models considered both ecological aspects and risks associated with transportation, which have been widely used in later research. Budak and Ustundag [19] proposed a MILP model to decide the suitable number of facilities and their locations for establishing an effective reverse logistics of wastes in Turkey. By considering an environmental impact, Alshraideh and Qdais [20] developed a stochastic model to optimize a capacitated vehicle routing schedule for of collection of medical wastes considering both transportation costs and the amount of gas emission. Mantzaras and Voudrias [21] proposed a nonlinear model to minimize the costs corresponding to the management of IMW in Greek. Temporary facilities are one important strategic decision in recent research. In addition, risks of disease spreading whether from hospitals or from transportation are considered a critical issue [22].

Regarding the uncertainty of the data arising from a limitation of data availability and imprecise in operations, much research has implemented fuzzy concepts to handle these uncertainties. For

example, Negarandeh and Tajdin [23] developed a MOMILP model to manage wastes from hospitals considering profitability, environmental impact, social impact, and resilience of the network under uncertain environments. They implemented robust fuzzy programming to cope with uncertainty where LP-metric and goal programming were used to find efficient results from conflicting objectives.

A summary of the literature on the reverse logistics of IMW is presented in Table I. It is clearly seen that previous works are still limited. Therefore, the purpose of this study is to develop a fuzzy multi-objective multi-period mixed-integer linear programming model for designing an effective reverse logistics network for IMW in outbreaks. The proposed model's objectives are to minimize total costs, risks at hospitals, and risks from transportation and treatments. The strategic decisions involve the establishment of temporary facilities, the size of the temporary treatment center, and the flow of the IMW. An integrated interactive fuzzy approach is employed to handle uncertainties in the costs and capacity of the facilities. By doing so, the optimal solutions can be generated to create a preferable trade-off among conflicting objectives under different degrees of feasibility. This study can assist the decision-makers in making better strategic decisions in designing the reverse logistics network for IMW in outbreaks under uncertain environments. The main contributions of this paper can be summarized as follows:

- This study proposed a fuzzy multi-objective multi-period mixed-integer linear programming model for designing an effective reverse logistics network for IMW in outbreaks considering data uncertainty and conflicting objectives (both financial efficiency and risks in operations).
- To handle the uncertainty of the data and balance the trade-off between conflicting objectives, an integrated interactive fuzzy approach is applied. Jimenez's approach is applied to handle the uncertainty with the feasibility concept. The Fuzzy Goal Programming (FGP) method is then used to generate effective solutions that assist decision-makers in making effective strategic decisions.
- To the best of our knowledge, this study is the first of its kind to integrate the Jimenez approach; and the Fuzzy Goal Programming (FGP) method to solve the reverse logistics network of IMW in outbreaks under an uncertain environment.

TABLE I  
SUMMARY OF RELATED RESEARCH

References	Model specification			Objectives			Problem formulation	Optimization
	Multi-objectives	Multi-periods	Data uncertainty	Financial aspect	Risk	Others		
Shih and Lin (2003)	x	x	-	x	x	-	DP, ILP	Multiple criteria optimization
Alshraideh and Qdais (2016)	x	x	-	x	-	x	MILP	Genetic algorithm
Budak and Ustundag (2017)	-	x	-	x	-	-	MILP	Solver software
Mantzara and Voudrias (2017)	-	x	-	x	-	-	MINLP	Solver software
Yu et al. (2020)	x	x	-	x	x	-	MOMILP	Interactive fuzzy approach
Kargar et al (2020)	x	-	-	x	x	x	MOMILP	Revised Multi-Choice Goal programming method
Negarandeh and Tajdin (2021)	x	-	x	x	-	x	RMOMILP	Chance Constraint Fuzzy Programming (CCFP) Improved Goal programming LP-metric
Zhao et al. (2021)	x	-	x	x	x	-	RMOMILP	Goal programming lexicographic weighted Tchebycheff AUGMECON
This study	x	x	x	x	x	-	FMOMILP	Integrated interactive fuzzy approach

Abbreviations: DP: Dynamic programming, ILP: Integer linear programming, MILP: Mixed-integer linear programming, MOMILP: Multi-objective mixed-integer linear programming, MINLP: Multi-objective stochastic mixed-integer nonlinear programming, RMOMILP: Robust multi-objective mixed-integer linear programming, FMOMILP: Fuzzy multi-objective mixed-integer linear programming.

### III. PROBLEM DESCRIPTION AND MATHEMATICAL MODEL

#### A. Problem Description

In order to design an effective reverse logistics network of IMW in outbreak circumstances under uncertain environments, the principal challenge is to balance between financial efficiency and risks that arise from operations, which include the risk of disease spreading at the hospitals, storage centers, treatment centers, and along the transportation routes. Unlike any normal reverse logistics network design, the amount of IMW dramatically increases in a very short horizon due to the outbreak. To handle this situation, the framework of the proposed reverse logistics network design for IMW management in outbreak circumstances is presented in Fig. 1. The network consists of hospitals, existing treatment centers, and temporary facilities, including temporary storage centers and temporary treatment centers.

Considering the rapid increase of IMW generated during outbreaks, temporary facilities help in providing adequate capacity for the treatment of the IMW. A FMOMILP model is presented to optimize the decisions of locations in establishing the temporary facilities, deciding the suitable size of temporary treatment centers, and determining the optimal flow of amount of IMW transferred among the facilities.

The problem assumptions are as follows:

- A set of capacity levels is provided to be chosen for each candidate location as temporary treatment centers. Each level is subject to a particular capacity limitation and incurs a particular installation cost.
- There is a lower limit on the utilization of facilities to be considered in each period.
- All uncertain parameters are assumed to have fuzziness under the triangular distribution.
- The total costs have a higher priority over the risk impact due to the preference of the decision-makers.

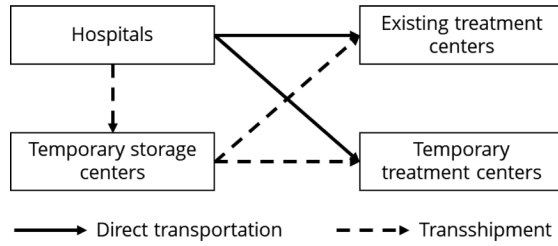


Fig. 1. The framework of the reverse logistics for IMW in outbreak circumstance.

**B. Mathematical Model**

*1) Notations*

The notations used in the mathematical model of the facility location problem are expressed as follows:

Please be noted, the symbol ( $\square$ ) represents the uncertain parameters in this model.

• Indexes

- $h$  Hospitals as well as other sources of medical waste
- $t$  Candidate locations for temporary storage centers
- $e$  Existing treatment centers
- $d$  Candidate locations for temporary treatment centers
- $p$  Periods
- $n$  Capacity levels

• Parameters

- $PbAh_h$  Risk probability at hospital  $h$
- $PbAt_t$  Risk probability at temporary storage center  $t$
- $PbAe_e$  Risk probability at existing treatment center  $e$
- $PbAd_d$  Risk probability at temporary treatment center  $d$
- $PbTh_{ht}$  Probability of transportation risk between hospital  $h$  and temporary storage center  $t$
- $PbTe_{te}$  Probability of transportation risk between temporary storage center  $t$  and existing treatment center  $e$
- $PbTd_{td}$  Probability of transportation risk between temporary storage center  $t$  and temporary treatment center  $d$
- $PbThe_{he}$  Probability of transportation risk between hospital  $h$  and existing treatment center  $e$
- $PbTh_{hd}$  Probability of transportation risk between hospital  $h$  and temporary treatment center  $d$
- $Npat^p_h$  Number of patients in hospital  $h$  in period  $p$
- $Pop_t$  Population exposure at temporary storage center  $t$
- $Pop_e$  Population exposure at existing treatment center  $e$
- $Pop_d$  Population exposure at temporary treatment center  $d$

$PopTh_{ht}$  Population exposure from transportation between hospital  $h$  and temporary storage center  $t$

$PopTe_{te}$  Population exposure from transportation between temporary storage center  $t$  and existing treatment center  $e$

$PopTd_{td}$  Population exposure from transportation between temporary storage center  $t$  and existing treatment center  $d$

$PopThe_{he}$  Population exposure from transportation between hospital  $h$  and existing treatment center  $e$

$PopTh_{hd}$  Population exposure from transportation between hospital  $h$  and existing treatment center  $d$

$RI$  Infection rate of the disease

$\widehat{Gw}_h^p$  Quantity of IMW generated at hospital  $h$  in period  $p$

$Cap_h$  Maximum capacity of IMW collection room in hospital  $h$

$\widehat{Cap}_t$  Capacity of temporary storage center  $t$

$Cap_e$  Capacity of existing treatment center  $e$

$\widehat{Cap}_{dn}$  Capacity of temporary treatment center  $d$  with capacity level  $n$

$LB_e$  Minimum quantity requirement of operating an existing treatment center  $e$

$LB_d$  Minimum quantity requirement of operating a temporary treatment center  $d$

$\widehat{inst}_t$  Cost of installing temporary storage center  $t$

$\widehat{insd}_{dn}$  Cost of installing temporary treatment center  $d$  with capacity level  $n$

$\widehat{pct}_t$  Cost of processing one unit of IMW at temporary storage center  $t$

$\widehat{pce}_e$  Cost of processing one unit of IMW at existing treatment center  $e$

$\widehat{pcd}_d$  Cost of processing one unit of IMW at temporary treatment center  $d$

$\widehat{tcht}_{ht}$  Cost of transporting one unit of IMW between hospital  $h$  and temporary treatment center  $t$

$\widehat{tcte}_{te}$  Cost of transporting one unit of IMW between temporary storage  $t$  and existing treatment center  $e$

$\widehat{tctd}_{td}$  Cost of transporting one unit of IMW between temporary storage  $t$  and temporary treatment center  $d$

$\widehat{tche}_{he}$  Cost of transporting one unit of IMW between hospital  $h$  and existing treatment center  $e$

$\widehat{tchd}_{hd}$  Cost of transporting one unit of IMW between hospital  $h$  and temporary treatment center  $d$

• Decision Variables

$Y_t$  1 if a temporary storage center is established at location  $t$ ; 0 otherwise

$Y_{dn}$  1 if a temporary treatment center with capacity level  $n$  is established at location  $d$ ; 0 otherwise

$OTpe^p$  1 if an existing treatment center  $e$  is operated in period  $p$ ; 0 otherwise

- $OTpd_d^p$  1 if a temporary treatment center  $d$  is operated in period  $p$ ; 0 otherwise
  - $UQ_h^p$  Quantity of uncollected IMW at hospital  $h$  in period  $p$
  - $Qt_t^p$  Quantity of IMW stored at temporary storage center  $t$  in period  $p$
  - $Qe_e^p$  Quantity of IMW treated at existing treatment center  $e$  in period  $p$
  - $Qd_d^p$  Quantity of IMW treated at temporary treatment center  $d$  in period  $p$
  - $QTh_t^p$  Quantity of IMW transported from hospital  $h$  to temporary storage center  $t$  in period  $p$
  - $QTte_{te}^p$  Quantity of IMW transported from temporary storage center  $t$  to existing treatment center  $e$  in period  $p$
  - $QTtd_{td}^p$  Quantity of IMW transported from temporary storage center  $t$  to temporary treatment center  $d$  in period  $p$
  - $QThe_{he}^p$  Quantity of IMW transported from hospital  $h$  to existing treatment center  $e$  in period  $p$
  - $QThd_{hd}^p$  Quantity of IMW transported from hospital  $h$  to temporary treatment center  $d$  in period  $p$
- 2) *Mathematical Model*

A mathematical model of a reverse logistic network of IMW in outbreak circumstance is formulated as follows:

- Objective functions

The mathematical model aims to balance the trade-off between financial performance and the risks from operations in drastic increases of IMW in outbreak circumstances.

$$\begin{aligned}
 Min z_1 = & \sum_{t=1}^T Y_t \widehat{inst}_t + \sum_{d=1}^D Y_{d_n} \widehat{insd}_{dn} + \\
 & \sum_{t=1}^T \sum_{p=1}^P \widehat{pct}_t Q_t^p + \sum_{e=1}^E \sum_{p=1}^P \widehat{pce}_e Qe_e^p + \\
 & \sum_{d=1}^D \sum_{p=1}^P \widehat{pcd}_d Qd_d^p + \sum_{h=1}^H \sum_{t=1}^T \sum_{p=1}^P \widehat{tcht}_{ht} QTh_t^p + \\
 & \sum_{t=1}^T \sum_{e=1}^E \sum_{p=1}^P \widehat{tcte}_{te} QTte_{te}^p + \\
 & \sum_{t=1}^T \sum_{d=1}^D \sum_{p=1}^P \widehat{tctd}_{td} QTtd_{td}^p + \\
 & \sum_{h=1}^H \sum_{e=1}^E \sum_{p=1}^P \widehat{tche}_{he} QThe_{he}^p + \\
 & \sum_{h=1}^H \sum_{d=1}^D \sum_{p=1}^P \widehat{tchd}_{hd} QThd_{hd}^p
 \end{aligned} \tag{1}$$

The first objective function as presented in Equation (1) represents the total costs of the reverse logistics network of IMW. The first and the second terms are installation costs of temporary facilities. The third is the processing cost at the temporary storage center. The fourth and the fifth terms are treatment costs. The other terms are transportation costs in the network.

The risks from operations are measured by a risk estimation model proposed by Nema and Gupta [24] where it concerns the probability of occurrence and the consequence of the risk.

$$Risk = Probability \times Consequence \tag{2}$$

Two objective functions including risk at hospitals and risk from transportation and treatment are formulated as shown in Equation (2). The risks are unitless, with the higher the risks, the greater the possibility of disease spreading.

$$Min z_2 = \sum_{p=1}^P \sum_{h=1}^H PbAh_h UQ_h^p Npat_h^p RI \tag{3}$$

The second objective function as presented in Equation (3) represents the risk at the hospitals where a great amount of IMW is generated in a very short horizon. According to Yu et al. [25], the probability of accidental risk at the hospitals is estimated by experts. The consequence of accidental risk at the hospital ( $PbAh_h$ ) is corresponding to the uncontrolled amount of IMW ( $UQ_h^p$ ) the number of patients at the hospital ( $Npat_h^p$ ), and the spreading rate of the disease ( $RI$ ). This objective aims to minimize the quantity of uncollected IMW at the hospital to reduce the risk of disease spreading to medical staff, patients, and the community around the hospital.

$$\begin{aligned}
 Min z_3 = & \sum_{h=1}^H \sum_{t=1}^T \sum_{p=1}^P PbTh_{ht} QTh_t^p PopTh_{ht} + \\
 & \sum_{t=1}^T \sum_{e=1}^E \sum_{p=1}^P PbTte_{te} QTte_{te}^p PopTte_{te} + \\
 & \sum_{t=1}^T \sum_{d=1}^D \sum_{p=1}^P PbTtd_{td} QTtd_{td}^p PopTtd_{td} + \\
 & \sum_{h=1}^H \sum_{e=1}^E \sum_{p=1}^P PbThe_{he} QThe_{he}^p PopThe_{he} + \\
 & \sum_{h=1}^H \sum_{d=1}^D \sum_{p=1}^P PbThd_{hd} QThd_{hd}^p PopThd_{hd} + \\
 & \sum_{t=1}^T \sum_{p=1}^P PbAt_t Qt_t^p Popt_t + \\
 & \sum_{e=1}^E \sum_{p=1}^P PbAe_e Qe_e^p Pope_e + \\
 & \sum_{d=1}^D \sum_{p=1}^P PbAd_d Qd_d^p Popd_d
 \end{aligned} \tag{4}$$

The third objective function as presented in Equation (4) represents the risk associated with transportation and treatment of IMW. The transportation risks are calculated by the probability of accidents along the route and the consequence of accidents along the route. According to Yu et al. [25], the probability of accidents along the route is corresponding to the probability of accidents ( $PopT$ ) and the amount of IMW transported ( $QT$ ). For processing risk at the storage center and treatment risk, the consequences are corresponding to the amount of IMW at the facilities ( $Q$ ), and population exposure ( $Pop$ ).

- Constraints

$$UQ_h^p = \widehat{Gw}_h^p + UQ_h^{p-1} - \sum_{t=1}^T QTh_t^p - \sum_{e=1}^E QThe_{he}^p - \sum_{d=1}^D QThd_{hd}^p, \forall h, p \tag{5}$$

$$Qt_t^p = Qt_t^p + \sum_{h=1}^H QTh_t^p - \sum_{e=1}^E QTte_{te}^p - \sum_{d=1}^D QTtd_{td}^p, \forall t, p \tag{6}$$

$$Qe_e^p = \sum_{t=1}^T QTte_{te}^p + \sum_{h=1}^H QThe_{he}^p, \forall e, p \tag{7}$$

$$Qd_d^p = \sum_{t=1}^T QTtd_{td}^p + \sum_{h=1}^H QThd_{hd}^p, \forall d, p \tag{8}$$

Equations (5) and (6) balance the flow among facilities in the network. Equations (7) and (8) calculate amount of IMW received at existing treatment centers and temporary treatment centers, respectively.

$$UQ_h^p \leq Cap_h, \forall h, p \tag{9}$$

$$Qt_t^p \leq Y_t \widehat{Capt}_t, \forall t, p \tag{10}$$

$$Qe_e^p \leq OTpe_e^p \widehat{Cape}_e, \forall e, p \tag{11}$$

$$Qe_e^p \geq LBe_e OTpe_e^p \widehat{Cape}_e, \forall e, p \tag{12}$$

$$Qd_d^p \leq OTpd_d^p \widehat{Capd}_d, \forall d, p \tag{13}$$

$$Qd_d^p \geq Lbd_d OTpd_d^p \widehat{Capd}_d, \forall d, p \tag{14}$$

Equation (9) ensures that the quantity of uncollected IMW does not exceed the capacity of the hospitals. Equations (10), (11), and (13) ensure the amount of IMW does not exceed the capacity of the facilities. Equations (12) and (14) represent a lower limit of IMW receiving at each facility.

$$OTpd_a^p \leq \sum_{n=1}^N Yd_{dn}, \forall d, p \tag{15}$$

$$\sum_{n=1}^N Yd_{dn} \leq 1, \forall d \tag{16}$$

Equations (15) ensures that a temporary facility cannot operate if it is not established. Equation (16) imposes that only one capacity level is chosen for a temporary treatment center. Equations (17) - (21) are non-negativity and binary constraints.

$$Yt_t, Yd_{dn} \in \{0,1\}, \forall t, d, n \tag{17}$$

$$OTpe_e^p, OTpd_a^p \in \{0,1\}, \forall e, d, p \tag{18}$$

$$UQ_h^p, Qt_t^p \geq 0, \forall h, t, p \tag{19}$$

$$Qe_e^p, Qd_a^p \geq 0, \forall e, d, p \tag{20}$$

$$QTh_{ht}^p, QTt_{te}^p, QTd_{td}^p, QTd_{td}^p, QTh_{hd}^p \geq 0, \forall h, t, e, d, p, n \tag{21}$$

IV. PROPOSED SOLUTION APPROACH

According to the uncertain environment of a reverse logistics network of IMW in outbreak circumstance, some uncertain parameters (i.e., IMW generated, costs and facilities' capacity) are described by triangular fuzzy numbers. In order to deal with such uncertainties, an integrated interactive fuzzy approach is applied. In the first phase, an equivalent auxiliary crisp model of Jimenez et al. [26] is used to turn a fuzzy number into a crisp number. In the second phase, FGP method is applied to generate the best solution based on the priority of the objectives. The flow chart of the proposed approach is presented in Fig. 2.

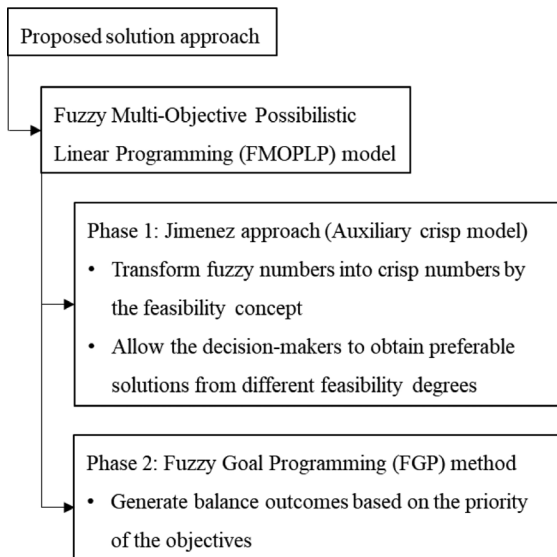


Fig. 2. Flow chart of the proposed solution approach.

A. Solving Fuzzy Multi-Objective Possibilistic Linear Programming (FMOPLP) Model

The Possibilistic Linear Programming (PLP) approach is used to handle the uncertainty and ill-known parameters. The imprecise parameters in our study include the amount of IMW generated, all related costs, and the facilities' capacity in which they are depicted by triangular fuzzy numbers. Each number is composed of three prominent data points which are the optimistic value point ( $a^o$ ), the most likely value point ( $a^m$ ), and the pessimistic value point ( $a^p$ ) as shown in Fig. 3.

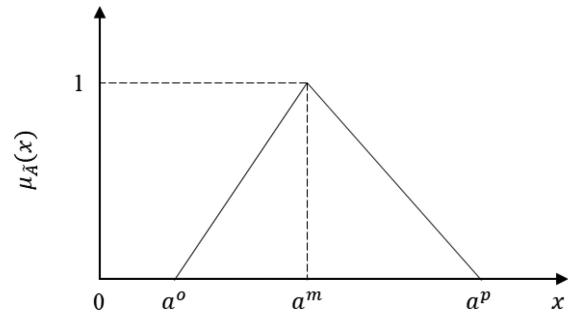


Fig. 3. Triangular distribution of  $\tilde{a}$

1) Phase 1: Auxiliary Crisp Model

The proposed reverse logistics network of IMW in the outbreak circumstance model contains fuzzy parameters that mimic the uncertainty of the practical environment in such a situation. By applying Jimenez et al. [26] approach, an interactive approach, the fuzzy possibilistic linear programming model is transformed into an auxiliary crisp model with several feasibility degrees ( $\alpha$  levels) based on the preference of the decision-makers. Moreover, this method provides computational efficiency since it maintains the models' linearity without increasing the number of objective functions.

To convert PLP model into an auxiliary crisp model, firstly, the membership function  $\mu_{\tilde{a}}(x)$  of is defined as follows:

$$\mu_{\tilde{a}}(x) = \begin{cases} f_a(x) = \frac{x-a^o}{a^m-a^o}, & \text{if } a^o \leq x \leq a^m \\ 1 & \text{if } x = a^m \\ g_a(x) = \frac{a^p-x}{a^p-a^m}, & \text{if } a^m \leq x \leq a^p \\ 0 & \text{otherwise} \end{cases} \tag{22}$$

According to Heilpern [27], the expected interval of a triangular fuzzy number  $\tilde{a}$ , denoted  $EI(\tilde{a})$ , and the expected value of a triangular fuzzy number  $\tilde{a}$ , denoted  $EV(\tilde{a})$ , are calculated as follows:

$$EI(\tilde{a}) = [E_1^a, E_2^a] = \left[ \int_0^1 f_a^{-1}(x) dx, \int_0^1 g_a^{-1}(x) dx \right] = \left[ \left( \frac{a^o+a^m}{2} \right), \left( \frac{a^m+a^p}{2} \right) \right] \tag{23}$$

$$EV(\tilde{a}) = \frac{E_1^a+E_2^a}{2} = \frac{a^o+2a^m+a^p}{4} \tag{24}$$



As determined by Jimenez [28], for any two fuzzy numbers  $\tilde{a}$  and  $\tilde{b}$ , the degree in which  $\tilde{a}$  is larger than  $\tilde{b}$  is as follows:

$$\mu_M(\tilde{a}, \tilde{b}) = \begin{cases} 0 & \text{if } E_2^a - E_1^b < 0 \\ \frac{E_2^a - E_1^b}{E_2^a - E_1^b - (E_1^a - E_2^b)} & \text{if } 0 \in [E_1^a - E_2^b, E_2^a - E_1^b] \\ 1 & \text{if } E_1^a - E_2^b > 0 \end{cases} \quad (25)$$

If  $\mu_M(\tilde{a}, \tilde{b}) \geq \alpha$ , it indicates that  $\tilde{a}$  is greater than or equal to  $\tilde{b}$  in a degree of  $\alpha$  and it is represented by  $\tilde{a} \geq_\alpha \tilde{b}$ . From Equation (25), this is equivalent to:

$$\frac{E_2^a - E_1^b}{E_2^a - E_1^b + E_2^b - E_1^a} \geq \alpha \quad (26)$$

According to Arenas et al. [29], for any two fuzzy numbers  $\tilde{a}$  and  $\tilde{b}$ , we say that  $\tilde{a}$  is indifferent to  $\tilde{b}$  in a degree of  $\alpha$ , denoted  $\frac{\alpha}{2} \leq \mu_M(\tilde{a}, \tilde{b}) \leq 1 - \frac{\alpha}{2}$ . This is equivalent to:

$$\frac{\alpha}{2} \leq \frac{E_2^a - E_1^b}{E_2^a - E_1^b + E_2^b - E_1^a} \leq 1 - \frac{\alpha}{2} \quad (27)$$

Fuzzy multi-objective linear programming can then be solved by the following formulations:

$$\text{Min } \tilde{z} = (\tilde{z}_1, \tilde{z}_2, \dots, \tilde{z}_k) = (\tilde{c}_1x, \tilde{c}_2x, \dots, \tilde{c}_kx) \quad (28)$$

$$\begin{aligned} \text{s.t. } & \tilde{a}_i x \geq \tilde{b}_i, i = 1, \dots, l \\ & \tilde{a}_i x = \tilde{b}_i, i = l + 1, \dots, m \\ & x \geq 0 \end{aligned}$$

Considering Equations (26) and (27), they are equivalent to:

$$\text{Min } \tilde{z} = (\tilde{z}_1, \tilde{z}_2, \dots, \tilde{z}_k) = (\tilde{c}_1x, \tilde{c}_2x, \dots, \tilde{c}_kx) \quad (29)$$

$$\begin{aligned} \text{s.t. } & [(1 - \alpha)E_2^{a_i} - \alpha E_1^{a_i}]x \geq \alpha E_2^{b_i} + (1 - \alpha)E_1^{b_i}, \\ & i = 1, \dots, l \\ & [(1 - \frac{\alpha}{2})E_2^{a_i} - \frac{\alpha}{2}E_1^{a_i}]x \geq \frac{\alpha}{2}E_2^{b_i} + (1 - \frac{\alpha}{2})E_1^{b_i}, \\ & i = l + 1, \dots, m \\ & [\frac{\alpha}{2}E_2^{a_i} - (1 - \frac{\alpha}{2})E_1^{a_i}]x \geq (1 - \frac{\alpha}{2})E_2^{b_i} + \frac{\alpha}{2}E_1^{b_i}, \\ & i = l + 1, \dots, m \end{aligned}$$

This approach enables the decision-makers to plan in an interactive manner with varying degrees of  $\alpha$ . It provides information for the decision-makers to determine the level of feasibility that they are willing to accept.

2) Phase 2: Applying Fuzzy Goal Programming (FGP) Method

The Fuzzy Goal Programming (FGP) method is one of the most widely used methods to solve multi-objective problems due to its ability to deal with uncertainty in the data and aspiration level of objectives. The FGP method is used in this study to solve a fuzzy multi-objective problem by minimizing the deviations of the objectives with a priority among the objectives. The more important objective is regarded as having a higher priority and should be satisfied first. Each objective is assigned a priority level  $k$ , with the highest priority being satisfied first.

A multi-objective problem with  $j$  objective minimization functions can be formulated as:

$$\text{Min } [z_1, z_2, \dots, z_j] \quad (30)$$

s.t. Problem constraints

To illustrate the FGP method, considering a problem with three minimization objectives, where the first objective ( $z_1$ ) has priority level 1, the second objective ( $z_2$ ) has priority level 2, and the third objective ( $z_3$ ) has priority level 3. The following is the steps in solving the FGP method:

Step 1: Solve the objective with priority level 1 (the most important objective).

$$\text{Min } z_1 \quad (31)$$

s.t. Problem constraints

Suppose the solution yield a minimum objective function value of  $z_1 = z_1^*$ .

Step 2: Solve the priority level 2's objective function subject to a deviation constraint of the priority level 1's objective function.

$$\text{Min } z_2 \quad (32)$$

s.t. Problem constraints

$$z_1 \leq z_1^* \times (1 + d_1)$$

where  $d_j$  is the percentage allowance of deviation of the objective function  $j$ . Suppose the solution yield a minimum objective function value of  $z_2 = z_2^*$ .

Step 3: Solve the priority level 3's objective function subject to a deviation constraint of the priority level 1's objective function and the priority level 2's objective function.

$$\text{Min } z_2 \quad (33)$$

s.t. Problem constraints

$$z_1 \leq z_1^* \times (1 + d_1)$$

$$z_2 \leq z_2^* \times (1 + d_2)$$

V. CASE STUDY

A. Case Description

To highlight the application of the proposed method, a case study of coronavirus disease (COVID-19) outbreak in Pathum Thani, Thailand is presented. The scope of the reverse logistics problem for medical waste management is composed of IMW generation sources (hospitals), storage centers, and treatment centers. Pathum Thani province, a part of the metropolitan region of Thailand, had a rapid increase in the number of COVID-19 patients during July and August which is presented in Fig. 4.

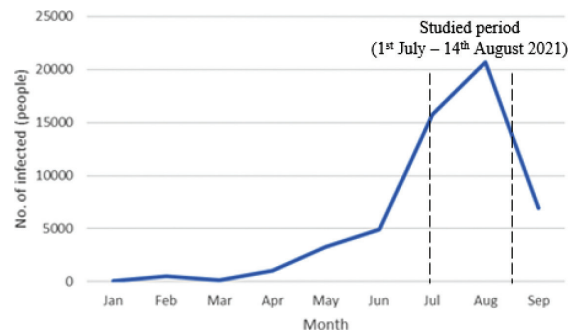


Fig. 4. No. of COVID-19 cases of Pathum Thani province from January - September 2021.

In this study, three districts of Pathum Thani province, including Muang district, Sam Khok district, and Lat Lum Kaeo district, are carried out as the case study. The planning horizon of the proposed model during the peak period of the outbreak, which is from 1st July-14th August 2021, which consists of 15 periods with 3 days each since IMW is normally picked up every 3 days.

The proposed model is composed of three echelons as presented in Fig. 4. The first echelon is comprised of ten IMW generation sources. To design an effective reverse logistics of IMW in this area, storage centers (the second echelon) are an alternative option to be used to store and aggregate the IMW that are overflowed from the hospitals. Then, the IMW are delivered to be treated at treatment centers (the third echelon). Currently, there is no storage center and treatment center for IMW in Pathum Thani province. The IMW of Pathum Thani province are normally treated by two existing treatment centers, one in Nonthaburi province and another in Ayutthaya province. However, these two incinerators have to be responsible for IMW from many nearby provinces and the incinerators will not be able to handle these wastes very soon since the number of patients keeps rising during this crisis. By concerning this problem, six potential locations for temporary storage centers and five potential locations for temporary treatment centers are studied to alleviate the facing problem by locating them in suitable areas. A digital map of the three districts of Pathum Thani province containing spatial data is analyzed using Quantum Geographic Information System (QGIS) 3.16.6 with criteria specified by the Pollution Control Department [30]. For example, a treatment center must be at least one kilometer away from residential areas and archaeological heritage sites. The locations of all facilities in the proposed reverse logistics network for IMW management can be presented in Fig. 5.

	Infected medical waste generation sources	Temporary storage centers	Temporary treatment centers
H1	▲ Lat Lum Kaeo Hospital	T1 ●	D1 ◆
H2	▲ Pathum Thani Hospital	T2 ●	D2 ◆
H3	▲ Sam Khok Hospital	T3 ●	D3 ◆
H4	▲ Nurulyakin mosque	T4 ●	D4 ◆
H5	▲ Buasuwarnpradit temple	T5 ●	D5 ◆
H6	▲ Borthong school	T6 ●	
H7	▲ Pathumthani Vocational Education College		
H8	▲ Ban Klang market		
H9	▲ Ban Mai community isolation		
H10	▲ Bang Toei community isolation		
			Existing treatment centers
			E1 ■
			E2 ■

Fig. 5. Facilities in the network

B. Input Parameters

Generally, the daily generation of IMW in Thailand is 0.54 kg/bed/day [31]. However, in the COVID-19 outbreak, there is an increase in generation of IMW due to a requirement in additional medical equipment, e.g., medical masks and personal protective equipment. According to evaluations from professionals, the daily IMW generation in most likely case is 2.85 kg/bed/day at hospitals and 1.82 kg/bed/day at field hospitals [32]. The amount of IMW generated at each hospital in each period is proportional to the number of patients and the daily IMW generation. The number of patients in hospitals (H1, H2, and H3) is estimated based on the number of new cases reported by the Pathum Thani province public health office and the assumption that the length of hospital stay for COVID-19 is 14 days. During this crisis, the field hospitals and community isolations (H4-H10) were full as soon as they opened. The estimated number of patients at each IMW generation sources in each period is presented in Table II.

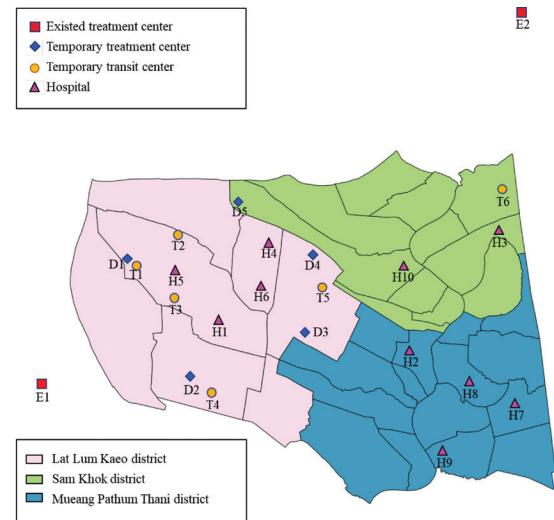


Fig. 6. The location of facilities of the reverse logistics for IMW management in Pathum Thani province

Considering facilities in the network, the lists of IMW generation sources and existing treatment centers are shown in Table III and IV, respectively. The capacities of the existing treatment centers in this case study are assumed to be a portion of their full capacities since these two treatment centers must service the IMW from other provinces as well. Six candidate locations for temporary storage centers and five candidate locations for temporary treatment centers are selected based on the criteria specified by [30]. The candidate locations for those temporary facilities and their population densities are shown in Table V and VI.

TABLE II  
ESTIMATED NUMBER OF PATIENTS AT EACH IMW GENERATION SOURCES IN EACH PERIOD

Period	Number of patients at each IMW generation sources (people)									
	H1	H2	H3	H4	H5	H6	H7	H8	H9	H10
1	464	186	39							
2	565	190	173							
3	577	145	208							
4	700	105	258				450			
5	758	89	281				1,350			
6	815	452	223				1,350			
7	922	683	352	90		90	1,350	300		300
8	1,070	825	616	90		90	1,350	450	300	900
9	1,232	1,101	1,037	90	160	90	1,350	450	300	900
10	1,291	1,348	1,241	90	240	90	1,350	450	300	900
11	1,309	988	1,715	90	240	90	1,350	450	300	900
12	1,390	725	1,511	90	240	90	1,350	450	300	900
13	1,241	654	2,036	90	240	90	1,350	450	300	900
14	1,052	446	1,924	90	240	90	1,350	450	300	900
15	915	210	1,938	90	240	90	1,350	450	300	900

TABLE III  
NAMES OF IMW GENERATION SOURCES

No.	IMW generation source	Maximum capacity of IMW collection room (kg/period)
1	Lat Lum Kaeo Hospital	8,160
2	Pathum Thani Hospital	4,650
3	Sam Khok Hospital	7,710
4	Nurulyakin mosque	480
5	Buasuwanpradit temple	1,320
6	Borthong school	480
7	Pathumthani Vocational Education College	7,380
8	Ban Klang market	2,460
9	Ban Mai community isolation	1,650
10	Bang Toei community isolation	4,920

TABLE IV  
NAMES OF EXISTING TREATMENT CENTERS

No.	Existing treatment center	Population density (people/km <sup>2</sup> )
1	Nonthaburi Provincial Administrative Organization's (PAO) waste processing facility	380.64
2	Bangpain Land company limited	4,650

TABLE V  
CANDIDATE LOCATION FOR TEMPORARY TREATMENT CENTERS

No.	Location (Latitude, Longitude)	Sub-district	Population density (people/km <sup>2</sup> )
1	14.066303, 100.362195	Rahaeng	403.71
2	14.012116, 100.399202	Lat Lum Kaeo	183.68
3	14.032922, 100.469977	Khu Bang Luang	347.36
4	14.074859, 100.468714	Khu Bang Luang	347.36
5	14.105289, 100.423597	Bang Toei	516.05

The traveling distances between two nodes in Pathum Thani province are obtained by using the fastest route in QGIS 3.16.6 and Google Map. For the transportation cost, it is proportional to the distance travelled and the weight of the IMW, which is estimated to be 0.185 baht/kg/km [25].

TABLE VI  
CANDIDATE LOCATION FOR  
TEMPORARY STORAGE CENTERS

No.	Location (Latitude, Longitude)	Sub-district	Population density (people/km <sup>2</sup> )
1	14.068801, 100.374156	Rahaeng	403.71
2	14.088797, 100.395403	Rahaeng	403.71
3	14.047686, 100.393543	Rahaeng	403.71
4	13.997883, 100.413293	Lat Lum Kaeo	183.68
5	14.055485, 100.475268	Khu Bang Luang	347.36
6	14.110869, 100.573855	Chiang Rak Noi	274.74

Considering the probability of accidental risk at the IMW generation sources ( $PbAh_h$ ), the risk is 0.003 for hospitals and 0.007 for temporary hospitals [25]. The accidental risk of the storage center ( $PbAt_t$ ) and treatment center ( $PbAe_e$  and  $PbAd_d$ ) are 0.0001 and 0.0006, respectively. According to Yu et al. [25] and Zhao et al. [33], the probability of risk along the route is calculated by Equation (34). The population exposure is calculated by Equation (35), where the affected radius is set to be 2.5 kilometers for treatment centers and 1 kilometer for storage centers. The population exposure along the route between facilities is calculated by Equation (36).

$$PbTh_{ht}, PbTt_{te}, PbTt_{td}, PbThe_{he}, PbTh_{hd} = \frac{0.4 \times 10^{-6} \times 0.9}{(km)} \times \text{travel distance (km)} \quad (34)$$

$$Popt_t, Pope_e, Popd_d = \pi r^2 (km^2) \times \text{population density (people/km}^2) \quad (35)$$

$$PbTh_{ht}, PbTt_{te}, PbTt_{td}, PbThe_{he}, PbTh_{hd} = 2(km^2) \times \text{population density (people/km}^2) \times \text{travel distance (km)} \quad (36)$$

The relevant costs and capacities of existing treatment centers, temporary treatment centers, and temporary storage centers are presented in Table VI, respectively. The installation cost of a temporary storage center is composed of costs of the land, its construction, and equipment. For temporary treatment centers, three capacity levels (S, M, and L) are provided as an alternative (decision variable), which incur different installation costs and are subject to different capacity limitations. The processing cost of temporary storage centers and temporary treatment centers in most likely cases is set to 0.9 Baht/kg and 3.23 Baht/kg, respectively. The size and cost parameter of temporary facilities are calculated based on [25], [34], [35]. The optimistic value and pessimistic value of the cost parameters and the amount of IMW generated are subject to 0.8 and 1.2 times of the most likely case, respectively.

TABLE VII  
COST PARAMETERS AND CAPACITY OF  
EXISTING TREATMENT CENTERS

No.	Processing cost (Baht)	Capacity (kg/period)
1	(10.4,13.00,15.6)	(453.6,567.0,680.4)
2	(3.60,4.50,5.40)	(2416.8,3021,3625.2)

TABLE VIII  
INSTALLATION COST AND CAPACITY OF TEMPORARY TREATMENT CENTERS

No.	Capacity level	Installation cost (Baht)	Capacity (kg/period)
1	S	(7477240,9346550,11215860)	(1920,2400,2400)
	M	(9995920,12494900,14993880)	(5760,7200,7200)
	L	(15932200,19915250,23898300)	(11520,14400,14400)
2	S	(8277240,10346550,12415860)	(1920,2400,2400)
	M	(11195920,13994900,16793880)	(5760,7200,7200)
	L	(17532200,21915250,26298300)	(11520,14400,14400)
3	S	(8437240,10546550,12655860)	(1920,2400,2400)
	M	(11435920,14294900,17153880)	(5760,7200,7200)
	L	(17852200,22315250,26778300)	(11520,14400,14400)
4	S	(8437240,10546550,12655860)	(1920,2400,2400)
	M	(11435920,14294900,17153880)	(5760,7200,7200)
	L	(17852200,22315250,26778300)	(11520,14400,14400)
5	S	(7157240,8946550,10735860)	(1920,2400,2400)
	M	(9515920,11894900,14273880)	(5760,7200,7200)
	L	(15292200,19115250,22938300)	(11520,14400,14400)

TABLE IX  
INSTALLATION COST AND CAPACITY OF  
TEMPORARY STORAGE CENTERS

No.	Installation cost (Baht)	Capacity (kg/period)
1	(5189000,6486250,7783500)	(25200,31500,31500)
2	(5189000,6486250,7783500)	(25200,31500,31500)
3	(5189000,6486250,7783500)	(25200,31500,31500)
4	(6789000,8486250,10183500)	(25200,31500,31500)
5	(8069000,10086250,12103500)	(25200,31500,31500)
6	(3909000,4886250,5863500)	(25200,31500,31500)

VI. RESULT AND DISCUSSION

A. Results

The feasibility degrees ( $\alpha$ ) is subjective to the preferences and experiences of the decision-makers. The  $\alpha$  level indicates the level of feasibility that the

decision-makers are willing to accept. In this case study, the  $\alpha$  level was fixed at 0.7 with 25% allowed percentage deviation for an illustrative purpose. Full details of the sensitivity analysis on different levels of the allowed percentage deviation are not included in this paper due to a suitable paper length. Fig. 6 presents the sensitivity analysis of the feasibility degree ( $\alpha$ ) with 25% allowed percentage deviation. It was found that as the  $\alpha$  increases, the total costs ( $z_1$ ) and the risk associated with transportation and treatment ( $z_3$ ) tend to become worse. The reason is that as the decision-makers have the desire to encounter the uncertainty with a higher confidence level in satisfying the constraints, the constraints become more restricted and fewer solution sets are feasible. However, this is not the case for risk at hospitals ( $z_2$ ) because a variety of factors contribute to the fluctuation of this objective function.

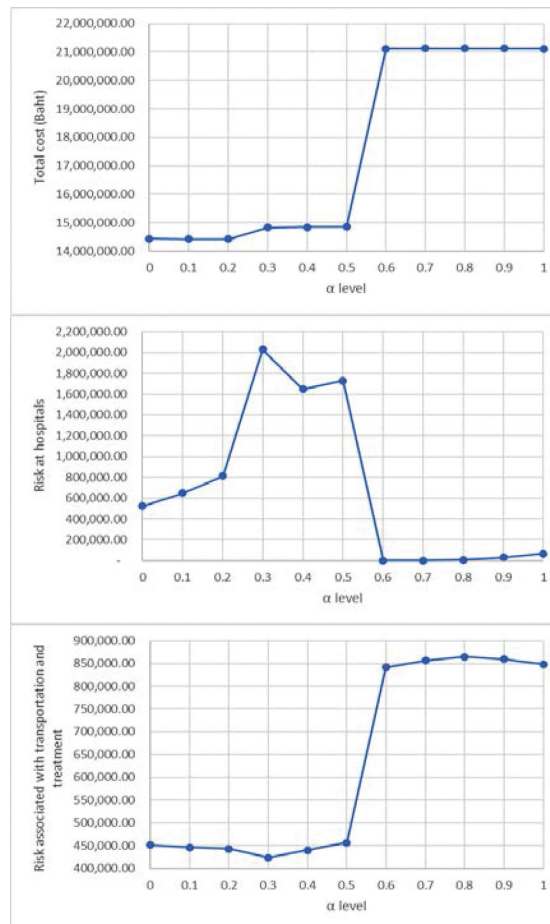


Fig. 7. The sensitivity analysis of the feasibility degree ( $\alpha$ ) with 25% allowed percentage deviation.

To clarify this issue, the risk at hospitals is directly correlated to the number of the uncollected wastes at the hospitals. One of the factors that leads to the fluctuation is the conflict between objectives. To reduce the risk at hospitals, a greater number of the IMW must be delivered out of the hospitals to be treated. This leads to an increase in transportations among facilities, treatments of the wastes, and establishment of more temporary facilities. It also lead to an increase in the total costs and the risk associated with transportation and treatment. For  $\alpha \geq 0.6$ , the solutions suggest establishing one temporary treatment center with capacity size L, resulting in a very low risk at hospital ( $z_2$ ) since most of the IMW can be treated.

To handle the FMOMILP model for the reverse logistics network design of IMW in outbreaks problem, the Fuzzy Goal Programming (FGP) method is applied to obtain an effective solution based on the priority of the objective functions. The priority of the objective functions in this case study are as follows:

- Priority level 1 – Minimize total costs ( $z_1$ )
- Priority level 2 – Minimize risk at hospitals ( $z_2$ )
- Priority level 3 – Minimize risk associated with transportation and treatments ( $z_3$ )

Table X shows the objective function values and the establishment of the temporary storage centers and temporary treatment centers from varying the allowed percentage deviations from 10% to 30%.

TABLE X  
RESULTS FROM VARIOUS ALLOWED PERCENTAGE DEVIATION

Objectives	PIS <sup>1</sup>	NIS <sup>2</sup>	Allowance percentage deviation				
			10%	15%	20%	25%	30%
$Z_1$ (Baht)	17,493,541.08	43,664,290.85	18,475,527.75 (+57.69% <sup>3</sup> )	19,945,979.89 (+54.32% <sup>3</sup> )	20,263,851.15 (+53.59% <sup>3</sup> )	21,123,563.91 (+51.62% <sup>3</sup> )	21,123,456.58 (+51.62% <sup>3</sup> )
$Z_2$	-	3,967,593.15	135,019.88 (+96.60% <sup>3</sup> )	135,007.57 (+96.60% <sup>3</sup> )	619.18 (+99.98% <sup>3</sup> )	644.97 (+99.98% <sup>3</sup> )	670.77 (+99.98% <sup>3</sup> )
$Z_3$	56,294.72	1,263,055.67	678,840.37 (+46.25% <sup>3</sup> )	460,085.94 (+63.57% <sup>3</sup> )	1,028,494.52 (+18.57% <sup>3</sup> )	856,024.77 (+32.23% <sup>3</sup> )	855,873.74 (+32.24% <sup>3</sup> )
Installed D			D1(size M)	D2(size M)	D5(size L)	D1(size L)	D1(size L)
Installed T			T6	T6	-	-	-

<sup>1</sup>Positive Ideal Solution (PIS) is the best value obtaining from the payoff table.

<sup>2</sup>Negative Ideal Solution (NIS) is the worst value obtaining from the payoff table.

<sup>3</sup>Percentage improved as compared to the NIS,

The optimal solutions in two cases of 10% to 15% allowed percentage deviation (little increase from the case of minimum total cost) select to establish a temporary storage center T6 at Chiang Rak Noi sub-district and a temporary treatment center with capacity size M at Rahaeng sub-district. However, in the cases of 20% to 30% allowed percentage deviation, where the total costs are allowed to moderately increase up to 30% from the case of minimum total costs, a temporary treatment center with capacity size L at Bang Toei sub-district for the case of 20% allowed percentage deviation and at Rahaeng sub-district for the cases of 25% and 30% allowed percentage deviation is selected. For these cases of moderate increase in the total costs, IMW is suggested to be delivered directly to the treatment centers without any storage. Since capacity size L is selected, the total costs and the risk associated with transportation and treatments increases, but the risk at hospitals is extremely low due to high IMW treatment capability of the facilities.

For an illustration of the result obtained from the IMW reverse logistics network design, the optimal solutions of 25% and 30% allowed percentage deviation cases are selected since their total costs and the risk associated with transportation and treatments increase in acceptable levels while their total costs slightly increase but the risk at hospitals improved dramatically up to 99.98% as compared to the NIS. Based on Table 10 with the case of 25% allowed percentage deviation, the total costs is 21,123,563.91 Baht, the risk at hospitals is 644.97, and the risk associated with transportation and treatments is 856,024.77 in which one temporary treatment center, D1(size L) at Rahaeng sub-district, is selected to be established. The risk associated with transportation and treatments is significantly higher than the risk at hospitals because it has the lowest priority level and optimizes last.

The allocation of IMW is presented in Table XI and the utilization of each facility is presented in Table XII. From Table XI and Table XII, the temporary

treatment center D1 serves as the primary treatment center and the two existing treatment centers are used as supplement when the capacity of the temporary treatment center D5 is reached. In the first 8 periods, none of the IMW are sent to the existing treatment centers because the temporary treatment center D1 is still capable of treating all IMW. However, as the amount of IMW increases, the IMW is overflowed to

the two existing treatment centers. For example, in period 9, the IMW from most hospitals are treated at the temporary treatment center D1. Once the capacity of the temporary treatment center D1 is full, the IMW is overflowed to the existing treatment centers E1 and E2, where the IMW from H1 and H3 are treated at E1, and the IMW from H9 is treated at E2.

TABLE XII  
ALLOCATION OF IMW IN EACH PERIOD

Allocation of IMW from hospitals to existing treatment centers															
Existing treatment centers	Period														
	1	2	3	4	5	6	7	8	9	10	11	12	13	14	15
E1									H1	H1	H1	H1	H1	H1	H1
									H9	H9	H9	H9	H9	H9	H9
E2									H3	H3	H3	H3	H3	H3	H3
Allocation of IMW from hospitals to temporary treatment centers															
TEMPORARY TREATMENT CENTERS	Period														
	1	2	3	4	5	6	7	8	9	10	11	12	13	14	15
D1	H1	H1	H1	H1	H1	H1	H1	H1	H1	H1	H1	H1	H1	H1	H1
	H2	H2	H2	H2	H2	H2	H2	H2	H2	H2	H2	H2	H2	H2	H2
	H3	H3	H3	H3	H3	H3	H3	H3	H3	H3	H3	H3	H3	H3	H3
				H7	H7	H7	H4	H4	H4	H4	H5	H4	H4	H4	H4
							H6	H6	H5	H5	H6	H5	H5	H5	H5
							H7	H7	H6	H6	H7	H6	H6	H6	H6
							H8	H8	H7	H7	H8	H7	H7	H7	H7
							H10	H9	H8	H8	H10	H8	H8	H8	H8
								H10	H10	H10		H10	H10	H10	H10

A comparison with the actual situation where there is no temporary facilities is also carried out as shown in Table XIII to show the huge damage from the excess amount of uncollected or untreated IMW from the actual situation. Because of an increase in IMW during the COVID-19 outbreak, the existing treatment centers were unable to treat all delivered

amount of IMW, and the remaining amount IMW eventually started to pile up. In the actual case, without these temporary facilities, the total costs is surely lower than the proposed situation but the IMW would be severely accumulated at the hospitals or at the existing treatment centers causing the risks to increase tremendously beyond the acceptable level.

TABLE XIII  
RESULTS COMPARISON WITH 25% ALLOWANCE PERCENTAGE DEVIATION

Actual situation			
Objective	Accumulate at hospitals	Accumulate at existing treatment centers	Proposed situation (Establish D1 (size L))
(Baht)	499,257.14	2,419,904.02	21,123,563.91
	5,346,463.77	1,826,198.57	644.97
	415,175.32	2,983,867.64	856,024.77
Excess amount of IMW remaining (kg)	258,453.27	302,113.82	None

The improper accumulation of IMW definitely caused concerns about the disease spreading to communities during that time [36]. Our proposed temporary facilities can lead to far better effective management of the IMW, lowering the risk of disease spreading. However, once the outbreak is over, the amount of IMW would return to a normal level. This temporary treatment center will still be useful because it can be used to treat the IMW and other wastes from Pathum Thani, where the IMW generation is expected to be 4,712 kg/day this year without the outbreak [37]. In addition, these facilities help Pathum Thani province to be ready or prepared for future outbreaks, which are likely to occur again soon. This will also reduce the processing cost of waste treatment as well as the transportation risk from using the existing treatment centers in nearby provinces. Most importantly, it certainly helps to avoid the risk of disease spreading from the huge excess amount of IMW (Table XIII) as reported in the past.

## VII. CONCLUSIONS

To handle the rapid increase of IMW due to outbreaks, an effective IMW reverse logistics network design using a fuzzy multi-objective multi-period mixed-integer linear programming model under an uncertain environment was proposed in this study. The model aimed to simultaneously minimize the total costs, the risk at hospitals, and the risk associated with transportation and treatments, by determining the optimal locations and size of temporary facilities and the flow of IMW among facilities. To deal with the uncertainty and the conflict among objectives, an integrated interactive fuzzy approach, which is an integration of an auxiliary model of Jimenez approach and the Fuzzy Goal Programming (FGP) method, was proposed. The auxiliary model was used to cope with uncertain parameters with feasibility concept, and the FGP method was applied to generate effective solutions based on the priority of the objective functions and the allowed percentage deviation determined by the decision-makers.

The effectiveness and applicability of the proposed methodology were demonstrated with an actual study of the COVID-19 outbreak in Pathum Thani province. The cases of 25% and 30% allowed percentage deviation with an establishment of one temporary treatment center, DI (size L) at Rahaeng sub-district were chosen because the total costs and the risk associated with transportation and treatments are in acceptable levels, whereas the risk at hospitals is very low. However, it would depend on the decision-makers to decide the best solution in their particular situations.

The primary limitation of this study is belonging to the data estimation. Since the COVID-19 outbreak is a new pandemic, and there has been an incomplete in the collected data and subjective knowledge of the

experts is still required in generating the appropriate data. As a result, further possible studies can be recommended as follows:

- More advanced methods in estimating the amount of IMW generated and the risk parameters could make the result more practical.
- An outbreak is an incident that incurs a high level of uncertainty. More advanced methods in handling the risks, e.g., robust programming, could be applied for better outcomes.
- For the network design, more facilities (e.g., different IMW sources and disposal centers) could be added. As the problems get bigger and more complex, metaheuristic algorithms could be considered.

## REFERENCES

- [1] P. Parthasarathy and S. Vivekanandan, "An Extensive Study on the COVID-19 Pandemic, an Emerging Global Crisis: Risks, Transmission, Impacts and Mitigation," *Journal of Infection and Public Health*, vol. 14, no. 2, pp. 249-259, Feb. 2021.
- [2] N. Waleekhajornlert and P. Sureeyatanapas, "Resilient Supplier Selection under Uncertainty Using the Extended TOPSIS Method: The Case of Electronic Components Procurement," *International Scientific Journal of Engineering and Technology*, vol. 4, no. 1, pp. 44-49, Jun. 2020.
- [3] Q. Cheng and L. Yu, "Operational Mechanism and Evaluation System for Emergency Logistics Risks," *International Journal of Intelligent Systems and Applications*, vol. 2, no. 2, pp. 25-32, Dec. 2010.
- [4] H. D. Sherali, J. Desai, and T. S. Glickman, "Allocating Emergency Response Resources to Minimize Risk with Equity Considerations," *American Journal of Mathematical and Management Sciences*, vol. 24, no. 3-4, pp. 367-410, Aug. 2013.
- [5] P. C. Nolz, F. Semet, and K. F. Doerner, "Risk Approaches for Delivering Disaster Relief Supplies," *OR Spectrum*, vol. 33, no. 3, pp. 543-569, Jun. 2011.
- [6] M. Abkowitz and P. Cheng, "Developing a Risk/Cost Framework for Routing Truck Movements of Hazardous Materials," *Accident Analysis & Prevention*, vol. 20, no. 1, pp. 39-51, Feb. 1988.
- [7] G. Jiang, Q. Wang, K. Wang et al., "A Novel Closed-Loop Supply Chain Network Design Considering Enterprise Profit and Service Level," *Sustainability*, vol. 12, no. 2, pp. 544, Jan. 2020.
- [8] N. M. Sander, "Capacity Planning of Aggregators and Multi-Objective Optimization Approach to Optimal Data Transmission in Cloud Providers for Meteorological Sensor Network," *International Scientific Journal of Engineering and Technology*, vol. 3, no. 1, pp. 15-24, Jun. 2019.
- [9] X. Li, B. Zhang, and H. Li, "Computing Efficient Solutions To Fuzzy Multiple Objective Linear Programming Problems," *Fuzzy Sets and Systems*, vol. 157, no. 10, pp. 1328-1332, May. 2006.
- [10] A. Charnes, W. W. Cooper, and R. Ferguson, "Optimal Estimation of Executive Compensation by Linear Programming," *Management Science*, vol. 1, no. 2, pp. 138-151, Jan. 1955.
- [11] A. Charnes and W. W. Cooper, "Management Models and Industrial Applications of Linear Programming," *Management Science*, vol. 4, no. 1, pp. 38-91, Oct. 1957.
- [12] S. Rivaz, S. H. Nasser, and M. Ziaseraji, "A Fuzzy Goal Programming Approach to Multiobjective Transportation Problems," *Fuzzy Information and Engineering*, vol. 12, no.2, pp. 139-149, Dec. 2020.
- [13] R. Narasimhan, "Goal Programming in a Fuzzy Environment," *Decision Science*, vol. 11, no. 2, pp. 325-336, Apr. 1980.



- [14] P. Rubin and R. Narasimhan, "Fuzzy Goal Programming with Nested Priorities," *Fuzzy Sets and Systems*, vol. 14, pp. 115-129, Nov. 1984.
- [15] S.R. Arora and R. Gupta, "Interactive Fuzzy Goal Programming Approach for Bilevel Programming Problem," *European Journal of Operational Research*, vol. 194, no. 2, pp. 368-376, Apr. 2009.
- [16] J. R. Stock, *Reverse Logistics: White Paper*, Illinois, USA: Council of Logistics Management, 1992, pp. 1-19.
- [17] M. Fleischmann, J. M. Bloemhof-Ruwaard et al., "Quantitative models for Reverse Logistics: A Review," *European Journal of Operational Research*, vol. 103, no. 1, pp. 1-17, Nov. 1997.
- [18] L.-H. Shih and Y.-T. Lin, "Multicriteria Optimization for Infectious Medical Waste Collection System Planning," *Practice Periodical Hazard. Toxic Radioactive Waste Manage.*, vol. 7, no. 2, pp. 78-85, Mar. 2003.
- [19] A. Budak and A. Ustundag, "Reverse Logistics Optimisation for Waste Collection and Disposal in Health Institutions: The Case of Turkey," *International Journal of Logistics Research and Applications*, vol. 20, no. 4, pp. 322-341, Sep. 2016.
- [20] H. Alshraideh and H. Abu Qdais, "Stochastic Modeling and Optimization of Medical Waste Collection in Northern Jordan," *Journal of Material Cycles and Waste Management*, vol. 19, no. 2, pp. 743-753, Feb. 2016.
- [21] G. Mantzaraz and E. A. Voudrias, "An Optimization Model for Collection, Haul, Transfer, Treatment and Disposal of Infectious Medical Waste: Application to a Greek Region," *Waste Management*, vol. 69, pp. 518-534, Nov. 2017.
- [22] S. Kargar, M. Pourmehdi, and M. M. Paydar, "Reverse Logistics Network Design for Medical Waste Management in the Epidemic Outbreak of the Novel Coronavirus (COVID-19)," *Science of the Total Environment*, vol. 746, pp. 141183, Dec. 2020.
- [23] R. Negarandeh and A. Tajdin, "A Robust Fuzzy Multi-Objective Programming Model to Design A Sustainable Hospital Waste Management Network Considering Resiliency and Uncertainty: A Case Study," *Waste Management & Research*, pp. vol. 40, no. 4, pp. 439-457, Aug. 2021.
- [24] A. Nema and S. K. Gupta, "Optimization of Regional Hazardous Waste Management Systems: An Improved Formulation," *Waste Management*, vol. 19, pp. 441-151, Nov. 1999.
- [25] H. Yu, X. Sun, and X. Zhao, "Reverse Logistics Network Design For Effective Management of Medical Waste in Epidemic Outbreaks: Insights from The Coronavirus Disease 2019 (COVID-19) Outbreak in Wuhan (China)," *International Journal of Environmental Research and Public Health*, vol. 17, no. 5, pp. 1770, Mar. 2020.
- [26] M. Jiménez, M. Arenas, A. Bilbao et al., "Linear Programming with Fuzzy Parameters: An Interactive Method Resolution," *European Journal of Operational Research*, vol. 177, no. 3, pp. 1599-1609, Mar. 2007.
- [27] S. Heilpern, "The Expected Value of a Fuzzy Number," *Fuzzy Sets and Systems*, vol. 47, no. 1, pp. 81-86, Apr. 1992.
- [28] M. Jiménez, "Ranking Fuzzy Numbers Through The Comparison of its Expected Intervals," *International Journal of Uncertainty, Fuzziness and Knowledge-Based Systems*, vol. 4, no. 4, pp. 379-388, Aug. 1996.
- [29] M. Arenas, A. Bilbao, B. Pérez et al., "Solving a Multiobjective Possibilistic Problem Through Compromise Programming," *European Journal of Operational Research*, vol. 164, no. 3, pp. 748-759, Feb. 2005.
- [30] Pollution Control Department. (2020, May 25). *Regulation and Guideline of Incineration Facility for Municipal Solid Waste*. [Online]. Available: <https://shorturl.asia/PycEA>
- [31] World Health Organization. Regional Office for South-East Asia. (2017, Apr. 19). *Report on Health-Care Waste Management (HCWM) Status in Countries of The South-East Asia Region*. World Health Organization. Regional Office for South-East Asia. [Online]. Available: <https://apps.who.int/iris/handle/10665/258761>
- [32] P. Boonsrangsom. (2021, May 3). *3 Levels of Management of Infectious Waste during COVID-19*. [Online]. Available: <https://shorturl.asia/h5Dvs>
- [33] J. Zhao, L. Huang, D. Lee et al., "Improved Approaches to the Network Design Problem in Regional Hazardous Waste Management Systems," *Transportation Research Part E: Logistics and Transportation Review*, vol. 88, pp. 52-75, Apr. 2016.
- [34] P. Sresanpila, and S. Sindhuchao, "Solving the Problem of the Selection of the Size and Multi Depot Location Case Study: Elimination of Infectious Waste of Community Hospitals in the Upper Part of Northeast Thailand," *UBU Engineering Journal*, vol. 9, no. 1, pp. 39-47, Jun. 2016.
- [35] R. Homchalee, B. Sameejam, and P. Kaewthong, "Location of Infectious Waste Incinerator of the Hospital in Maha Sarakham Province," *Thai Journal of Operations Research*, vol. 7, no. 2, pp. 30-41, Dec. 2019.
- [36] P. Rujivanarom. (2021, Aug. 10). *Crumbling Under Mountains of Waste*. [Online]. Available: <https://www.bangkokpost.com/thailand/general/2162751/crumbling-under-mountains-of-waste>
- [37] Nonthaburi Provincial Administrative Organization's. (2019, Apr 23). *Project for System Optimization Disposal of Infectious Waste (Phase 2)*. [Online]. Available: [http://nont-pro.go.th/public/news\\_upload/backend/files\\_222\\_2.pdf](http://nont-pro.go.th/public/news_upload/backend/files_222_2.pdf).



**Pornpawee Supsermpol** is currently a Master student in the School of Manufacturing Systems and Mechanical Engineering, Sirindhorn International Institute of Technology, Thammasat University, Thailand. Her research interests are in the area of fuzzy multi-objectives optimization, reverse logistics and supply chain network design.



**Sun Olapiriyakul** is an Assistant Professor of the Industrial Engineering and Logistics Systems program at Sirindhorn International Institute of Technology (SIIT) of Thammasat University, Thailand. After earning a BEng in mechanical engineering from SIIT, Thailand, and an MSc in industrial engineering from San Jose State University, US, he received a doctoral scholarship from Royal Thai Government in 2005 to study in industrial engineering and conduct research related to nanotechnology. He completed his Ph.D. in industrial engineering at New Jersey Institute of Technology, US, in 2010, with his dissertation titled: End-of-life Management of Nanotechnology Products. His current research focuses on the sustainable supply chain network design, urban freight transport, and workforce scheduling. His approach to research revolves around the use of industrial engineering principles in conjunction with sustainability concepts and environmental impact assessment methodologies.



**Navee Chiadamrong** is an Associate Professor from the School of Manufacturing Systems and Mechanical Engineering, Sirindhorn International Institute of Technology, Thammasat University, Thailand where

teaches and researches in the area of production planning and control methods and supply chain management. He received his MSc in Engineering Business Management from the Warwick University and Ph.D. in Manufacturing Engineering and Operational Management from the University of Nottingham, England. Some of his recent articles have appeared in International Journal of Production Economics, Computers and Industrial Engineering, Journal of Simulation, and TQM & Business Excellence.

# PAPER FORMAT (IEEE Style)

## I. FORMAT

- Your paper must use a paper size corresponding to A 4 which is 210 mm (8.27 inch) Wide and 297 mm (11.69 inch)
- Your paper must be in two column format
- Articles not more than 15 pages in length, single-sided A4 paper, margins (top, bottom, left, right) are 1 inch (2.54 cm)
- Abstract and References and content set to double columns,
- English font is Times New Roman, as follows:

TABLE I  
FONT SIZES FOR PAPERS

Content	Font Size	Labelling
Title (Single column)	18 (CT)	bold
Authors (Single column)	11 (CT)	bold
Authors Information (Single column)	10 (CT)	regular
Abstract	10 (LRJ)	bold
Index Terms (Keywords)	10 (LRJ)	bold
Content	10 (LRJ)	regular
Heading1	10 (CT)	bold (Capitalization)
Heading 2	10 (LJ)	regular
Table Title (Place above the Table)	8 (CT)	regular
Table content	8 (CT)	regular
Figure caption (Place below the figure)	8 (LJ)	regular
Reference Head	10 (CT)	regular (Capitalization)
Reference	8 (LJ)	regular
Author Profiles	10 (LRJ)	bold author name/ profile regular

CT=Centre Text, LJ=Left Justified, RJ=Right Justified, LRJ=Left & Right Justified

## II. COMPOSITION OF THE ARTICLE

### A. Article title

B. *Authors information*, Write (all) the author's name, affiliation, department, city, country and E-mail (set to Single Column) all.

C. *Abstract*, Must be under 200 words and not include subheadings or citations. Define all symbols used in the abstract. Do not delete the blank line immediately above the abstract.

D. *Index Terms*, Enter key words or phrases in alphabetical order, separated by commas.

### E. Content

1) *Academic article*, should include: Introduction, Content, and Conclusion.

2) *Research article*, should include: introduction, literature review, Materials methods, Results, Discussion, and conclusion.

Clearly summarize the important findings of the paper. It should contain such as objectives, methods and major results.

### F. Introduction

The Introduction section of reference text expands on the background of the work (some overlap with the Abstract is acceptable). The introduction should not include subheadings.

G. *Pictures, table, etc.*, Must be use in numerical order in the article, provided the source correctly, cannot use other people' copyright.

Chart should be colored contrastingly or in black and white.

### H. Reference

1) *Cited in the main text*. Indicate the number in the [ ] mark at the end of the text or the name of the referring person. Let the numbers be in the same line of content as [1].

2) *Cited after the article*. Put all bibliographical reference after articles, and order according to the author's name, please refer IEEE format. The footer reference format is as follows.

## III. RERERENCES

References in research articles and scholarly articles. For academic and research journals, INTERNATIONAL SCIENTIFIC JOURNAL OF ENGINEERING AND TECHNOLOGY (ISJET). The technology defines referrals according to the IEEE format. All references should be listed at the end of the paper using the following.

### Basic format for books:

J. K. Author, "Title of chapter in the book," in *Title of His Published Book*, xth ed. City of Publisher, Country if not USA: Abbrev. of Publisher, year, ch. x, sec. x, pp. xxx-xxx.

### Examples:

- [1] G. O. Young, "Synthetic structure of industrial plastics," in *Plastics*, 2nd ed., vol. 3, J. Peters, Ed. New York: McGraw-Hill, 1964, pp. 15-64.
- [2] W.-K. Chen, *Linear Networks and Systems*. Belmont, CA: Wadsworth, 1993, pp. 123-135.

### Basic format for periodicals:

J. K. Author, "Name of paper," *Abbrev. Title of Periodical*, vol. x, no. x, pp. xxx-xxx, Abbrev. Month. year.

### Examples:

- [3] J. U. Duncombe, "Infrared navigation—Part I: An assessment of feasibility," *IEEE Trans. Electron Devices*, vol. ED-11, no. 1, pp. 34-39, Jan. 1959.
- [4] E. P. Wigner, "Theory of traveling-wave optical laser," *Phys. Rev.*, vol. 134, pp. A635-A646, Dec. 1965.
- [5] E. H. Miller, "A note on reflector arrays," *IEEE Trans. Antennas Propagat.*, to be published.

**Basic format for reports:**

J. K. Author, "Title of report," Abbrev. Name of Co., City of Co., Abbrev. State, Rep. xxx, year.

**Examples:**

- [6] E. E. Reber, R. L. Michell, and C. J. Carter, "Oxygen absorption in the earth's atmosphere," Aerospace Corp., Los Angeles, CA, Tech. Rep. TR-0200 (4230-46)-3, Nov. 1988.
- [7] J. H. Davis and J. R. Cogdell, "Calibration program for the 16-foot antenna," Elect. Eng. Res. Lab., Univ. Texas, Austin, Tech. Memo. NGL-006-69-3, Nov. 15, 1987.

**Basic format for handbooks:**

Name of Manual/Handbook, x ed., Abbrev. Name of Co., City of Co., Abbrev. State, year, pp. xxx-xxx.

**Examples:**

- [8] *Transmission Systems for Communications*, 3rd ed., Western Electric Co., Winston-Salem, NC, 1985, pp. 44-60.
- [9] *Motorola Semiconductor Data Manual*, Motorola Semiconductor Products Inc., Phoenix, AZ, 1989.

**Basic format for books (when available online):**

Author. (year, month day). Title. (edition) [Type of medium]. volume (issue). Available: site/path/file

**Example:**

- [10] J. Jones. (1991, May 10). *Networks*. (2nd ed.) [Online]. Available: <http://www.atm.com>

**Basic format for journals (when available online):**

Author. (year, month). Title. *Journal*. [Type of medium]. volume (issue), pages. Available: site/path/file

**Example:**

- [11] R. J. Vidmar. (1992, Aug.). On the use of atmospheric plasmas as electromagnetic reflectors. *IEEE Trans. Plasma Sci.* [Online]. 21(3), pp. 876-880. Available: <http://www.halcyon.com/pub/journals/21ps03-vidmar>

**Basic format for papers presented at conferences (when available online):**

Author. (year, month). Title. Presented at Conference title. [Type of Medium]. Available: site/path/file

**Example:**

- [12] PROCESS Corp., MA. Intranets: Internet technologies deployed behind the firewall for corporate productivity. Presented at INET96 Annual Meeting. [Online]. Available: <http://home.process.com/Intranets/wp2.htm>

**Basic format for reports and handbooks (when available online):**

Author. (year, month). Title. Comp any . City, State or Country. [Type of Medium]. Available: site/path/file

**Example:**

- [13] S. L. Talleen. (1996, Apr.). The Intranet Architecture: Managing information in the new paradigm. Amdahl Corp., CA. [Online]. Available: <http://www.amdahl.com/doc/products/bsg/intra/intra/html>

**Basic format for computer programs and electronic documents (when available online):**

ISO recommends that capitalization follow the accepted practice for the language or script in which the information is given.

**Example:**

- [14] A. Harriman. (1993, June). Compendium of genealogical software. *Humanist*. [Online]. Available e-mail: HUMANIST@NYVM.ORG Message: get GENEALOGY REPORT

**Basic format for patents (when available online):**

Name of the invention, by inventor's name. (year, month day). Patent Number [Type of medium]. Available: site/path/file

**Example:**

- [15] Musical toothbrush with adjustable neck and mirror, by L.M.R. Brooks. (1992, May 19). *Patent D 326 189* [Online]. Available: NEXIS Library: LEXPAT File: DESIGN

**Basic format for conference proceedings (published):**

J. K. Author, "Title of paper," in *Abbreviated Name of Conf.*, City of Conf., Abbrev. State (if given), year, pp. xxxxxx.

**Example:**

- [16] D. B. Payne and J. R. Stern, "Wavelength-switched passively coupled single-mode optical network," in *Proc. IOOC-ECOC*, 1985, pp. 585-590.

**Example for papers presented at conferences (unpublished):**

- [17] D. Ebehard and E. Voges, "Digital single sideband detection for interferometric sensors," presented at the 2nd Int. Conf. Optical Fiber Sensors, Stuttgart, Germany, Jan. 2-5, 1984.

**Basic format for patents:**

J. K. Author, "Title of patent," U.S. Patent x xxx xxx, Abbrev. Month. day, year.

**Example:**

- [18] G. Brandli and M. Dick, "Alternating current fed power supply," U.S. Patent 4 084 217, Nov. 4, 1978.

**Basic format for theses (M.S.) and dissertations (Ph.D.):**

J. K. Author, "Title of thesis," M.S. thesis, Abbrev. Dept., Abbrev. Univ., City of Univ., Abbrev. State, year.

J. K. Author, "Title of dissertation," Ph.D. dissertation, Abbrev. Dept., Abbrev. Univ., City of Univ., Abbrev. State, year.

**Examples:**

- [19] J. O. Williams, "Narrow-band analyzer," Ph.D. dissertation, Dept. Elect. Eng., Harvard Univ., Cambridge, MA, 1993.
- [20] N. Kawasaki, "Parametric study of thermal and chemical nonequilibrium nozzle flow," M.S. thesis, Dept. Electron. Eng., Osaka Univ., Osaka, Japan, 1993.

**Basic format for the most common types of unpublished references:**

J. K. Author, private communication, Abbrev. Month, year.

J. K. Author, "Title of paper," unpublished.

J. K. Author, "Title of paper," to be published.

**Examples:**

- [21] A. Harrison, private communication, May 1995.
- [22] B. Smith, "An approach to graphs of linear forms," unpublished.
- [23] A. Brahms, "Representation error for real numbers in binary computer arithmetic," IEEE Computer Group Repository, Paper R-67-85.

**Basic format for standards:**

Title of Standard, Standard number, date.

**Examples:**

- [24] IEEE Criteria for Class IE Electric Systems, IEEE Standard 308, 1969.
- [25] Letter Symbols for Quantities, ANSI Standard Y10.5-1968.



**First A. Author** and the other authors may include biographies at the end of regular papers. Biographies are often not included in conference related papers. The first paragraph may contain a place and/or date of birth (list place, then date).

Next, the author's educational background is listed. The degrees should be listed with type of degree in what field, which institution, city, state, and country, and year the degree was earned. The author's major field of study should be lower-cased.

The second paragraph uses the pronoun of the person (he or she) and not the author's last name. It lists military and work experience, including summer and fellowship jobs. Job titles are capitalized. The current job must have a location; previous positions may be listed without one. Information concerning previous publications may be included. Try not to list more than three books or published articles. The format for listing publishers of a book within the biography is: title of book (city, state: publisher name, year) similar to a reference. Current and previous research interests end the paragraph.

The third paragraph begins with the author's title and last name (e.g., Dr. Smith, Prof. Jones, Mr. Kajor, Ms. Hunter). List any memberships in professional societies. Finally, list any awards and work for committees and publications. If a photograph is provided, the biography will be indented around it. The photograph is placed at the top left of the biography, and should be of good quality, professional-looking, and black and white (see above example). Personal hobbies will be deleted from the biography. Following are two examples of an author's biography.



**Second B. Author** was born in Greenwich Village, New York City, in 1977. He received the B.S. and M.S. degrees in aerospace engineering from the University of Virginia, Charlottesville, in 2001 and the Ph.D. degree in mechanical engineering from Drexel

University, Philadelphia, PA, in 2008. From 2001 to 2004, he was a Research Assistant with the Princeton Plasma Physics Laboratory. Since 2009, he has been an

Assistant Professor with the Mechanical Engineering Department, Texas A&M University, College Station. He is the author of three books, more than 150 articles, and more than 70 inventions. His research interests include high-pressure and high-density nonthermal plasma discharge processes and applications, microscale plasma discharges, discharges in liquids, spectroscopic diagnostics, plasma propulsion, and innovation plasma applications. He is an Associate Editor of the journal *Earth, Moon, Planets*, and holds two patents.

Mr. Author was a recipient of the International Association of Geomagnetism and Aeronomy Young Scientist Award for Excellence in 2008, the IEEE Electromagnetic Compatibility Society Best Symposium Paper Award in 2011, and the American Geophysical Union Outstanding Student Paper Award in Fall 2005.



**Third C. Author** received the B.S. degree in mechanical engineering from National Chung Cheng University, Chiayi, Taiwan, in 2004 and the M.S. degree in mechanical engineering from National Tsing Hua University, Hsinchu, Taiwan, in 2006. He is currently

pursuing the Ph.D. degree in mechanical engineering at Texas A&M University, College Station.

From 2008 to 2009, he was a Research Assistant with the Institute of Physics, Academia Sinica, Tapei, Taiwan. His research interest includes the development of surface processing and biological/medical treatment techniques using nonthermal atmospheric pressure plasmas, fundamental study of plasma sources, and fabrication of micro- or nanostructured surfaces.

Mr. Author's awards and honors include the Frew Fellowship (Australian Academy of Science), the I. I. Rabi Prize (APS), the European Frequency and Time Forum Award, the Carl Zeiss Research Award, the William F. Meggers Award and the Adolph Lomb Medal (OSA).

**Remark:** More detail information, Please read Preparation of Papers for INTERNATIONAL SCIENTIFIC JOURNAL OF ENGINEERING AND TECHNOLOGY (ISJET), <https://ph02.tci-thaijo.org/index.php/isjet/index>



**Panyapiwat Institute of Management (PIM)**  
85/1 Moo 2, Chaengwattana Rd,  
Bang Talat, Pakkred, Nonthaburi 11120, Thailand  
Tel. +66 2855 1560 Fax. +66 2855 0392  
<https://www.tci-thaijo.org/index.php/isjet/index>  
<https://isjet.pim.ac.th>  
E-mail: [isjet@pim.ac.th](mailto:isjet@pim.ac.th)